2024

Enabling outer planet exploration : performance and feasibility of nuclear thermal propulsion for rendezvous missions

Saroj Kumar

ENABLING OUTER PLANET EXPLORATION: PERFORMANCE AND FEASIBILITY OF NUCLEAR THERMAL PROPULSION FOR RENDEZVOUS MISSIONS

Saroj Kumar

A DISSERTATION

Submitted in partial fulfillment of the requirements
for the degree of Doctor of Philosophy
in
The Department of Mechanical and Aerospace Engineering
to
The Graduate School
of
The University of Alabama in Huntsville

May 2024

Approved by:

Dr. L. Dale Thomas, Research Advisor
Dr. Jason T. Cassibry, Committee Chair
Dr. Robert Frederick, Committee Member
Dr. Matthew Turner, Committee Member
Dr. Gabriel Xu, Committee Member
Dr. George J. Nelson, Department Chair
Dr. Shankar Mahalingam, College Dean
Dr. Jon Hakkila, Graduate Dean

Abstract

ENABLING OUTER PLANET EXPLORATION: PERFORMANCE AND FEASIBILITY OF NUCLEAR THERMAL PROPULSION FOR RENDEZVOUS MISSIONS

Saroj Kumar

A dissertation submitted in partial fulfillment of the requirements for the degree of Doctor of Philosophy

Mechanical and Aerospace Engineering

The University of Alabama in Huntsville

May 2024

Nuclear Thermal Propulsion (NTP) provides the compelling alternative between the chemical and electric propulsion systems for outer planet robotic missions. High-thrust and high-specific impulse (over twice the best chemical propulsion engine) NTP systems can enable outer planet missions that have been limited due to the large ΔV requirements. This dissertation identifies an enabling mission architecture and NTP engine thrust class for rendezvous missions to the Gas giant and Ice giant systems. The work presented in the dissertation demonstrates the performance impact of the NTP system and its feasibility for robotic missions using a systems engineering model driven by the model based systems engineering (MBSE) which is coupled with the domain engineering analysis models and systems engineering architectural models. The performance metrics are chosen based on the finite maneuver analysis and design reference mission trade tree to determine the solution space of NTP for high energy missions. The developed spacecraft integrated system model allows rapid mission analysis for engine thrust class ranging from 5 klbf to 30 klbf

and I_{sp} from 850 s to 900 s for expendable and non-expendable architectures. The direct spacecraft injection analysis showed payload delivery of over 12% to Jupiter and over 30% to Saturn for NTP system on a commercial heavy lift launch vehicle when compared with standalone super heavy-lift launch vehicles. The point design studies demonstrated the enhanced capability of NTP system by reducing the trip times to Gas giant missions by a factor of two or more. Engine trade analysis shows 12.5 to 15 klbf NTP engines are optimum for rendezvous missions to the outer planets using expendable configuration, which consists of a spacecraft and NTP injection stage with injection stage being used for trans-planetary injection and plane change maneuver only and spacecraft's storable propellant to be used for planetary orbit insertion. Payload mass delivery using an expendable configuration for a Jupiter rendezvous mission is shown to outperform non-expendable configuration (NTP system to be used for both trans-planetary injection and planetary orbit insertion) by 5.67% for Hohmann transfers. However, non-expendable configurations have shown similar payload delivery for high energy Type-I trajectory missions with trip times of 1.49 years.

Acknowledgements

I would like to take a moment to express my deepest gratitude and thank those who have been instrumental to me reaching this point in my life. This was not just the four years of dedication and hard work but a goal since my under-graduation days, with many people supporting me along the way.

First and foremost, I would like to sincerely thank my advisor, Dr. L Dale Thomas, for his unwavering support in pursuit of my research interest. Thank you Dr. Thomas for your guidance, mentorship both professionally and personally and endless patience. I would also like to thank my committee chair Dr. Jason Cassibry for his insightful feedback on my research and your willingness to invest your time and expertise in my development have been truly invaluable.

The quality of this dissertation would not have been what it is currently without the invaluable advice from my committee members Dr. Matthew Turner, Dr. Gabriel Xu and Dr. Robert Frederick. I extend my appreciation to each of you for taking out time to review my research progress routinely and providing your feedback and constructive criticism, which greatly enhanced the quality of this work.

To my colleagues at CSIL and PRC, thank you for providing me the supportive environment throughout my research. In particular, I would like to thank *Daria Nikitaeva, Alex Aueron, Shreyas Raghu, Samantha Rawlins, Diana Gorokhovskaya and Will Ziehm* for all the support and engaging discussions on topics ranging from advanced propulsion concepts, systems engineering to integrated modeling and simulation.

I would like to take this opportunity to acknowledge Dr. Mike Houts at NASA MSFC for supporting the work presented in this dissertation. Dr. Russ Joyner at the Aerojet Rocketdyne for helping me understand the NTP engine designs and

the impact of using HALEU on engine performance parameters. I would also like to acknowledge Dr. Alfred Nash (team lead, Team X) and his team at the Jet Propulsion Laboratory for giving me the opportunity to learn about the mission concept development process and the art of writing successful proposals during my internship.

I would like to thank my friends in India, Germany and here in the US who have been some of my biggest supporters throughout my time in graduate school. I would like to especially thank *Amit Patel, Bryan Winterling, Jayesh Chaudhary, Pratik Bhardwaj and Swarnalatha K V Kumar* for all the encouragement to achieve something greater than average and being friends for life!

On a more personal level, I would like to thank my family. Mummy and Papa for supporting an providing me the best opportunity to pursue my academic endeavours. My sister, Anjali, for always encouraging me to pursue my passion in the field of space exploration.

Finally and most importantly, I would like to thank my wife, Sneha. I hope the sacrifice of putting your life on hold while I could work on my research will pay off. Thank you for your constant encouragement when it all seemed impossible.

To my teachers

For always inspiring me

Table of Contents

List of Figures

List of Tables

List of Symbols

Symbol	Description
C_3	Characteristic energy
C_p	average molar heat capacity
F_{ext}	total external forces
I_{sp}	Specific impulse, s
$LH2$	Liquid Hydrogen
R_{D}	heliocentric orbital radii of the destination celestial body
V_∞	hyperbolic excess velocity
ΔV	Change in velocity, km/s
μ	gravitational parameter
μ_{sun}	gravitational parameter of the Sun
f_p	sum of all perturbing acceleration
m	total mass of the spacecraft
t	time
v	spacecraft velocity
v_e	effective exhaust velocity

Symbol	Description
a	semi-major axis of the transfer orbit
J	conversion from thermal to mechanical units
K	Kelvin
M	molecular weight of gas
mT	metric tons
MW	Megawatt
T	temperature

Chapter 1. Introduction

Nuclear Thermal Propulsion (NTP) has distinctly shown its relevance in enabling future human missions to Mars [1, 2]. However, the utilization of this advanced propulsion for robotic missions has not been explored extensively. NTP powered missions using expendable configurations have potential to improve the capability in terms of spacecraft mass and trip times when compared with the current available in-space propulsion solutions. There has never been an effort to develop a quantified framework that assesses the enabling mission architectures and NTP engine parameters desirable for ambitious missions to the outer solar system exploration.

1.1 Problem Statement

The overall question of this dissertation can be stated as: *Can a robotic mission using NTP system be designed which enables the missions recommended by the planetary science and astrobiology decadal survey which is within the constraints of the planetary science division?*

The research questions associated with the above statement are:

- What is the potential difference in performance parameters for NTP systems in comparison to traditional propulsion systems towards enabling ambitious missions to the outer solar system exploration?
- What is an enabling mission architecture for the robotic missions using NTP systems?
- What is the enabling engine thrust class for targeted robotic missions?

The performance parameters imply the payload injection capability, impact on Initial Mass in Low Earth Orbit (IMLEO) with long finite maneuvers and high-fidelity trajectory design. Mission constraints comprises of nuclear safe orbit requirements, NTP system and spacecraft design which is within the requirement of a commercially available launch vehicle and architectures considering $LH2$ propellant boil-off for long duration missions.

1.2 Dissertation Objectives

The main contribution of this dissertation is to provide the solution space of NTP systems for missions to the outer solar system. The Design Reference Missions are used to fulfill the knowledge gaps on mission architectures and engine parameters using the quantifiable figures of merit. The low level goals in order to answer the research questions are mentioned below along with the Table 1.1 matrix indicating the objectives needed to answer the dissertation research questions.

- Develop a detailed systems engineering model using MBSE approach which is tightly coupled with the domain engineering model.
- Develop the Spacecraft Integrated System Model which is able to perform end-to-end mission analysis based on the architecture generated by the design structure matrix.
- Define the Design Reference Missions trade tree in such a way that it clearly articulates the NTP system performance for planetary science missions.
- Calculate the initial capability of the NTP system using the expendable configuration and evaluate its performance by comparing it with chemical propulsion system.
- Perform the exhaustive engine system trades and determine the enabling engine thrust parameters for robotic missions.
- Evaluate the performance of expendable and non-expendable mission architectures and recommend the possible solution space for both architectures.

Table 1.1: Low level goals matrix to provide the answers to the dissertation research questions.

Low level goals to answer research questions	**Potential difference in performance parameters for NTP systems in comparison to traditional propulsion systems?**	**Enabling mission architecture for the robotic missions using NTP systems?**	**Enabling engine thrust class for targeted robotic missions?**
Develop systems engineering model coupled with the domain engineering model	**X**	**X**	**X**
Develop the Spacecraft Integrated System Model	**X**	**X**	**X**
Define the Design Reference Missions trade tree		**X**	**X**
Calculate the initial capability of the NTP system	**X**		
Perform engine system trades for robotic missions			**X**
Evaluate the performance multiple mission architectures	**X**	**X**	

1.3 Dissertation Organization

This dissertation is primarily divided into four chapters (Chapter 2-5) contributing towards the solution space for NTP systems and methodology proposed to quantify the NTP engine parameters with respect to the robotic missions.

Chapter 2 provides the detailed literature review and identifies three knowledge gaps: (1) insufficiency of the available detailed mission analysis in determining the difference in overall mission performance of NTP system in comparison to traditional propulsion systems, (2) current planetary mission architecture solutions and its limitation on concepts of operations applicability for nuclear fission powered systems and (3) studies on robotic missions using NTP considering arbitrary engine parameters thus the need to determine the engine parameters applicable for robotic missions.

Chapter 3 proposes the overall model integration and execution approach by dynamically coupling the structure model with analytical models. The modules in design structure matrix are introduced to provide the foundation for detailed analysis in Chapter 4 and 5. The UAH NTP 330MW engine model described in the chapter is used for point design studies. Trajectory models of various fidelity levels were used throughout the dissertation however, the final results presented in this dissertation are based on the high-fidelity numerical propagator.

Chapter 4 presents the results on the performance parameters of NTP system and compares them with the traditional propulsion system. The point

design studies using the expendable configuration are discussed for rendezvous mission to Gas and Ice giant systems.

Chapter 5 explores the complete tradespace as described in the DRM trade tree to determine the enabling NTP engine parameters for robotic missions to the outer planets. The chapter also discusses the challenges with the non-expendable configuration and potential missions suitable for both type of architectures.

Chapter 6 summarizes the insights from the dissertation and its contribution of the body of knowledge, as well as suggested leads for future work.

1.4 Publication History

Much of the research work in this dissertation has been presented at various conferences focusing in the area of advance propulsion concepts. Results presented in Chapter 4 have already been published in the AIAA *Journal of Spacecraft and Rockets* (JSR) and ANS *Journal on Nuclear Technology* (NT). Publications based on Chapter 3 and Chapter 5 will be submitted to the Journals on Systems Engineering, JSR and NT. The authors relevant journal and conference publications history is listed in Appendix A.

Chapter 2. Literature Review

To frame the design problem, the past and present work concerning the literature review of the dissertation can be summarized into two focus areas:
(1) Reviewing literature towards the robotic exploration of our solar system and identifying current challenges for missions to the outer planets. This led to the first research question (RQ #1) *"Can those problems be addressed?"*;
(2) Literature review on the Nuclear Thermal Propulsion systems to understand whether this advanced propulsion technology can answer the first research question (*"Can we?"*). This also led to the subsequent research questions on the enabling mission architectures and the Nuclear Thermal Propulsion engine parameters (RQ #2 and RQ #3 respectively) which has been described in this chapter in detail.

2.1 Robotic Exploration of Our Solar System

The genesis of robotic exploration of solar system bodies can be traced back to the early days of the space age when the world's major space agencies embarked on ambitious missions to study and explore celestial objects beyond Earth. In 1959, the Soviet Luna 2 became the first spacecraft to reach Earth's escape velocity and achieved a heliocentric orbit [3]. Although, the primary ob-

jective of the mission was to impact the lunar surface but due to the malfunction with the launch vehicle the spacecraft missed the Moon by 5,900km [4]. Over the last seven decades more than 250 spacecrafts have travelled beyond the Earth's orbit to study celestial bodies in our solar system and beyond. Figure 2.1 shows the distribution of the target planets in the solar system for total or partially successful planetary science missions by nation/space agencies from the year 1958 to 2022.

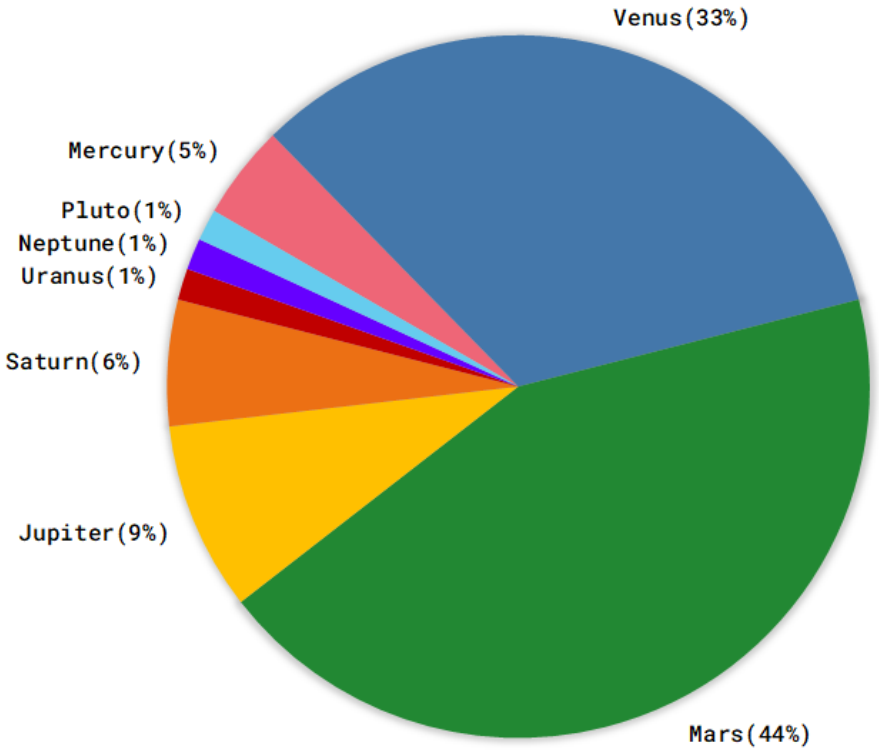

Figure 2.1: Distribution of the target planets for total or partial successful planetary science missions (1958 - 2022).

Among the missions sent to the targeted planets, over 82% of the missions have been to explore the planets in the inner solar system with majority of them being towards exploring the Earth's neighbouring planets Venus and Mars. On the other hand there have been only 18% of the missions targeted to explore the planets in the outer solar system.

NASA's planetary science missions under the planetary science program consist of a balanced mix of missions in three different cost classes - small, medium, and large ("flagship"). The large ("flagship") class missions are strategic missions which address broad, high-priority science objectives using complex scientific instruments with long-term measurements [5]. The development of large ("flagship") missions is led by a NASA center and due to the mission objectives the overall spacecraft mass is heaviest in its class and often requires the longest development time. Some of the past large ("flagship") missions are Voyager, Galileo, Cassini and Mars Science Laboratory (MSL) etc.[6]. Currently, Europa Clipper mission is in development under this mission category with planned launch in 2024. The total expected lifecycle cost for large ("flagship") missions is between $2000M -$3000M USD, however due to the high-priority scientific instruments development and very low single point failure requirements and other reasons the flagship class missions often cost in excess of the mentioned lifecycle cost [7, 8].

Medium-class spacecraft are under the New Frontiers (NF) program, which tackles a specific solar system exploration goal that conducts a high-science-return investigation [9]. The New Frontiers missions are PI-led and are managed by limited numbers of NASA centers. There have been three missions under this

program namely New Horizons which was a Pluto flyby mission, Juno mission to study gas giant planet Jupiter and asteroid sample return OSIRIS-REx mission [10]. Currently, the next New Frontiers mission in development is a robotic rotorcraft to Saturn's moon Titan [11]. The total lifecycle cost cap for New Frontiers class missions is less than $1000M USD with targeted launch of a new mission every 60 months.

Discovery program is the smallest category mission under the planetary science program. This program is also a PI-led mission and addresses focused science objectives in our solar system with lower cost and faster development time. Some examples of the past Discovery missions include Dawn mission to Ceres, Mars lander InSight mission etc. The current active mission under this program is the Lucy space probe which will study multiple Jupiter trojan asteroids. Currently, there are three missions in development phase under the program namely Psyche mission to metallic asteroid 16Psyche and DAVINCI (Deep Atmosphere Venus Investigation of Noble gases, Chemistry, and Imaging) and VERITAS (Venus Emissivity, Radio Science, InSAR, Topography, and Spectroscopy) missions to Venus. The total lifecycle cost cap of Discovery series planetary missions is $500M USD with trageted launch of a new mission every 36 months. Table 2.1 shows the examples of different classes of planetary science missions. Figure 2.2 shows the relationship between spacecraft dry mass and mission cost of NASA's planetary science missions from 2001 - 2022.

Table 2.1: Representative Small, Medium, and Large Planetary Science Missions.

Spacecraft	Mission Goals	Dry mass	Mission class
Dawn [12]	Study protoplanets in the main asteroid belt: Vesta and Ceres	747 kg	Small
Juno [13]	Reveal the story of the formation and evolution of the planet Jupiter	1,593 kg	Medium
Cassini [14]	Study Saturn system	2,125 kg	Large

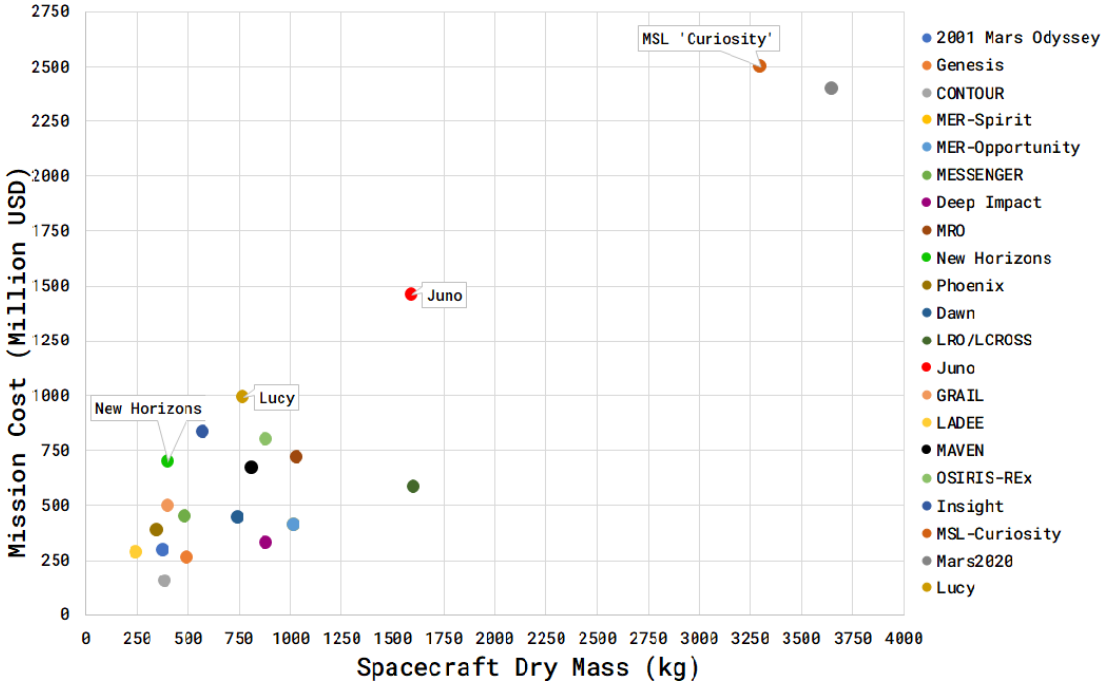

Figure 2.2: Mission cost vs spacecraft dry mass of NASA's planetary science missions from 2001 - 2022.

2.2 Outer Solar System Exploration

Missions to the outer solar system have provided invaluable insights into the distant realms of our cosmic neighborhood. These missions involve spacecraft traveling beyond the asteroid belt to explore planets like Jupiter, Saturn, Uranus, and Neptune, as well as their moons and surrounding environments. There have been a total of eight spacecrafts to the outer solar system with primary mission to explore the outer planets or dwarf planet in the Kuiper belt region. Table 2.2 lists the summary of missions to the outer solar system. Exploring the outer planets is a complex and challenging endeavour that involves a combinations of mission design and architectural considerations within the program requirements. Some of the factors contributing to the relatively limited number of missions to the outer solar system are:

- **Trip time and Mission Duration:** Exploring the outer planets requires longer mission duration's. For example, rendezvous missions to the gas giants using conventional chemical propulsion systems can take five to ten years reach their destinations. The science operations of the missions only begins after the spacecraft is in the orbit of the target planetary body and this phase can be time limited depending on the spacecraft health parameters.

- **Limited Launch Opportunities:** If the available launch vehicle cannot inject the spacecraft in a direct Type-I trajectory then missions often requires gravity assist trajectories to reach farther destinations. The align-

ment of planets and the specific trajectories required for outer planet missions may limit the launch windows available. Missions need to be launched during specific windows to achieve efficient trajectories, and missing these windows can result in significantly longer travel times and increased costs.

Table 2.2: Missions to the outer solar system and beyond with primary objective to explore outer planets and Kupiter belt region.

Spacecraft	**Destination**	**Mission type**
Pioneer 10	Jupiter	Flyby
Pioneer 11	Jupiter, Saturn	Flyby
Voyager 1	Jupiter, Saturn	Flyby
Voyager 2	Jupiter, Saturn, Uranus, Neptune	Flyby
Galileo	Jupiter	Rendezvous
Cassini-Huygens	Saturn	Rendezvous
New Horizons	Pluto and KBOs	Flyby
Juno	Jupiter	Rendezvous

- **Limited Payload Capability:** The limited spacecraft mass for missions to the outer solar system is a critical constraint that impacts mission design, instrument selection, propulsion systems, and overall mission capabil-

ities. This constraint arises from several factors such as propulsion requirements, scientific instruments to achieve the mission objectives in line with the decadal surveys and power subsystem etc.

2.3 Nuclear Thermal Propulsion

The fundamental principle of Nuclear Thermal Propulsion is remarkably simple when compared with chemical propulsion systems. In NTP system, the heat energy from fission reactor is transferred to the propellant which is then ejected through a de Laval nozzle. A schematic of a nuclear thermal propulsion engine is shown in figure 2.3 [15]. The fuel is injected into the reactor core where it is heated to temperatures of about 2,500 K or above and then ejected via nozzle [16]. The temperature of the propellant heating is actually limited due to the structural integrity of the NTP engine. A small amount of propellant is also used to run the turbopumps which feed the propellant to the reactor core.

The benefits of Nuclear Thermal Propulsion can be shown via ideal rocket equation,

$$\Delta V = I_{sp} g_0 \ln\left(\frac{m_0}{m_f}\right). \tag{2.1}$$

The specific impulse in the rocket equation is dependent on the square root of the ratio of the absolute temperature of the exhaust gas to the molecular weight of the exhaust gas [17]. Thus, to improve the performance of the system, one needs to have the highest exhaust temperature with the lowest molecular weight of the propellant.

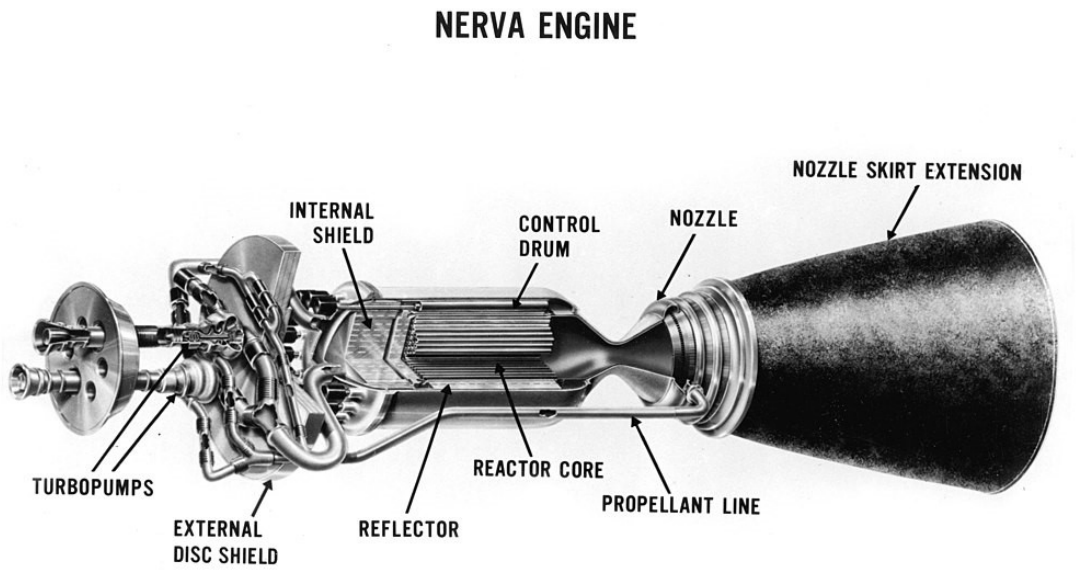

Figure 2.3: Schematic of the NERVA Nuclear Rocket Engine [15].

The NTP engines do not require propellant combustion to generate heat but use heat source from the nuclear reactor to generate much higher exhaust temperatures of the propellant. The NTP system is generally designed with hydrogen as fuel and does not require an oxidizer which in turn lowers the molecular weight of the exhaust gas. This significantly improves the specific impulse of the propulsion system. The best chemical propulsion system today are limited to a specific impulse of about 450 seconds and only slight improvements can be expected. On the other hand, NTP systems using solid core reactor have already demonstrated in ground testing a specific impulse of about 900 seconds *i.e.,* about twice as efficient when compared with the best chemical propulsion engines [18, 19]. The specific impulse of a nuclear engine is doubled when compared to any state-of-

the-art chemical engine because the propellant of choice, hydrogen has molecular weight of two as against 9 or 10 from the combination of liquid oxygen and liquid hydrogen used in the highest efficient chemical engines [20, 21]. A general schematic of a spacecraft using NTP system is shown in figure 2.4 which consists of a nuclear power source, heat exchange system, propellant tanks, and payload [22]. In the heat exchange systems the heat generated from the core is transferred to the liquid propellant before being ejected from the nozzle. The NTP system will also require a radiation shield due to the reactivity from the nuclear core which can pose a challenge to the payload most importantly if the radiation contains neutrons as the hardware may suffer from activation which can affect the material properties such as mechanical resistance [23].

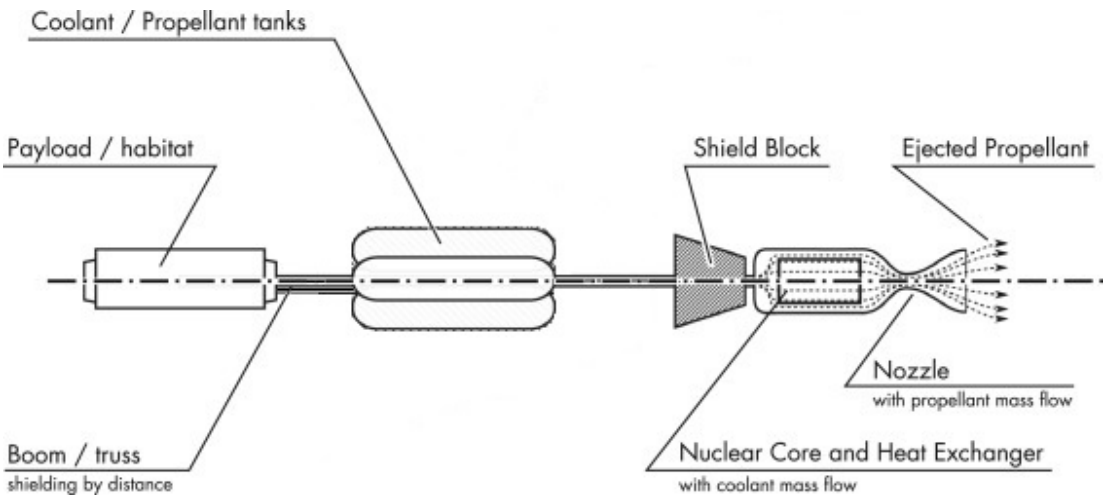

Figure 2.4: Schematic of spacecraft using NTP system [22].

The NTP system can demonstrate even higher performance when temperature limits are relaxed and concepts such as liquid core and gas core reactors are

implemented which have capability to generate specific impulse between 1500 to 6000s [24, 25].

2.3.1 Current Operational In-Space Propulsion Systems

The current operational in-space propulsion systems for interplanetary missions can be categorized in two areas (i) Chemical propulsion systems and (ii) Solar electric propulsion systems. Figure 2.5 below illustrates the thrust vs specific impulse of the majority of the current operational propulsion systems.

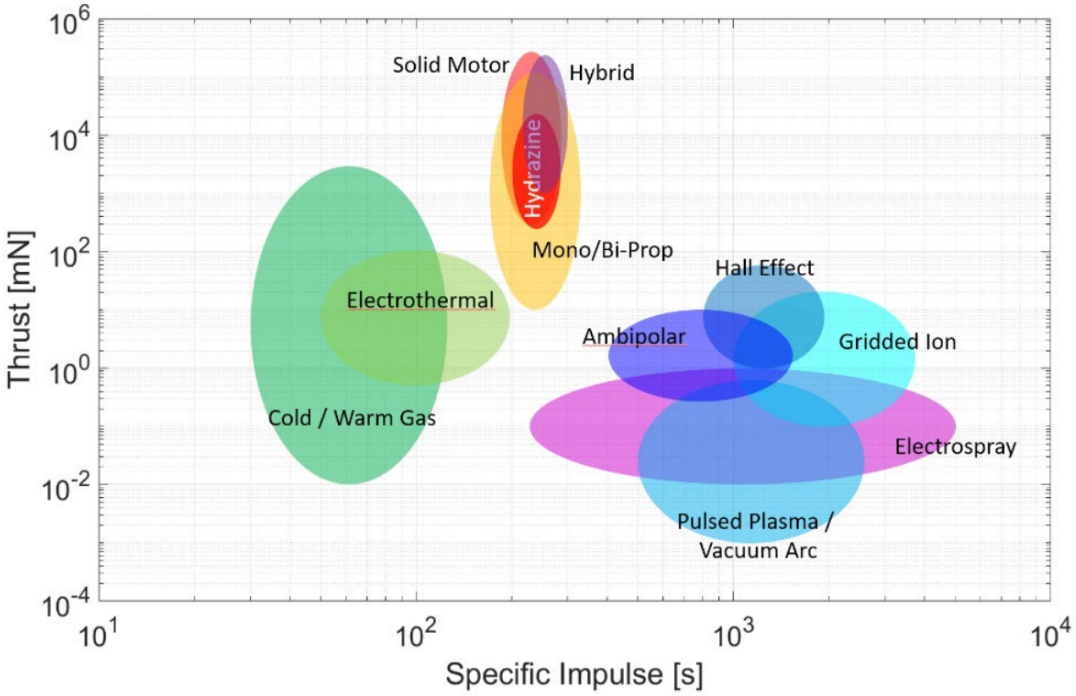

Figure 2.5: Thrust vs specific impulse of typical in-space propulsion systems [26].

2.3.1.1 Chemical Propulsion Systems

The thrust produced by the spacecraft using the chemical propulsion system is derived from the heat of the reaction which produces high-temperature gas that is expanded and ejected through a de Laval nozzle thereby converting thermal energy into kinetic energy. Assuming all the thermal energy is converted to kinetic energy, an energy balance can be used to derive the exhaust velocity of the gas which is shown in the equation 2.2 below:

$$v_e = \left(\frac{2JC_pT}{M}\right)^2, \tag{2.2}$$

where v_e represents the effective exhaust velocity, J represents the conversion from thermal to mechanical units, C_p represents the average molar heat capacity, T represents the temperature, and M represents the molecular weight of gas. For long duration planetary science missions to the outer planets, if a multi-ton class spacecraft is to be delivered then the propulsion system must achieve high propellant exhaust velocities. Unfortunately, for chemical propulsion system the exhaust velocities of about 4000 m/s are fundamentally limited by the available reaction energies of the chemical propellants combustion. Therefore, to enable large missions using chemical propulsion systems engineers design spacecraft trajectory using planetary gravity assist maneuvers rather than direct ballistic transfers which increases the overall interplanetary trip time. Figure 2.6 shows the example of Earth to Saturn transfer for flagship class Cassini mission using Venus-Venus-Earth-Jupiter Gravity Assist (VVEJGA) interplanetary trajectory.

Missions to Ice giant planets Uranus and Neptune are currently dependent on the Radioisotope Power System (RPS) to power the spacecraft. One of the challenge of long trip times due to the dependence of chemical propulsion system is that the RPS system have flight design life of 14 yrs from the date of launch [27]. Therefore, it is recommended for the missions to complete the primary science mission within this period of time which has been a challenge using chemical propulsion systems.

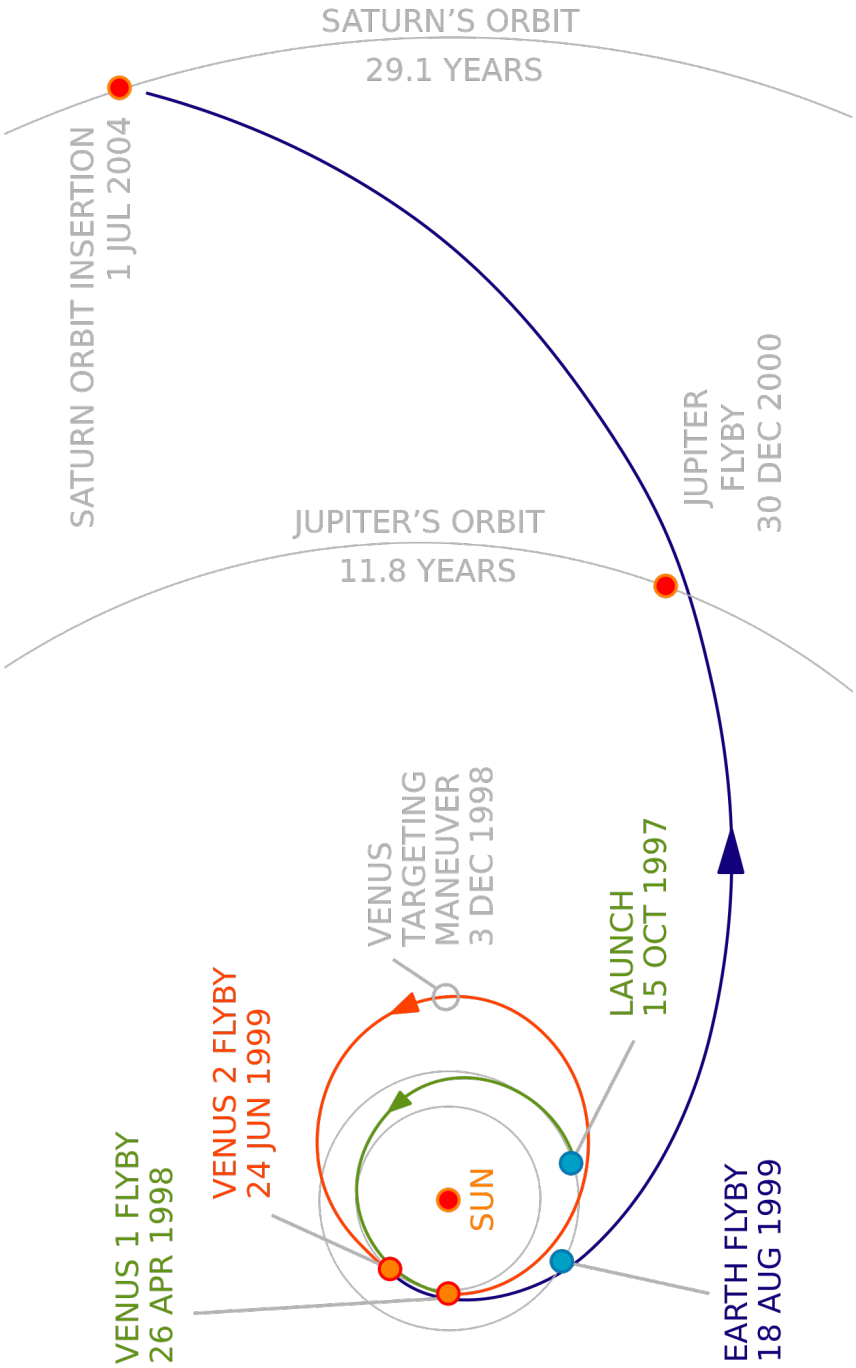

Figure 2.6: Cassini-VVEJGA Interplanetary Trajectory to Saturn [28].

2.3.1.2 Solar Electric Propulsion Systems

Solar Electric Propulsion (SEP) comprises three types of design approaches to achieve high exhaust velocities in order to reduce the total propellant required for the mission. The design approaches can be classified as: electrothermal propulsion where the propellant is electrically heated and then ejected through the nozzle; electrostatic propulsion in which the ionized gas is accelerated through an electric field; and finally electromagnetic propulsion wherein the ionized gas is accelerated using simultaneous application of electric and magnetic forces [29].

The propellant ejected in the SEP systems is upto twenty times faster than a conventional chemical propulsion system thereby reducing the overall propellant mass requirement for a particular mission. SEP systems are however limited by the available electric power on-board the spacecraft which is generated by the spacecraft's solar panels. The power generated by the spacecraft's solar panels is inversely proportional to the square of the distance between the spacecraft and the Sun. Figure 2.7 shows the solar irradiance vs the distance from the Sun. SEP system can be provided sufficient electrical power for missions to the inner solar system however, due to very low solar irradiance in the outer solar system the overall mass and volume requirement for spacecraft's solar arrays will be prohibitively large therefore missions to the outer solar system using electric propulsion would generally require nuclear power sources [30].

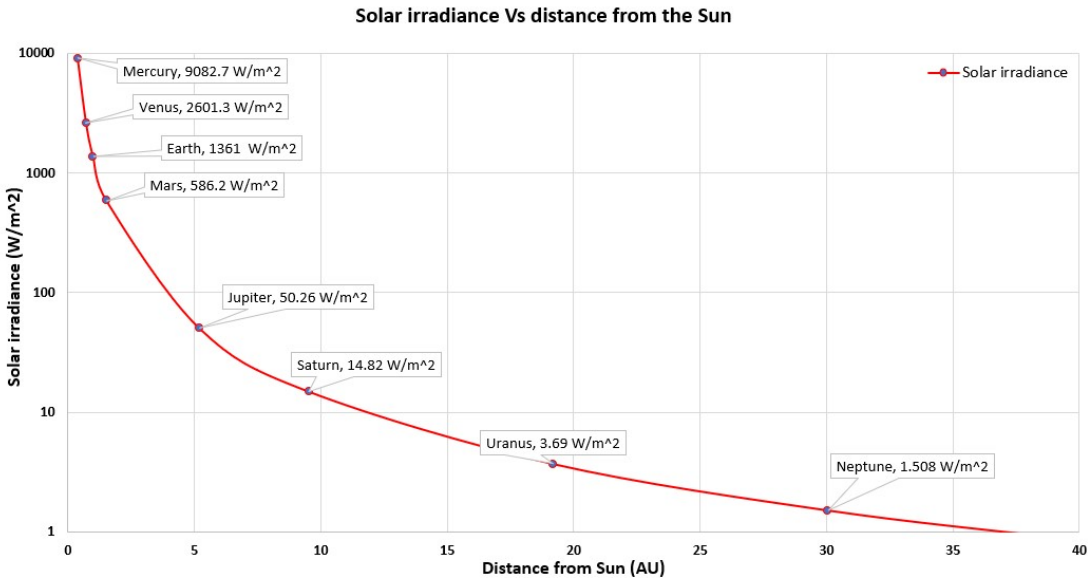

Figure 2.7: Solar irradiance Vs distance.

2.3.2 Nuclear Thermal Propulsion for Outer Solar System Exploration

Nuclear Thermal Propulsion is an ideal alternative for both Chemical and Solar Electric Propulsion systems due to its high thrust capability when compared with SEP systems and high specific impulse capabilities when compared with Chemical propulsion systems. This distinct capability offers missions with high acceleration in a short operating period than the other higher efficient SEP alternatives thereby resulting missions with short trip times. The higher specific impulse with almost twice as efficient when compared with the highest performing LOX/LH2 chemical propulsion systems allows higher payload delivery capability with similar Initial Mass in Low Earth Orbit (IMLEO).

The importance of effective exhaust velocity in terms of payload fraction vs ΔV can be demonstrated using the figure 2.8. With the increase in effective exhaust velocity the payload delivery increases exponentially as the ΔV requirement for the mission increases.

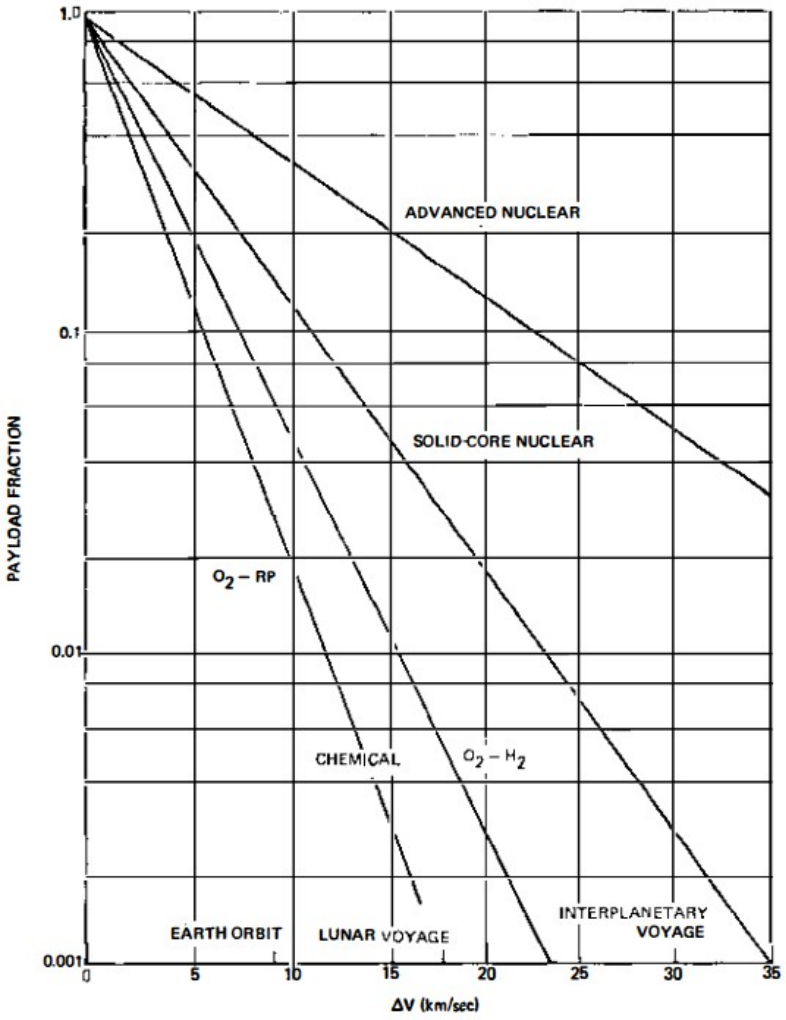

Figure 2.8: Propulsion system performance for Chemical, Solid-Core Nuclear and Advanced Nuclear powered missions [31].

The IMLEO as a function of mission ΔV for chemical and nuclear thermal propulsion systems as a single in-space vehicle is shown in figure 2.9 [32] which elucidates that the practical limit of a chemical propulsion system for a 0.5mT payload delivery is projected to be ∼10 km/s and ∼22 km/s for nuclear thermal propulsion. Figure 2.9 also shows the enhanced capability of NTP for direct transfer outer planet missions to Jupiter, Saturn and Pluto.

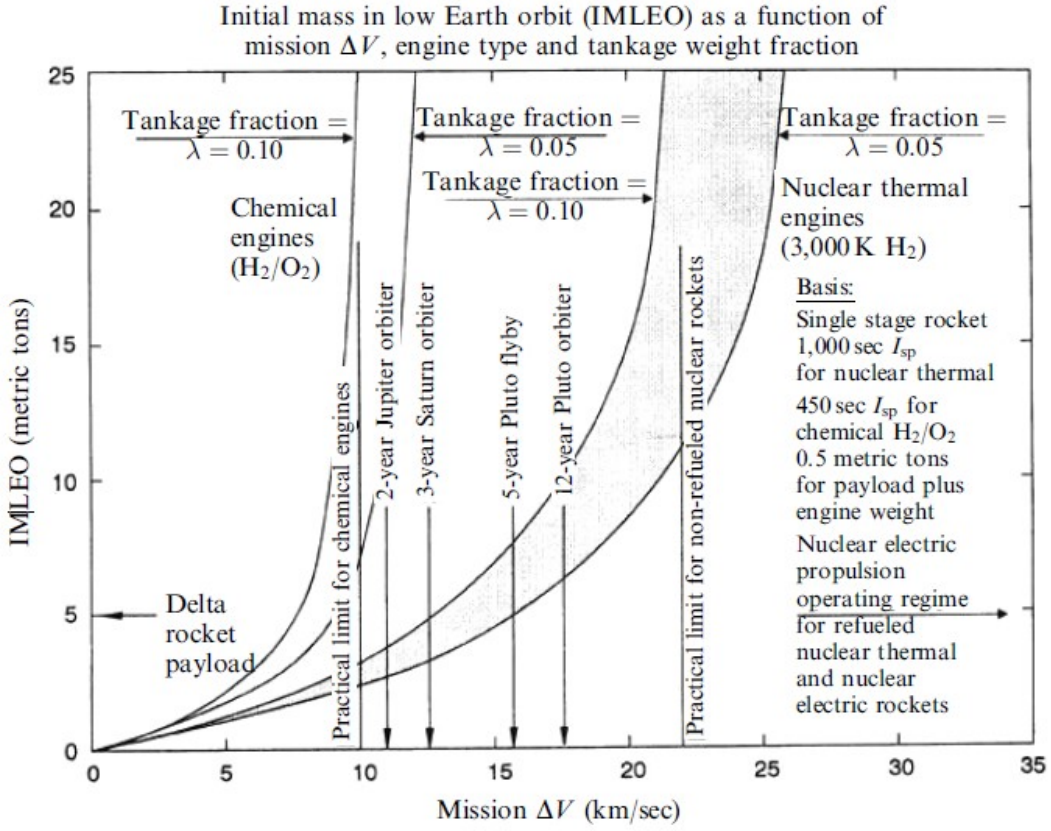

Figure 2.9: IMLEO as a function of mission ΔV [32].

Numerous mission concept studies have been conducted on NTP technology to Moon and Mars which have mostly concentrated towards enabling human

missions [33, 34, 35, 36, 37]. While there have been limited studies demonstrating the capabilities of NTP systems for science/robotic missions to outer planets and beyond, general trends on reduced trip times and enhanced payload delivery are applicable to missions beyond the distances of Mars. The majority of mission studies on NTP systems for outer planets have examined missions such as gas giant rendezvous, Europa sample return, Pluto orbiter and sample return, direct mission to Uranus and Neptune [38, 39, 40, 41, 42, 43]. Major studies to the gas giant systems using nuclear propulsion are mentioned in the table 2.3 which includes rendezvous missions to Jupiter, Saturn, Titan and Europa sample return. Most of the studies are based on smaller high performance bi-modal MITEE (MInature ReacTor EnginE) concept which is based on Particle Bed Reactor (PBR) technology [38]. The studies have focused on bi-modal nuclear propulsion system due to its ability to produce high thrust to escape out of planetary gravity well and achieve high ΔV for outer planet missions. Another advantage of MITEE is its low engine mass ($\sim$350kg) and therefore the spacecraft can be launched using medium lift launch vehicles. The Jupiter, Saturn orbiter and Europa sample return mission are studied using MITEE engine concepts. Due to the lightweight propulsion system and its bi-modal design, the ΔV capability of the system is much more than an NTP module used only for spacecraft injection. The Titan orbiter and lander mission is studied using regular NTP system where NTP injection stage is dropped after Earth escape maneuver and spacecraft is captured around Titan using aerocapture technique [44].

Table 2.3: NTP powered missions to the gas giant systems [38, 41, 43].

Mission	**Reactor Power (MW)**	**Engine Thrust (N)**	**Specific impulse (s)**	**IMLEO (kg)**	**Payload (kg)**	**Trip time (years)**
Titan orbiter lander	75	27,000	980	8,491	1,110	6.4
Europa sample return	75	14,268	1,000	3,350	470*	Earth - Europa: 02; Europa - Earth: 3.3
Jupiter Orbiter	75	14,000	1,000	3,395	600	02
Saturn orbiter	75	14,000	1,000	4,173	600	03
Saturn orbiter	340	66,723	960	20,000	341	2.3

*Payload includes lander, autonomous submarine vehicle, sample return tank and aeroshield.

Mission studies to ice giants, Pluto and near helio-pause region are mentioned in table 2.4. The studies to Neptune, Uranus orbiter and Pluto flyby missions were performed using expendable mode NTP system. The mission to Neptune was studied using solid core nuclear fission reactor design [21]. The goal was to determine the NTP performance towards delivering 1500 kg payload to Neptune orbit. The mission to Uranus was studied using LEU NTP engine system design and utilizing SLS Block 2 launch vehicle to deliver the spacecraft in LEO parking orbit [45]. Due to the enhanced performance of the launch vehicle and high thrust NTP system, a payload of about 3000 kg can be inserted into Uranus orbit. The Pluto flyby mission is studied using a small NTP engine design and utilizing Titan IV heavy lift launch vehicle [46]. The study also investigated mission capability using lightweight tankage/ structural materials such as graphite/epoxy and aluminum-lithium in place of traditional aluminum alloys. The Pluto system orbiter lander mission was studied using bi-modal SNTP system [47]. The SNTP system is designed using compact PBR and is highly efficient than competing systems. Figure 2.10 below illustrates the propulsion system along with the Closed Brayton Cycle (CBC) power conversion subsystem. The study on mission to near helio-pause region at about 100AU using NTP system utilizes upgraded 75 MW MITEE engine which has a total mass of about 200 kg and specific impulse of 1000s [32].

Table 2.4: NTP Powered Mission concepts to the Ice Giants, Pluto and near helio-pause region [32, 39, 45].

Mission	**Reactor Power (MW)**	**Engine Thrust (N)**	**Specific impulse (s)**	**IMLEO (kg)**	**Payload (kg)**	**Trip time (years)**
Neptune orbiter	300	72,600	860	50,000	1,500	09
Uranus orbiter	550	111,205	894	34,000	3,000	12.5
Pluto flyby	340	66,723	960	20,000	508	9.15
Pluto orbiter	75	14,000	1,000	3,985	200	13
Pluto system orbiter lander	400	73,000	900	21,500	2894	11.5
100AU fast flyby	75	14,000	1,000	8,100	200	12

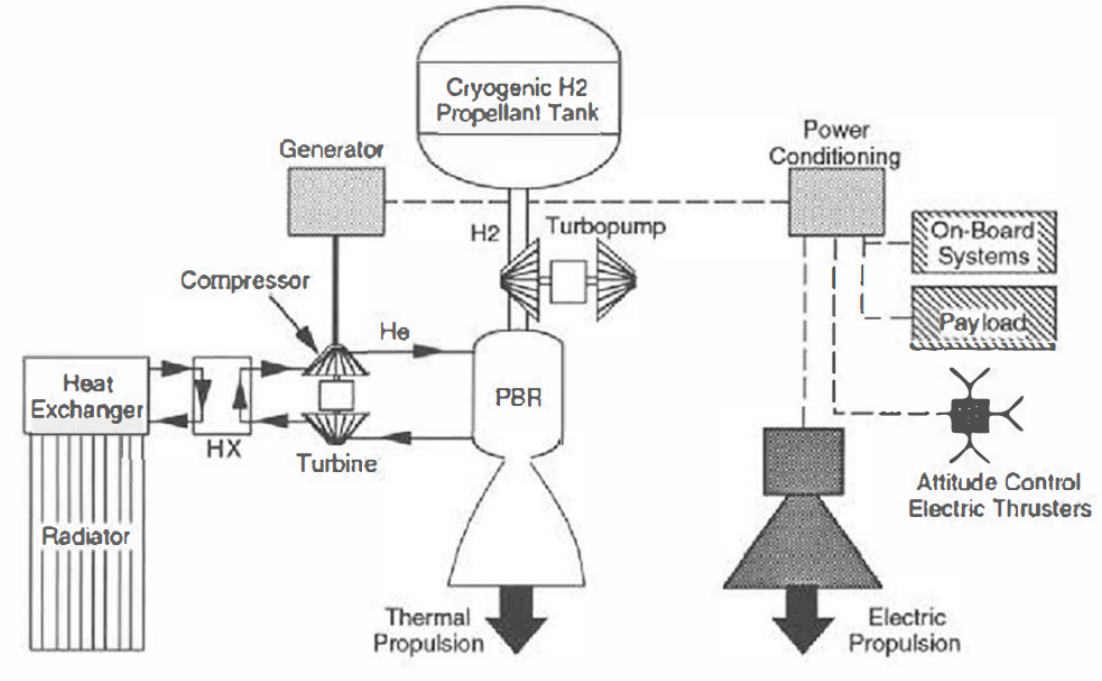

Figure 2.10: Schematic of bi-modal SNTP system and power conversion subsystem [47].

2.3.2.1 Gap identification #1

High fidelity mission concepts for an NTP system is clearly an important study required to accurately determine the capability of the propulsion system and compare its performance with the traditional propulsion systems. In the literature, it is observed that the majority of NTP performance parameters have been identified depending upon the mission constraints for a human mission to Mars. NTP powered cargo and crewed Mars mission systems analysis has shown the TMI requirements for a conjunction class mission to be at 155 mT and 293 mT respectively [48]. To enable the mission, the NTP engine requirements were

derived based on the engine burn duration, total number of burns for round-trip mission and total thrust range. The nominal burn duration requirement was set at 60 minutes along with 10 burns needed for the mission. This requirement then determined that the total engine thrust range during TMI and TEI to be at 240-350 klbf. Based on the mission analysis NTP engine sensitivity trades, NTP engine of 75 klbf nominal thrust is recommended to be used in the clusters of 3-4 engines [49, 50]. Studies have also analyzed crewed missions to Mars for different aggregate orbits and engine-out scenarios. Recent studies for a 2033 Mars mission have determined that based on the crew vehicle stack gross mass of 150 mT - 290 mT will require 15 klbf - 25 klbf thrust per engine with total number of engine in the cluster of 2, 3 and 4 [51].

The values of the performance of an NTP engine for robotic missions have not been determined. The studies focusing on the robotic missions using NTP are also not aligned with the NASA's planetary science missions program such as the delivered payload does not meets the traditional requirements for flagship or NF class missions. The IMLEO parameters also at times exceed the available launch vehicle capabilities. The studies also lacked details on the maneuver analysis for the selected NTP engine parameters and ignored the impact of ΔV losses during the engine run duration. For accurate performance determination of the NTP for robotic missions, it is needed to perform end-to-end high-fidelity integrated mission analysis starting from determining the launch vehicles mass and volume capability to place the spacecraft in the parking orbit, NTP engine finite burn analysis and the impact on total ΔV due to gravity losses etc. Therefore,

the task is to perform pre-phase A level mission concept which can demonstrate the NTP's game changing capability towards the exploration of outer solar system. This establishes the Research Question #1, *"What is the potential difference in performance parameters for NTP systems in comparison to traditional propulsion systems towards enabling ambitious missions to the outer solar system exploration?"*

2.4 Planetary Mission Architectures

The architecture design is not defined for a single mission or its requirements but a large trade space by evaluating alternative mission concepts. Planetary missions architectures involves multiple elements such as spacecraft design, launch vehicle and its capability to place the spacecraft in the parking orbit, propulsion element for trans-planetary injection and planetary capture maneuvers for rendezvous and round-trip missions. This section will describe the mission architectures for planetary science missions to the outer solar system using traditional propulsion systems and review of mission concept studies using NTP systems.

2.4.1 Mission Architectures for Traditional Propulsion Systems

Mission design for the medium and large class robotic missions to the outer solar system often use multiple planetary gravity assists in order to achieve the required C_3 energy due to the limitations of the traditional propulsion systems. The spacecraft is injected by the launch vehicle in the low Earth orbit and post this

an upper stage kick motor provides the required C_3 energy to the spacecraft's next encounter with the planetary body for gravity assist. Depending on the mission, multiple gravity assist maneuvers may be required to accelerate the spacecraft and gain velocity to reach the targeted planetary body. Table 2.5 shows the mission timeline of Cassini interplanetary trajectory which is typical for chemical powered missions. The required gravity assists are dependent on the orbital alignments of multiple planetary bodies which limits the launch windows and launching the spacecraft beyond the optimum date dramatically increases the required launch energy per unit mass in order to reduce the post launch ΔV from spacecraft's onboard propulsion systems.

Post trans-planetary injection maneuver, the Deep Space Maneuvers (DSM), Trajectory Correction Maneuver (TCM) and Plantary Orbit Insertion maneuvers are performed by the spacecraft's propulsion module subsystem which typically includes a bipropellant system with engine thrust ranging from 400 N to more than 1000 N.

Depending upon the science mission objectives and other constraints the mission design includes the trade-off of spacecraft mass vs trip time. New Horizons mission design to Pluto focused on shortening the trip by limiting the mass of the spacecraft. With spacecraft wet mass of 478 kg, the launch vehicle was able to inject the spacecraft in a direct ballistic flight from Earth to Pluto with Jupiter flyby [52]. The spacecraft was able to flyby Pluto in a record 9.5 year trip time after its launch.

Table 2.5: Cassini interplanetary trajectory mission events.

Mission Events	**Date**	**Comments**
Launch	October 15, 1997	$C_3 = 18.1\ km^2/s^2$
Venus 1 flyby	April 26, 1998	Altitude at periapsis = 284 km; velocity = 11.8 km/s
Deep Space Maneuver	December 03, 1998	Venus targeting maneuver; ΔV = 466 m/s
Venus 2 flyby	June 24, 1999	Altitude at periapsis = 623 km; velocity = 13.0 km/s
Earth flyby	August 18, 1999	Altitude at periapsis = 1,171 km; velocity = 19.1 km/s
Jupiter flyby	December 30, 2000	Altitude at periapsis = 137 Jupiter Radii; velocity = 11.5 km/s
Saturn Orbit Insertion	July 01, 2004	ΔV = 626 m/s

Although there has not been an SEP powered mission to the outer planets, multiple point design have been conducted to explore the initial architecture assessments. Mission studies to the Ice giant planets Uranus and Neptune using SEP have determined that the increased flight system mass due to the SEP system has detrimental impact on science payload mass and the overall trip times [53]. Figure 2.11 shows the mission design architecture for Ice giants using SEP

system. The designed interplanetary trajectory depends on a 25 kW SEP stage and uses multiple planetary flybys including to Venus, Earth and Jupiter. The spacecraft is designed to be launched using a commercial heavy lift launch vehicle and has a total time of flight of 11 years to Uranus and 13 years to Neptune.

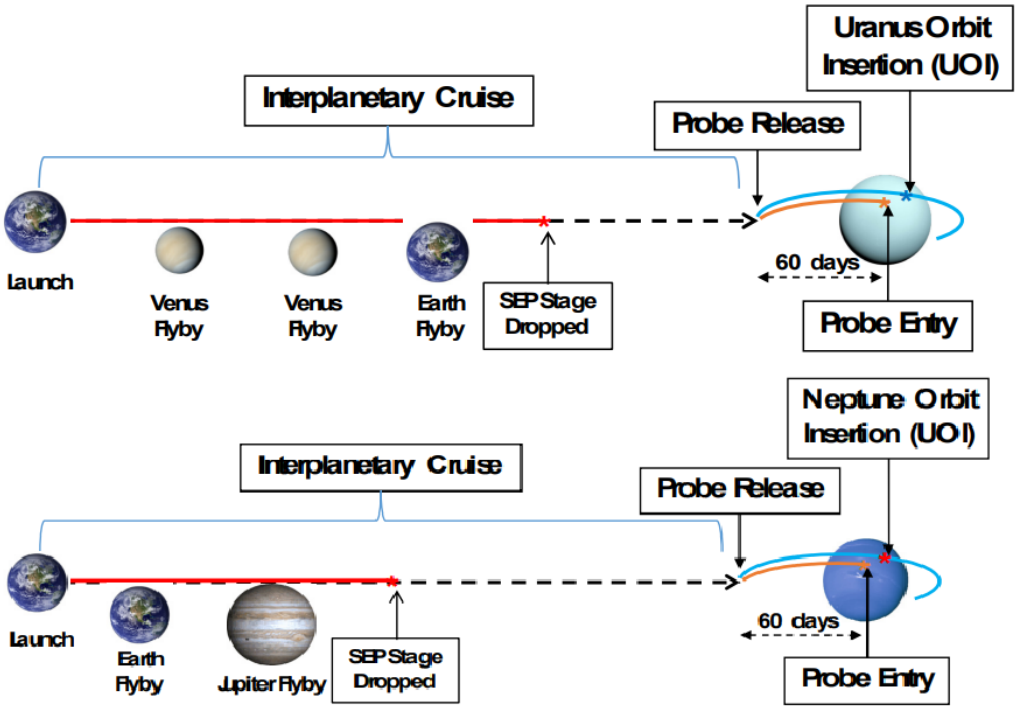

Figure 2.11: Mission design architectures for Ice Giants using SEP system [53].

2.4.2 Mission Architectures for NTP Systems

Mission concepts using NTP for robotic missions have implemented two architectures (1) NTP system utilization for only Earth escape maneuver which is also known as 'expendable mission mode' and uses chemical propulsion for planetary orbit insertion and (2) NTP system as the only propulsion system for

Earth escape and planetary orbit insertion [46, 54]. The expendable and non-expendable mission architectures used in the literature can be shown graphically using figure 2.13. Table 2.6 summarizes literature on NTP powered expendable and non-expendable architectures for rendezvous missions to Pluto. Both the concepts have been presented with their respective advantages such as in expendable mission mode the challenges of keeping propellant at cryogenic temperatures for long duration and reactor restart are eliminated. Due to the NTP use case for only single burn the thermal protection systems complexity is reduced because long term LH2 storage is not required. However, using the second option gives the NTP system advantage especially for bimodal concepts in which the NTP system can provide the electrical power to the spacecraft during cruise and science phases of the mission. Figure 2.12 describes the MITEE-B engine NTP and electrical power propulsion mode. The Minature Reactor Engine Bi-Modal (MITEE) concept study has analysed that the engine with 3.2 klbf thrust and 1000 s of I_{sp} can also generate power output of 1 KW(e) [55]. The one kilowatt of continuous electrical power can eliminate the need of RPS system thereby providing greater operational capability.

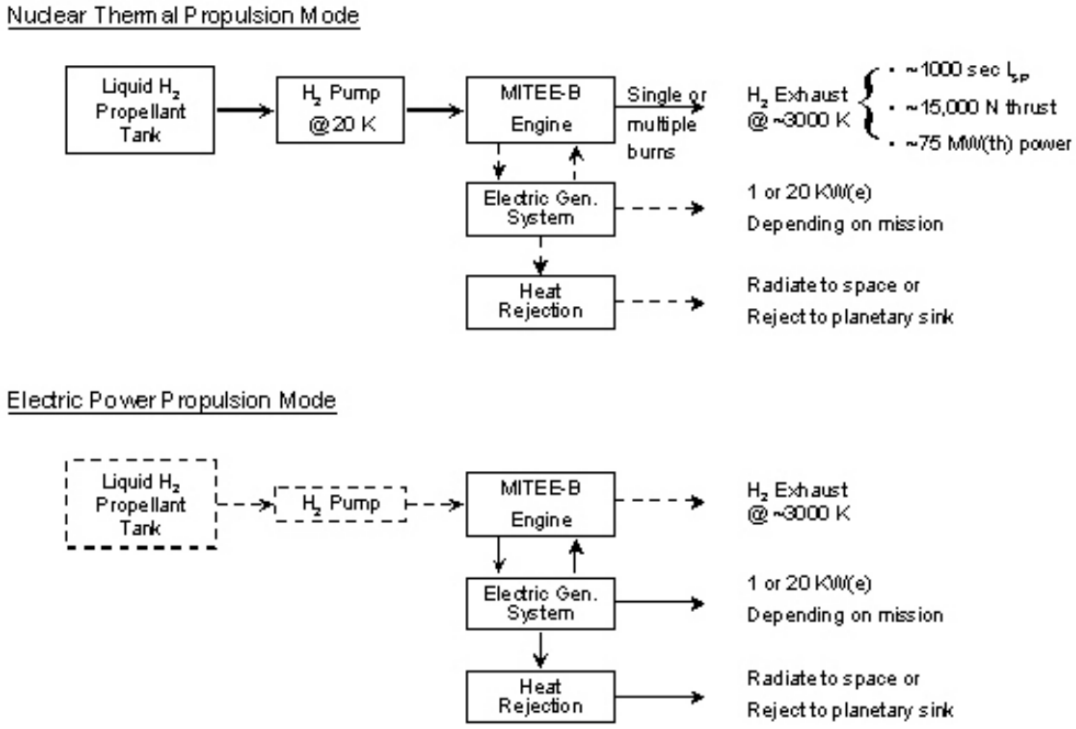

Figure 2.12: Bi-modal NTP engine operational modes [55].

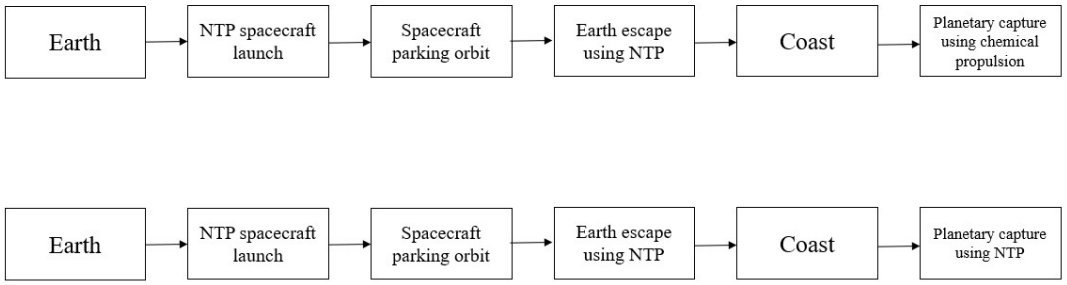

Figure 2.13: Mission architectures using NTP system for robotic missions.

Table 2.6: NTP powered mission architectures for Pluto rendezvous missions.

Mission	**IMLEO (mT)**	**Departure Orbit (LEO: 185x184km)**	**NTP System Thrust/I_{sp}**	ΔV **(km/s)**	**Trajectory**	**Trip time (years)**	**Payload (kg)**
Expendable	20	LEO	15klbf/960s	7.902	E-JGA-P	13	351
Non-expendable	12.5	LEO	3.1klbf/1000s	20.43	E-P direct	11	500
Expendable	20	LEO	10klbf/870s	7.59	E-JGA-P	16	491
Non-expendable	21.5	LEO	16.4klbf/900s	19.87	E-P direct	11.5	1410

2.4.2.1 Gap identification #2

The NTP powered robotic missions have used traditional architectures with LEO (180x180km) departures post separation from the launch vehicle. However, NTP mission architectures need to consider the failure scenarios during the engine run time in LEO. NTP fission reactor is essentially non-radioactive during the launch sequence and it is activated for high-power operation only in stable LEO parking orbit. Once, the high-power operation begins for trans-planetary injection maneuver, fission system radiological inventory steadily increases as fission products build up [56]. This challenge needs to be incorporated in mission architectures such that in case of any failure, the NTP system orbital lifetime is at least until fission products naturally convert back into non-radioactive isotopes. Figure 2.14 illustrates the radiation dose rate for different engine run time as a function of decay time for NERVA engine reactor [57]. For the 25 minute engine run duration of 1855 MW reactor the ionizing radiation levels decrease rapidly over the first 300 years due to the decay of the short lived isotopes. The shorter engine run duration have significantly lower radiation dose from the reactor in the initial years however, the dose rate close to 300 years is similar irrespective of the engine run duration.

Literature studies have explored the potential nuclear-safe parking orbits by determining the estimated orbital lifetime for parking orbits which do not significantly impact the launch vehicle Earth-to-Orbit payload capability [57, 58]. The studies have recommended parking orbits such as 148x800 km, 500 km circular and 800 km circular etc for intial operation of the NTP system. It also needs

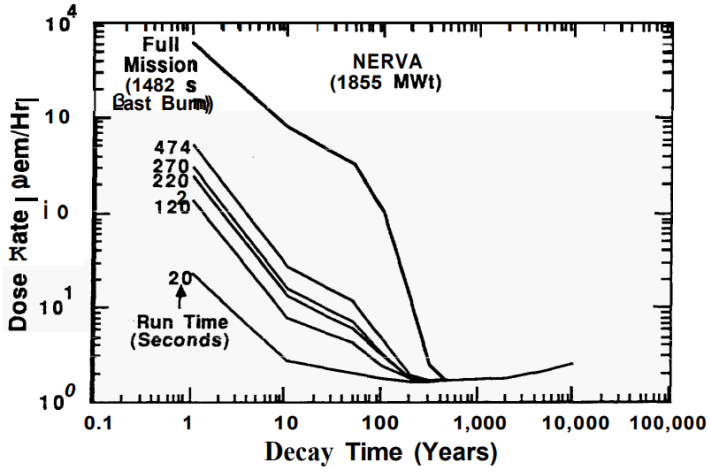

Figure 2.14: NERVA Radiation dose rate as a function of engine run time and decay time [57].

to be noted that these studies were conducted in 1980s and 1990s and since then there has been a dramatic changes in the on-orbit spacial density of spacecrafts and satellite fragmentations. Therefore, it is now required that the potential nuclear-safe orbit analysis to be updated by including spacial density of objects in LEO and HEO as a parameter. Figure 2.15 portrays the spacial density as a function of near Earth altitude upto 2000 km [59].

While the mission architectures for NTP have demonstrated the higher performance for non-expendable missions. There is no detailed analysis on the challenges of using NTP for planetary capture maneuvers with respect to the long term storage of LH2. The published mission concepts have been focused on specific individual analysis such as engine performance, launch vehicle capability and trajectory design, and no literature has integrated the mission phases and used their synthesis as a coupled tool to design more optimal mission architecture

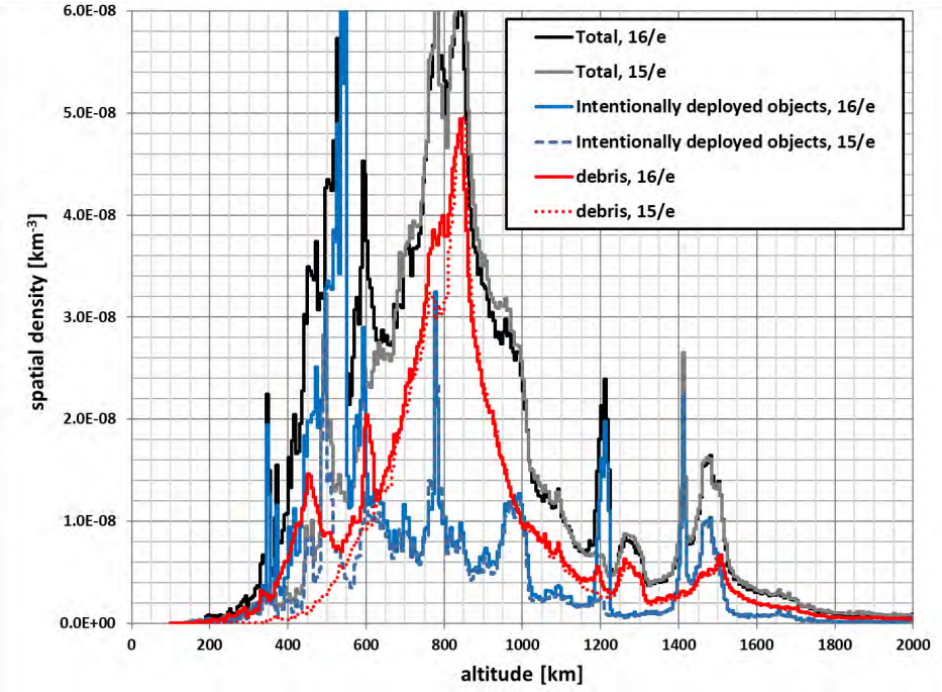

Figure 2.15: Spacial density of objects in near Earth altitude [59].

whose goals can be quantitatively defined. Therefore, the Research Question #2 can be identified as *"What is an enabling mission architecture for the robotic missions using NTP systems?"*

2.5 NTP Engine - How Small Is Big Enough

2.5.1 NTP Engine Development

The NTP development program started with the Project Rover in 1955 and is currently in progress under the NASA's Space Nuclear Propulsion (SNP) program. The Project Rover was stated by the Air Force with intention to use the propulsion system in the Intercontinental Ballistic Missiles (ICBM), later the

project was transferred to NASA in 1958 when NASA explored the NTP use case towards upper stages for Saturn V and later in-space propulsion for missions to Mars. Since, then the majority of NTPs development has been by keeping its use case for future human missions to Mars [60, 61]. Therefore, the NTP engine performance objectives have been selected towards enabling human missions to Mars. The selected optimum thrust, I_{sp} and chamber pressure parameters for an 'all-up' mission to Mars were 50,000 lbf - 125,000 lbf, 925 seconds and 500 psia - 1000 psia respectively [62]. Later, during the SNTP program NTP systems engineering studies were performed for lunar/Mars transportation system to allow an early test and application of NTP transportation system [63]. The critical technical performance objectives required for enabling lunar/Mars missions are mentioned in table 2.7.

Table 2.7: Critical technical performance objectives for Lunar/Mars transportation [64].

Parameters	**Objectives**
Thrust	25 klbf to 75 klbf
I_{sp}	$>$ 875 s
Thrust/Weight	$>$3
Engine life	$>$ 270 minutes at rated thrust
Restart capability	Multiple ($>$10)
Single burn duration	60 minutes (max.)

In 2009, NASA's Design reference architecture 5.0 for human missions to Mars described the system and operations that would be used for the first three missions to explore the surface of Mars by humans [2]. NTP was preferred transportation technology for both crew and cargo vehicles for long surface stay mission with core propulsion stage requiring three 25-klbf engines to be used to perform primary mission maneuvers. Recent studies have explored the Mars opposition mission using High-Assay Low Enriched Uranium (HALEU) NTP engine systems and have demonstrated that engine trades for Mars architecture also require a three NTP engine system of each with 25-klbf thrust [48]. Figure 2.16 shows the LEU NTP Mars Crew Vehicle Point of Departure Configuration using 25-klbf engine systems [65].

2.5.2 NTP Engine for Robotic Missions

With the focus of NTP for human missions to Mars, the NTP engine design has been towards larger engine class with thrust range of 25 klbf - 125 klbf for LEO aggregation orbit and 15klbf - 25 klbf for Lunar Distant Highly Elliptical Orbit (LDHEO) aggregation orbit. On the other hand, smaller class engines can enable robotic missions and can also meet the requirements of host of missions such as technology demonstrator and for cislunar operations. The development and operation of a smaller class engine can also provide experience with flight hardware that can be incorporated towards the development of larger thrust class engines for human missions to Mars.

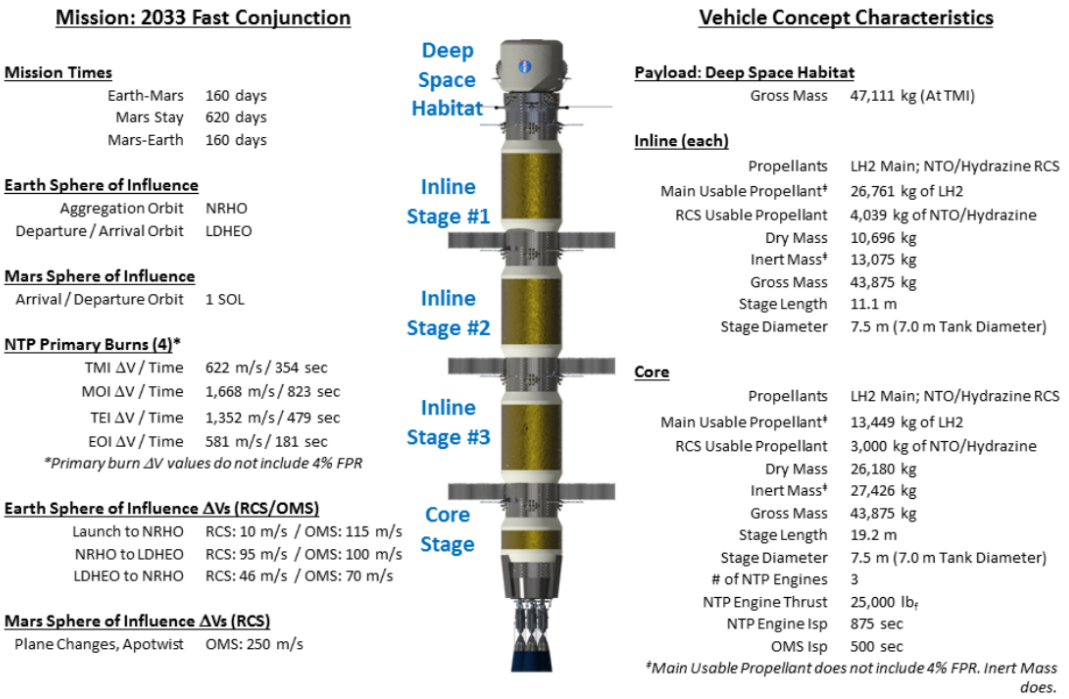

Figure 2.16: LEU NTP Mars crew vehicle point of departure configuration [65].

Mission concept studies for planetary robotic missions have considered wide range of engine thrust class. Small reactor engine with reactor power of 75 MW with thrust output of 3200 lbf has been analyzed for fly-by and rendezvous mission to Pluto and sample return from Europa [54]. Zubrin *et al.* in 1992 proposed a 10 klbf thrust class NTP engine with I_{sp} ranging from 850 s - 900 s for missions to Ice giants albeit with orbiter mass requirements not meeting with current planetary science missions program [66]. Studies have also looked at using 15 klbf and 16.5 klbf engine class for host of missions to the outer planets using both thrust only and bi-modal concepts [46, 47]. Finally, there has also been a study on the use of 25 klbf engine for missions to Jupiter and Uranus [67]. Figure

2.16 shows the schematic of NTP one-pass moderator block and fuel element of a 25 klbf engine [68].

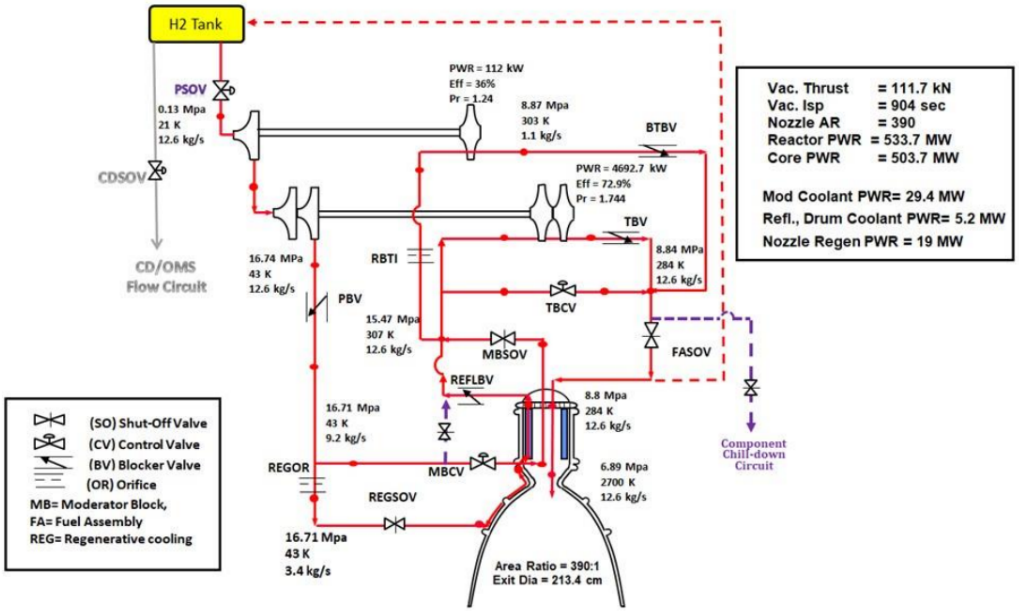

Figure 2.17: Schematic of NTP one-pass moderator block and fuel element of 25 klbf engine [68].

2.5.2.1 Gap identification #3

With majority of the NTP engine design and performance evaluation focused towards human mission to Mars there has been little focus on engine performance requirement for planetary robotic missions. The studies on NTP powered missions for robotic exploration have considered arbitrary engine parameters starting from 3.2 klbf to 25 klbf of thrust level and I_{sp} range from 850 to 1000 s. Therefore, it is needed to perform a trade space exploration of the NTP engine parameters for the selected Design Reference Missions (DRM) in order to deter-

mine the solution space of NTP system for missions to the outer solar system exploration.

Literature review also determined that the mission analysis did not include the engine performance during the maneuvers and used impulsive burn analysis. For accurate results, it is critical to perform finite maneuver analysis in order to understand the total engine run time limits, ΔV losses and its impact on the overall system design. Therefore, based on the knowledge gap identified in this section the Research Question #3 can be established as *"What is the enabling engine thrust class for targeted robotic missions?"*

2.6 Chapter Summary

The three gaps identified in this chapter after the detailed literature review led to the research questions which are summarized below:

First, point design studies for NTP system are needed for the potential planetary missions in the outer solar system to determine the difference in performance parameters of NTP in comparison to traditional propulsion systems. This will require the development of a systems engineering model which will be driven by the MBSE framework. The model and the MBSE framework has been described in the Chapter 3.

Second, mission architectures used by the traditional propulsion systems will not be applicable for the NTP systems. Therefore, the enabling mission architectures for the NTP systems will have to be determined by evaluating multiple mission scenarios. The technical feasibility of these architectures will be deter-

mined by the output metrics such as mission sensitivity for different departure and arrival scenarios, NTP system performance and trip-times etc.

Third, there is lack of understanding on the best NTP engine performance parameters for mission focusing robotic exploration. This requires a detailed trade space exploration for the selected DRMs in order to determine the solution space of enabling NTP engine parameters for robotic missions to the outer solar system. The analysis to answer this question will include finite maneuver analysis, ΔV loss determination and engine run time evaluation etc.

Research Question #1 *What is the potential difference in performance parameters for NTP systems in comparison to traditional propulsion systems towards enabling ambitious missions to the outer solar system exploration?*

Research Question #2

What is an enabling mission architecture for the robotic missions using NTP systems?

Research Question #3

What is the enabling engine thrust class for targeted robotic missions?

Chapter 3. Approach and Methodology

With the identification of research questions pertaining the use of NTP for robotic mission, this chapter will describe the approach and methodology for the selected DRMs in order to fill the knowledge gaps. For this purpose, a Spacecraft Integrated System Model (SISM) is developed using model-based approach. The SISM results are then used to perform the trade space of the mission architectures and compare the NTP engine performance which are driven by both technology and space mission architecture constraints.

3.1 Overall Approach

The overall model integration and execution approach between the tightly-coupled domain engineering analysis models and systems engineering architecture model is shown graphically in Figure 3.1. The model will take mission requirements and technology constraints as input and generates outputs as NTP system performance for each architecture evaluation for the mission classified. The overall model described iterates over the engineering analysis model and the systems engineering architectural model such that it (a) determines the feasibility of mission architecture and engine trade space via systems engineering model and (b)

evaluates the NTP system performance metrics for each conceptual mission which is driven by the analytical models from each domain.

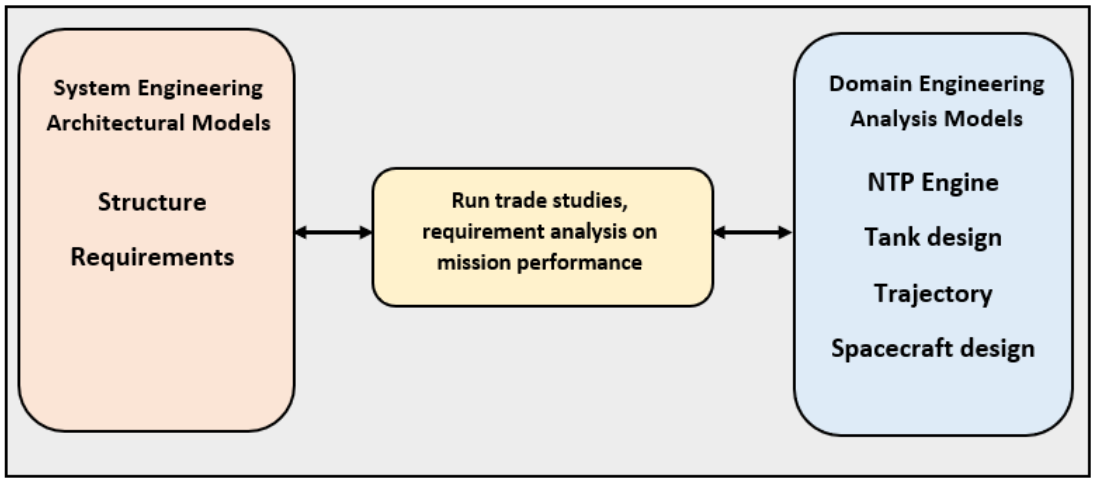

Figure 3.1: Overall model integration and execution approach for Spacecraft Integrated System Model (SISM).

The model's utility is to determine the NTP engine parameters that enable robotic missions by maximizing the spacecraft dry mass delivery and minimizes the IMLEO. Domain engineering analytical models will be used to answer the Research Question #1 by performing point design studies and comparing the performance with traditional propulsion systems. Research Questions #2 and #3 will be answered using systems engineering model as described in detail in Section 3.2. The development of SISM was divided into three phases as shown in Figure 3.2, the phase I involved the development of the Model Based Systems Engineering (MBSE) framework and performed mission analysis using standalone simulation models. The phase II of the model development involved integration of domain engineering analysis models with the systems engineering architectural model.

Lastly, the phase III of the model development involved requirement analysis and trade space exploration of the the NTP mission architectures.

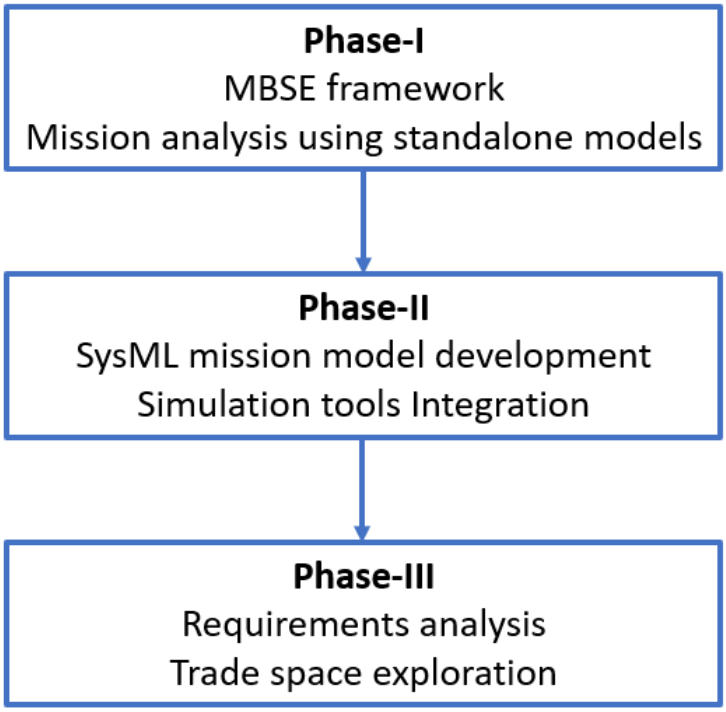

Figure 3.2: SISM Development phases [69].

3.2 Systems Engineering Model

This section describes the systems engineering model which is driven by the MBSE framework. The use of MBSE approach allows the modules to be customized or replaced depending on the mission requirements. Figure 3.3 describes the systems engineering model which contains modules with information on input and output parameters. A high-fidelity mission design requires analysis in multiple domains such as detailed calculations on IMLEO, launch vehicle

performance, trajectory analysis etc. which are performed on different engineering analysis tools. Because this exercise is multidisciplinary in nature, the issues arising during the design of one system do not exist in isolation, but feed upon other systems as well. This problem is solved iteratively until multiple cross dependent parameters are satisfied. Therefore, the utilization of model-based approach becomes critical in this scenario towards performing rapid mission analysis for different architectures including multiple engine thrust class for trade space exploration.

Physics based models have traditionally been used to perform analysis for in-space transportation system over the decades to validate system level designs. However, one of the mission design problem which needs to be addressed is integrating dependencies of individual state-of-the-art analytical models with the systems engineering models. Due to the technical constraints involving multiple systems for a high precision interplanetary mission requirements, there is a need to model a systems engineering environment to integrate analytical models for a single source of truth across all modules. The conceptual in-space transportation system design process consists of a variety of disciplines making up a system level design problem. The process during the conceptual phase includes the following [70]:

- Specification of requirements based on mission classification.
- Design of in-space propulsion system.

- End-to-end mission trajectory calculation based on the designed propulsion system.
- Estimation of mass and dimensions of the propulsion system and spacecraft.
- Feedback from the results from the analytical models for optimization and modification of the overall system to meet mission requirements.

The development of systems engineering model in this document is inspired by the Harmony integrated systems and software development process [71]. The Harmony process is similar to the "Vee" lifestyle development model which includes subsets as Harmony-SE and Harmony-SWE [72]. The Harmony-SE consists of the system architecture baseline description which includes requirement analysis and system analysis and design. The Harmony-SWE consists software implementation, module integration and system acceptance process. For the scope of this thesis, systems architecture baseline processes have been included which includes process elements as requirement analysis and architectural design using the developed structure modules.

As seen in Figure 3.3, the systems engineering model consists of modules as a design structure matrix or an N2 diagram. These modules are mission classification, spacecraft, NTP system, launch vehicle and cost. The vertical arrows are represented as inputs and the horizontal arrows represent outputs. The mission classification is the first module which provides the initial input parameters. The module specifies the mission type such as discovery, new frontiers or flagship class planetary science mission. Depending upon the mission type and

science objectives derived from the planetary science and astrobiology decadal survey the mission classification module also defines if the robotic mission will be a flyby, rendezvous or a round-trip mission. The output from the mission classification module is then used in the form of mission requirements to the modules mentioned in the waterfall sequence. The spacecraft module determines the spacecraft specifications such as dimensions, dry mass and the onboard chemical propellant requirements depending upon the ΔV requirements for the selected architecture. These parameters are approximated based on the historical trend for the spacecraft development under the NASA's planetary science division as discussed in the section 2.1.1. In general, referring to the data set from the Figure 2.2 spacecraft dry mass of over 2.5 mT for gas giant missions and 1.5 mT for ice giant mission can be categorized under the flagship class missions and spacecraft dry mass of about 2 mT and 1 mT for gas giant and ice giant rendezvous missions respectively can be categorized under the new frontiers class mission.

The design of NTP system consists of the engine system and propellant tank specifications. The module requirements are derived from the outputs of the mission classification and spacecraft modules. The details of NTP system analytical model is discussed in section 3.4. The launch vehicle module ensures that the overall NTP system and spacecraft mass and its dimensions are within the requirements of the available launch vehicles. Finally, the last module of the systems engineering model is cost estimation. In the document, the mission cost is determined as a function of spacecraft dry mass plus the launch vehicle cost. Considering the NTP system is currently in the development phase, the

cost estimate of the propulsion system is beyond the scope of this thesis. Due to the cost cap requirements the planetary science missions to the outer planets are designed for the new frontiers and the flagship class mission and only commercial launch vehicles such as SpaceX Falcon Heavy, United Launch Alliance (ULA) Vulcan Heavy and Blue Origin New Glenn are considered for the mission analysis. The technical feasibility of the final architecture is determined based on the output metrics defined which are mission sensitivity for departure orbit, NTP system performance, IMLEO, trip-time and cost.

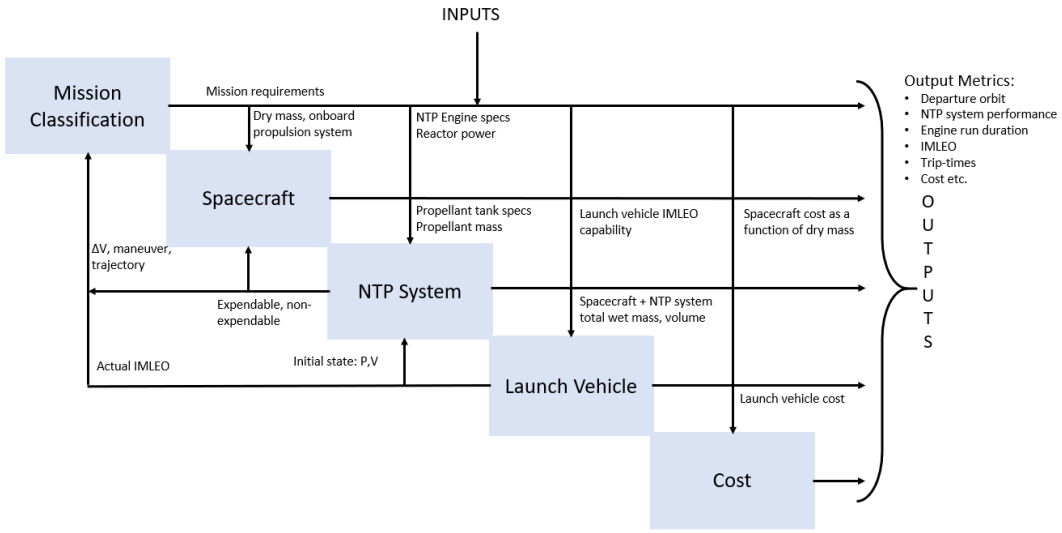

Figure 3.3: Systems Engineering model described as an N2 diagram which includes modules that drive the robotic mission formulation.

3.2.1 Systems Engineering Structure and Requirements Model

An architectural framework of the systems engineering model is developed to describe the cohesive set of elements, properties and constraints of the system.

Each element properties and constraints are connected via a single repository of the structure model in order to have a single source of truth to evaluate the overall mission architecture. This approach also allows for rapid changes in the architecture which is a typical need during the early phase of the mission formulation. Figure 3.4 shows the structure model consisting of architecture elements for mission formulation phase using the NTP system. The information contained in the elements of the structure model are assigned with the relationship to the overall mission model. The parent elements of the structure model includes the description of the propulsion system, mission types, targeted planetary body and mission enterprise details such as spacecraft specifications, trajectory details and launch vehicle constraints. Accordingly, the child elements include propulsion system parameters such as engine performance, propellant requirement and tank constraints for targeted mission using expendable or non-expendable configurations. The described framework makes it easy to add elements depending on the mission profile to evaluate multiple architectures.

The description of mission requirements diagram for robotic rendezvous mission can be seen in Figure 3.5. The mission design requirements are divided into functional, performance and physical requirements. The functional and performance requirements include NTP engine and reactor requirements through which the total engine run time and maximum propellant requirements are derived. The ΔV and propellant requirements are derived using the initial patched conic analysis calculations for a direct transfer trajectory. LEO parking orbit constraints are determined based on the minimum required altitude for the final-

end-of-life storage and beyond maximum internationally deployed objects and debris belt in LEO. The physical requirements are based on the spacecraft and NTP system configuration and commercial launch vehicle compatibility.

3.2.2 Integrated Modeling Environment

Once the role of MBSE application for the mission analysis was decided, the next step was to work on the current available MBSE capabilities to develop the system model. The first task involved capturing the top level system model description in Systems Modeling Language (SysML) Block Definition Diagram. Following the structure model development, the SysML requirements model is developed for each element of the structure defining capability or constraints that must be satisfied. The system modeling environment utilizes SysML/MagicDraw plugin from Dassault Systems to develop the descriptive models of the mission concepts. For analytical models, Matlab, Systems Tool Kit and Excel are used to perform the launch vehicle, NTP system performance and trajectory analysis as per the simulation settings and constraints. Figure 3.6 shows the complete cycle of the integrated modeling environment which begins with the requirements as defined according to the mission classification modules for each elements. The system descriptive model is then updated as per the preferred architecture for the robotic mission. The results from the launch vehicle and NTP system performance are then used to converge the spacecraft trajectory involving Earth departure phase, interplanetary transfer phase and planetary capture phase for the rendezvous mission. The results from the analytical models once the mission

has closed are then exported to the data explorer to perform trade space exploration to determine the optimum NTP engine parameters and architecture for the selected mission. The results are then exported via Ansys ModelCenter to update the descriptive model and for validation against the requirements defined in the SysML system model. The described modeling environment allows for a consistent design along with mitigation of any missing requirements. This approach also allows traceability of the elements in each module, allowing the user to view large information of subsystem parameters in a single model repository.

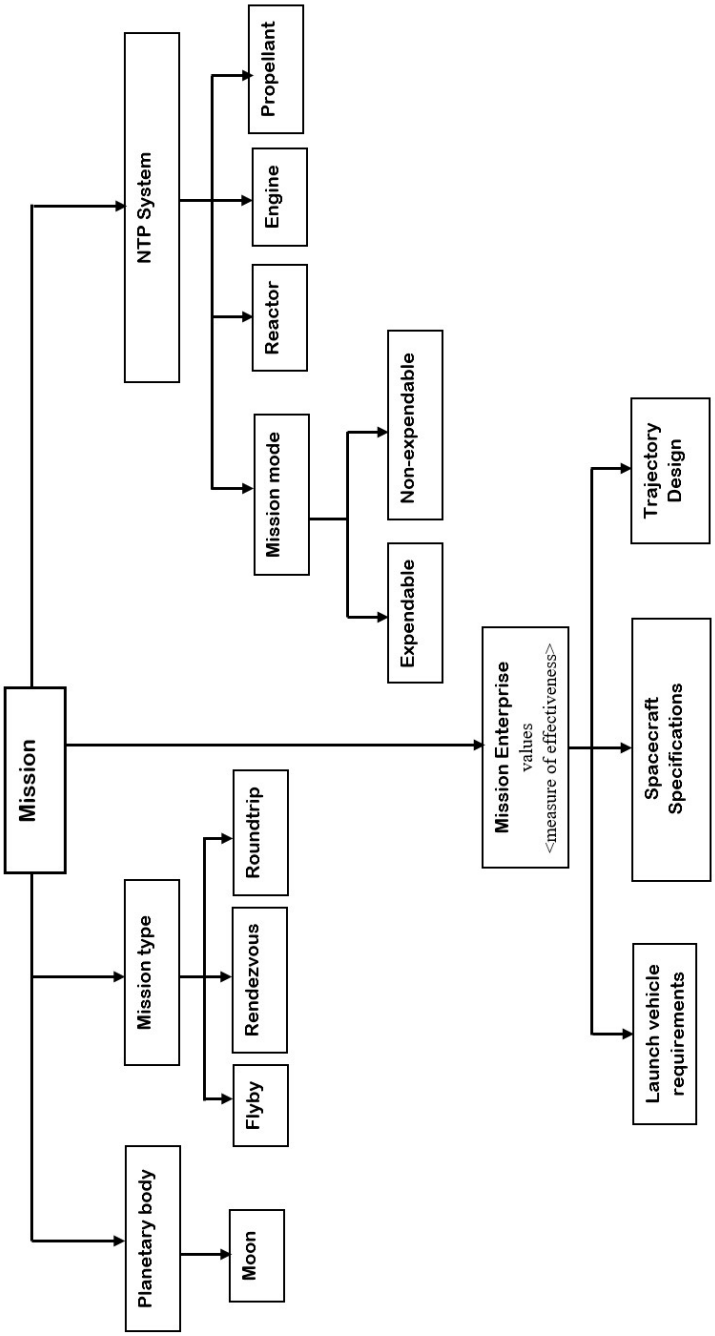

Figure 3.4: Elements of structure model for mission design framework [73].

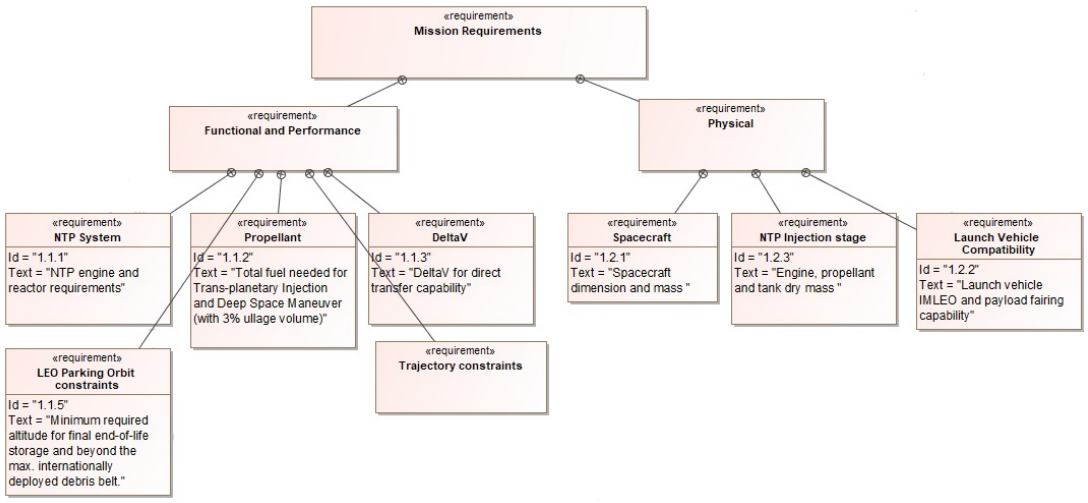

Figure 3.5: Mission requirements diagram for NTP powered rendezvous missions [74].

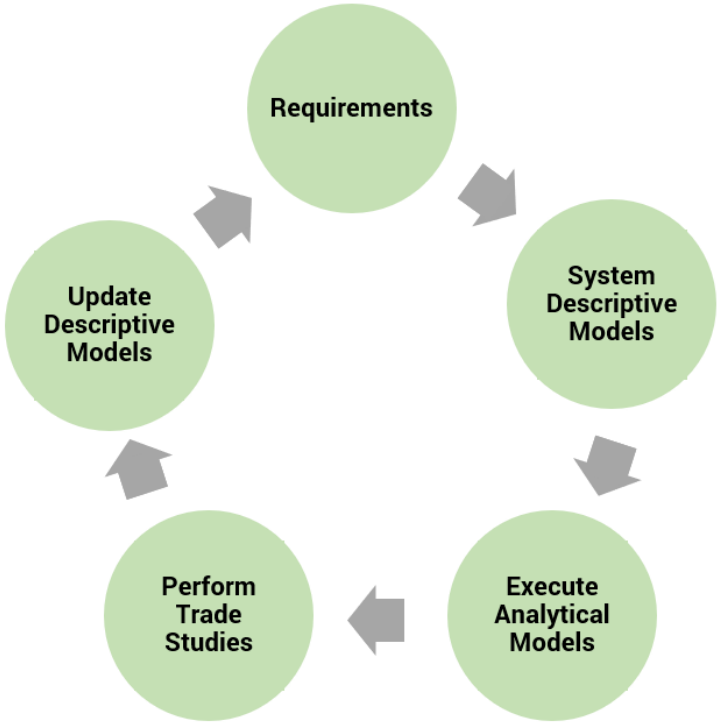

Figure 3.6: Integrated modeling environment.

3.3 NTP System Analytical Models

3.3.1 Engine Model

The NTP engine model developed by D.Nikitaev at the University of Alabama in Huntsville (UAH) has been used for the point design studies [75]. The engine model was developed in reference to the Aerojet Rocketdyne Power Balance Model (AR-PBM) 5.7 [76]. The AR-PBM 5.7 NTP engine uses ceramic fuel element and has reactor power of 330 MW with 15 klbf of thrust and 900 s of specific impulse. The UAH NTP 330 MW engine model was bench marked against the AR-PBM 5.7 and resulted with error margin of within 2% [77]. Figure 3.7 shows the detailed flow schematic of the AR-PBM 5.7 engine model in 22 steps starting with hydrogen release from the propellant tank to the exit from the nozzle. The engine performance including transient states (startup and shutdown) states for thrust, specific impulse and reactor power can be seen in figures 3.8. The details on engine startup and shutdown transient states are further described in the Appendix B.

For trade space exploration to determine the optimum engine performance with respect to thrust and specific impulse a constant thrust and specific impulse model was implemented. This was due to the fact that the use of engine transient states in the point design studies did not impact the mission performance parameters such as trip time, ΔV and engine run time duration significantly.

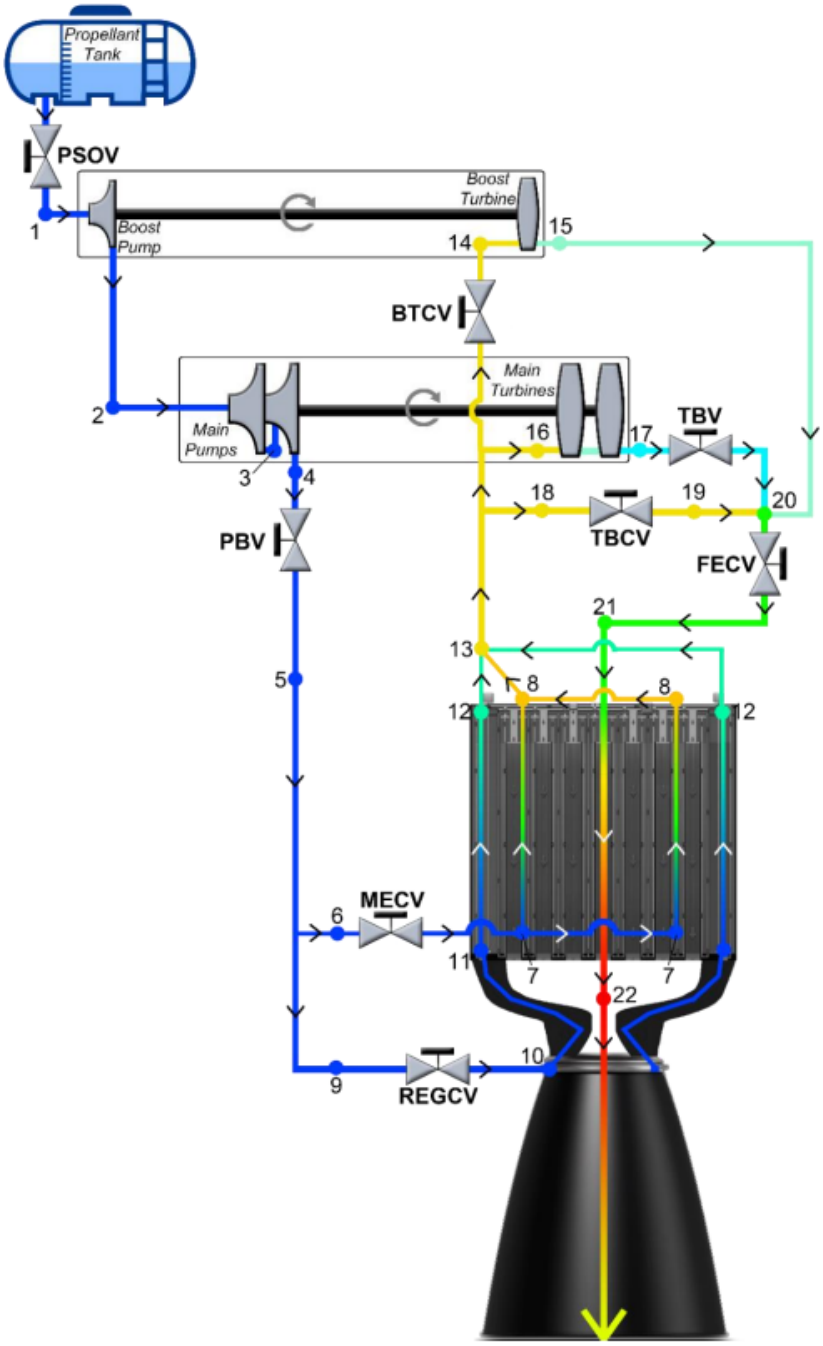

Figure 3.7: Aerojet Rocketdyne NTP engine schematic (Adapted from AR PBM 5.7[76]).

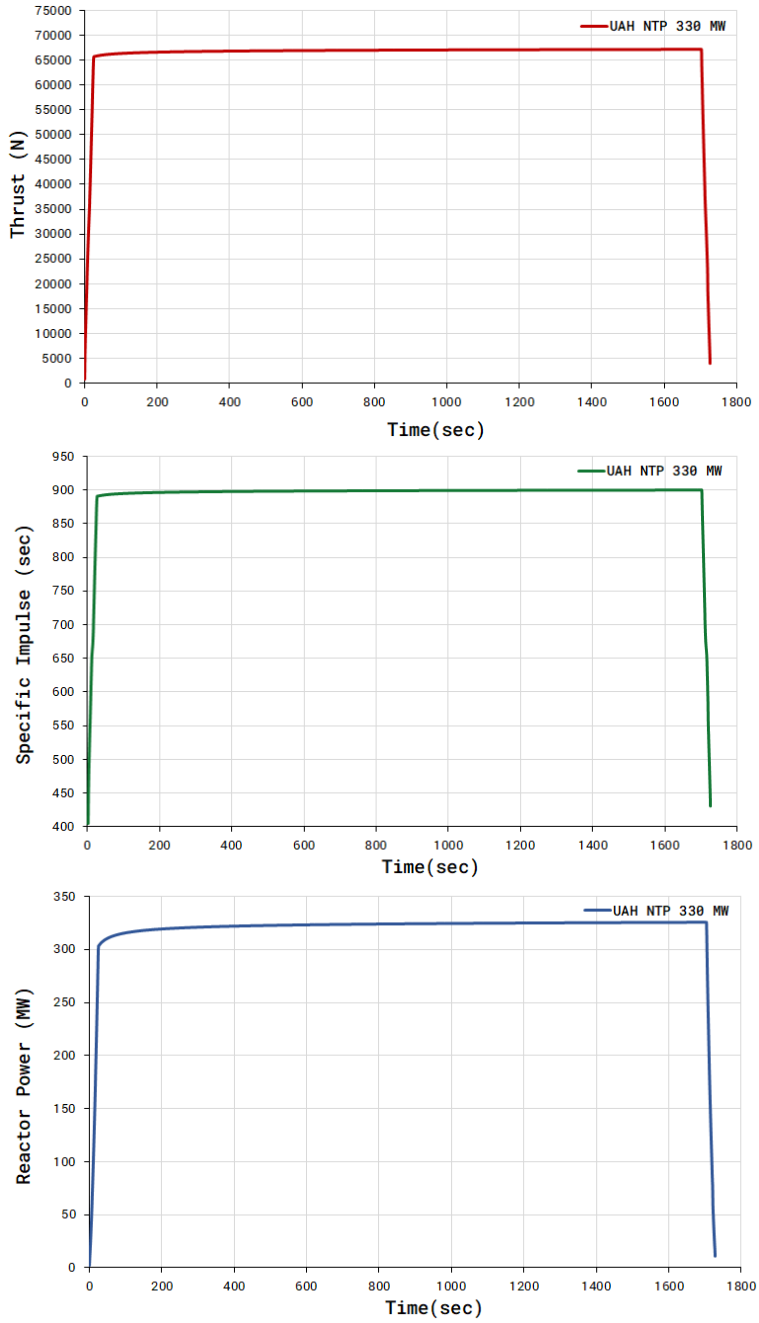

Figure 3.8: UAH NTP 330 MW engine performance parameters for thrust, specific impulse and reactor power.

3.3.2 Propellant Tank MER Analysis

It is imperative to include the realistic propellant tank calculations early in the mission design process to minimize the performance risk later in the design period. The propellant tank model used on this document involves determining Mass Estimating Relations for a LH2 propellant tank MERs with respect to its volume and mass. The first step in designing the tank is to have the total LH2 requirement for the mission which is in turn determined from the total ΔV requirement including ΔV losses. The MERs for the tank include the 3% ullage volume and cryogenic insulation mass. Using the propellant tank regression data as shown in Figure 3.9, the LH2 tank volume and cryogenic insulation MERs can be calculated as:

$$M_{LH_2Tank}(kg) = 9.09V_{LH_2}(m^3) \tag{3.1}$$

$$M_{LH_2Insulation}(kg) = 2.88A_{tank}(kg/m^2). \tag{3.2}$$

The final calculated propellant mass fraction is at 0.85 which is comparable to the tanks used in the large upper stage launch vehicles.

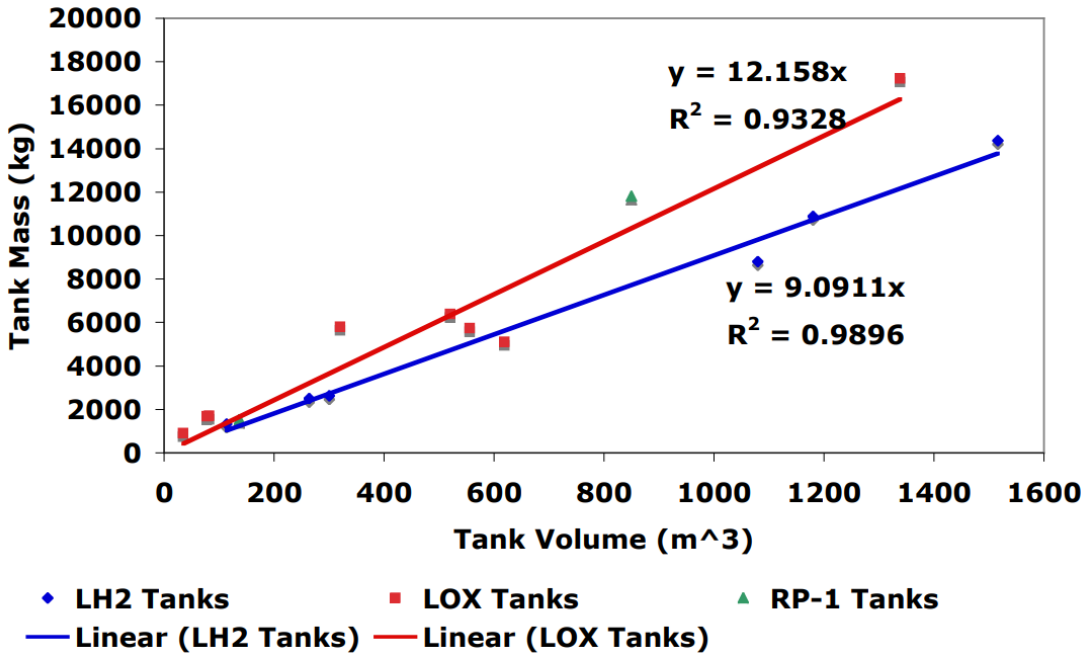

Figure 3.9: Propellant tank regression data [78].

3.3.3 Trajectory Analysis

The spacecraft's equation of motion in orbit can be determined using Newton's laws of motion. We know Newton's second law as,

$$\frac{d(mv)}{dt} = \sum F_{ext}, \tag{3.3}$$

where m is the total mass of the spacecraft, v is the spacecraft's velocity, t is time and F_{ext} is total external forces. Solving the above equation for two body problem with perturbations gives,

$$\frac{d^2r}{dt^2} = -\frac{\mu}{r^3}\vec{r} + f_p, \tag{3.4}$$

where μ is called as gravitational parameter and f_p is the sum of all perturbing acceleration including central body direct non spherical perturbation, direct third body point mass perturbation, indirect third body point mass perturbation, spacecraft thrust atmospheric drag and solar radiation pressure perturbation.

The orbit propagators are used to determine the motion of the spacecraft over a period of time. With the implementation of Newton's laws, the trajectory of the spacecraft can be determined based on its initial state and the perturbing forces acting on the spacecraft. There are three different types of orbit propagation techniques namely, numerical integration [79], analytical [80]and semianalytical [81, 82, 83].

The analytical propagation method approximates the spacecraft's ephimeris using only the initial state of the spacecraft and time. The central body for the

spacecraft is always considered as a point mass. Some of the models include the J2 perturbations (effect of asymmetry in Earth's gravitational field) and J4 perturbations (effect of Earth's oblateness) and simple atmospheric drag model. These propagators are also known as low fidelity propagators due to inaccuracies when the model propagates for a longer period of time. These are best used to determine a spacecraft's trajectory around Earth to track and communicate without having to maneuver the spacecraft.

The semianalytical propagation method provides more accuracy than the analytical propagation technique. It uses numerical methods with less approximations to determine spacecraft's trajectory. These propagators are also known as medium fidelity propagators. Draper Semianalytic Satellite Theory (DSST) orbit propagator can be categorized under semianalytical propagators which is used for maneuver planning of spacecraft in Earth's orbit and maintain space object catalog [84, 85]. The semianalytical propagators available in STK are Long term Orbit Predictor (LOP) and SGP4 for non-LEO satellites.

The numerical propagators are the most accurate when compared with the analytical and semianalytical propagation techniques. Thus, they are also known as high fidelity orbit propagators. These propagators typically use all the forces acting on spacecraft to determine the realistic trajectory. Numerical propagators are used for spacecraft operations and studies which involve high accuracy analysis. STK Astrogator module includes high fidelity numerical propagators namely known as High Precision Orbit Propagator (HPOP). The trajectory analysis presented in this document uses STK Astrogator module using HPOP.

STK's Astrogator propagator analysis module is intended to design and analyze spacecraft trajectories and orbital maneuvers. The astrogator module executes the Mission Control Sequence (MCS) designed by the user which calculates the spacecraft's ephemeris. The capabilities of astrogator other than orbit propagation also includes modeling impulsive and finite maneuver of the engine model. The algorithm used for the interplanetary trajectory uses numerical integration using cowell's formulation with variation of parameters for orbit propagation. Gravitational and atmospheric models of the planetary bodies are used from the available data from NASA JPL. The trajectory constraints and targeting methods include differential corrector which allows the user to determine the values of the control parameters for satisfy the mission requirements. The user interface and mission control segments available in the Astrogator analysis module are described in detail in Appendix C.

3.4 Design Reference Missions

A well defined Design Reference Mission (DRM) is critical to the development of a space mission concept [86]. The DRMs are to be defined in such a way that it addresses the science and technical objectives as defined by the scientific and engineering community. In this document, the DRMs are selected around the technical objectives of the NTP systems that help to clearly articulate the propulsion system performance for the NASA's planetary science missions program. The DRMs are used to provide the traceability from the NTP performance objectives to the mission requirements and can be used to examine the options and implications of the observations such as identifying the solution space of the propulsion system. To help answer the Research Questions, the DRMs are divided into two categories (i) Point design reference missions and (ii) Design reference mission trade tree.

3.4.1 Point Design Reference Missions

The point design reference missions were identified in order to answer Research Question #1. Figure 3.10 shows the DRM matrix to demonstrate the performance of NTP system towards enabling missions to the outer solar system. The goal of the point design missions is to demonstrate the enhanced capability of NTP for robotic missions to the outer planets and compare the performance with the missions using traditional propulsion systems. For even comparison with

the actual and conceptual missions using traditional propulsion system the target destinations of all four outer planets were considered for rendezvous missions.

The selected mission architecture for the interplanetary missions uses expendable mission mode configuration which consists of NTP injection stage and spacecraft. The NTP injection which consists of an NTP engine system and LH2 propellant tank is used during the Earth departure phase. Type-I direct transfer and Hohmann transfer trajectories are considered for missions to the gas giant (Jupiter, Saturn) and ice giant (Uranus, Neptune) systems. The Planetary Orbit Insertion (POI) is performed using storable chemical propulsion system. The UAH NTP 330 MW engine model is used to analyse the finite maneuver analysis during the Earth departure phase. Further details on the mission architecture, performance and its comparison with traditional missions to the outer planets is discussed in Chapter 4.

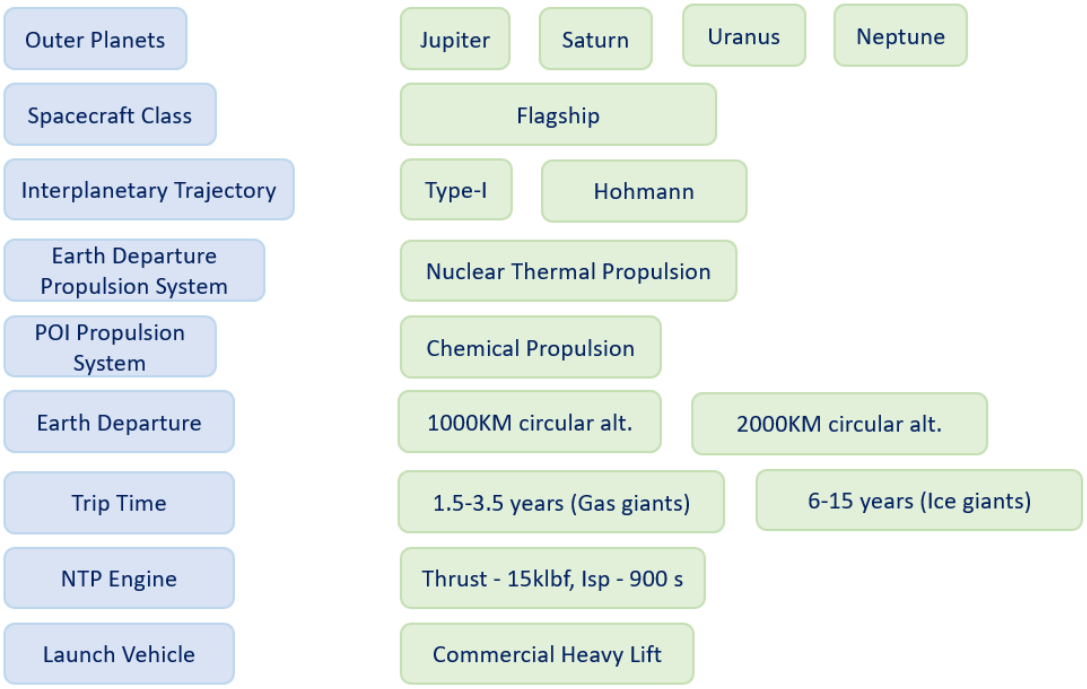

Figure 3.10: Point design reference missions to the outer planets using NTP system.

3.4.2 Design Reference Mission Trade Tree

The design reference mission trades to determine the enabling architecture and optimum NTP engine parameters for robotic missions to the outer planet destinations is illustrated in Figure 3.11. Jupiter and Neptune were each selected mission for trades among the gas giant and ice giant planets. The mission architecture and engine trades to the Jupiter is critical to be analyzed for two reasons (i) robotic missions to the Jupiter system has been one of the preferred destination by the scientific community to explore not just the gas giant planets but also its moons such as Europa, Callisto and Io etc. and (ii) for missions beyond the 5 AU distances, Jupiter also acts as the preferred choice to be used for the gravity assist maneuver. The second destination of Neptune system was considered primarily due to is vast distance and being the farthest plant in the solar system and has traditionally been a challenge to realize a mission using chemical/ SEP systems. The planetary mission categories of both new frontiers and flagship class were included in the mission trades. All three possible interplanetary trajectories (direct fast transfer, gravity assist and Hohmann transfers) were considered for mission using NTP system for Earth departure. Unlike for point design, both chemical and NTP system was traded for planetary orbit insertion maneuvers. Earth departure from nuclear safe orbit of beyond 1000 km circular to 2000 km circular altitude was included in the analysis perform the sensitivity analysis of the NTP performance based on the departure orbits. Constant thrust and specific impulse NTP engine model is used in the DRM with thrust range from 5 klbf to

30 klbf and specific impulse range from 850 sec to 900 sec. Mass and payload volume constraints with respect to the commercial heavy lift launch vehicle have been included in the analysis. Results on the NTP engine trades and mission architectures are described in detail in Chapter 5.

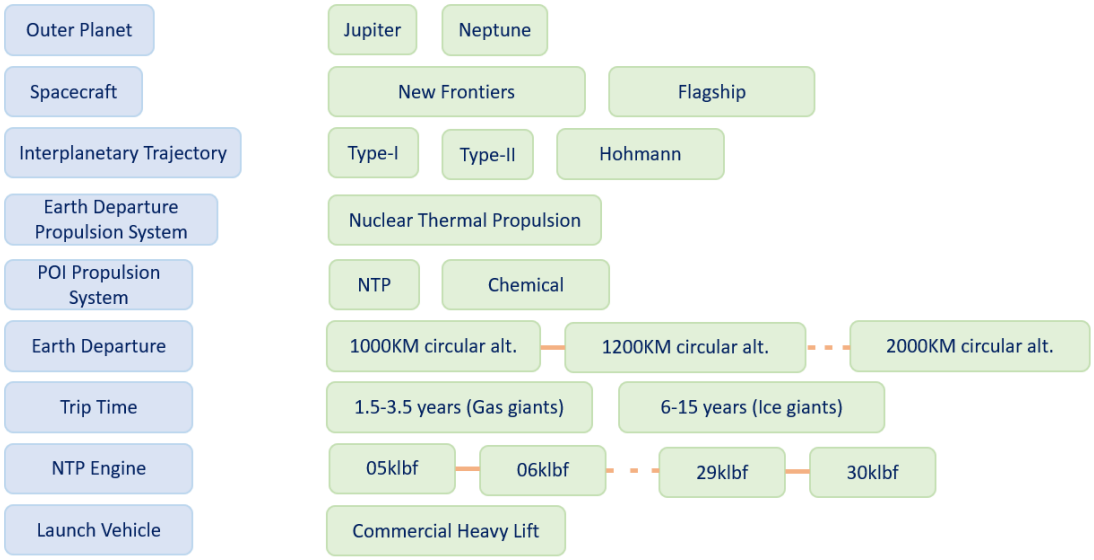

Figure 3.11: NTP key design reference mission trades for missions to the outer planets.

3.5 Model Validation

The development of Spacecraft Integrated System Model (SISM) which includes the systems engineering model and analytical models of subsystems for mission formulation described in this chapter provides the ability to create the digital test bed on which the research questions of this dissertation may be answered. The developed SISM represent a significant contribution to the community focused on space mission formulation and NTP system development.

The systems engineering model was validated during and after the integration of the structure and requirements model by demonstrating NTP demo mission which involved increasing the orbit of the spacecraft in LEO [87]. Another NTP mission for a lunar rendezvous mission was implemented to validate the requirements model against the actual mission parameters outputs [88].

The analytical model of NTP engine 'UAH NTP 330 MW' has already been verified against the benchmark Aerojet Rocketdyne AR-PBM 5.7 which in comparison had error margin of less than 1% for 20 of the 22 states and under 4% for the remaining two states. The constant thrust and specific impulse engine model for trade space exploration relies on the rocket equation, propellant mass subtractions for every delta time interval. Due to the simplicity of the model basic calculations were deemed sufficient to verify the model against the literature. The propellant tank mass estimation model is derived from the equations presented in the section 3.3.2 and the available tank regression data. The final results including the tank mass fraction are compared with the historical liquid hydrogen Earth departure stages [89]. The calculated propellant mass fraction of 0.85 is within the required range of 0.8-0.9. The trajectory analysis involved initial estimation using patched conic analysis which is performed using the equations available in the literature. For, high-fidelity trajectory analysis including the finite maneuver analysis the trajectory design is performed using the STK software with details of the algorithms used having been explained in the section 3.3.3 and Appendix C. Finally, the finite maneuver analysis model used in the mission analysis has been validated with results from the literature on engine burn duration for lunar

and Mars mission [90]. The same model was then used for mission analysis with results published in the peer review journals AIAA JSR and ANS NT [74, 91].

3.6 Quantifiable Figures of Merit for Engine Trades

The NTP system has mostly been projected and compared with other propulsion systems with its 900 sec specific impulse capability and poor thrust to weight ratios. However, the relative advantages of a propulsion system should not be ascertained by using only two parameters. Multiple quantifiable figures of merit are to be determined for robotic missions to the outer planets using NTP system. The figures of merit required to answer the research questions are identified based on the vehicle and system level parameters which will impact the capability of the system either adversely or favourably in enabling the planetary science missions. The figures of merit used in this study have been derived based on the Exploration Systems Mission Directorate strategy to task to technology development approach [92] and discussed in Appendix D. The following performance factors are identified which would be most significant towards determining the optimum engine parameters and architectures for missions to the outer solar system:

- Initial Mass in Low Earth Orbit (IMLEO) vs engine thrust.
- Departure ΔV vs engine thrust.
- Engine run time to achieve the departure ΔV including losses.
- Spacecraft mass delivered vs trip time.

Along with the above performance parameters, sensitivity analysis of specific impulse and departure orbit will also be needed to be performed to determine the performance of the propulsion system at the NTP system level.

3.7 Chapter Summary

This chapter introduces the coupled systems engineering model using MBSE approach and the analytical models for evaluation of the NTP system parameters. The overall systems engineering architectural model consist of structure and requirements model which is integrated with the domain engineering analysis models. The systems engineering model described in the N2 format comprises of modules which are mission classification, spacecraft, NTP system, launch vehicle and cost. These modules are integrated in a waterfall sequence but with each module having the input and output parameters connected with the other modules. The integration of systems engineering model with the analytical model is described in section 3.2.2 which consists of five steps to perform mission analysis and trade space exploration. An existing analytical model of the NTP engine is used to perform the point design study and analyse the impact of engine transient states in the overall ΔV capability. Analytical models of propellant tank, trajectory design and launch vehicle performance are modelled using the mathematical relations described in section 3.3.

The DRM trade tree to answer the research questions is presented in the section 3.4 which includes the DRM for point design reference mission to perform the NTP powered mission analysis to the outer planets and eventually compare

the overall mission parameters with traditional propulsion systems. The DRM trade tree in section 3.4.2 will be used to determine the optimum engine parameters and mission architectures which fits within the NASA's planetary science missions program. Finally, section 3.5 and 3.6 discuss the model validation approach for the systems and analytical models implemented in the dissertation and quantifiable figures of merit to perform engine trades.

Chapter 4. Point Design Studies

Chapter 3 described the overall model integration and execution approach for Spacecraft Integrated System Model which includes the systems engineering architecture models and domain engineering analysis models. The systems engineering model and its output metrics for the selected DRMs can assess the NTP system performance required to answer the research questions. This chapter starts with assessing the standalone commercial launch vehicle performance for a direct insertion capability to the gas giant planets and comparison with NTP system being used as an injection stage with the standalone commercial launch vehicle. Point design study results for the selected reference missions to the outer planets (Jupiter, Saturn, Uranus and Neptune) as described in the chapter 3 are presented in the section 4.3 and 4.4.

4.1 Direct Spacecraft Injection Performance

Determining the direct spacecraft injection performance primarily means calculating the C_3 versus payload mass of the propulsion system. This calculation is performed for the most efficient transfer orbit in order to maximize the payload delivery mass thereby requiring the use of Hohmann transfer between the Earth

and the destination celestial body. The first step is to determine the hyperbolic excess velocity by:

$$V_\infty = \sqrt{\frac{\mu_{\text{sun}}}{R_{\text{Earth}}}} \left(\sqrt{\frac{2R_{\text{D}}}{R_{\text{E}} + R_{\text{D}}}} - 1 \right), \tag{4.1}$$

where V_∞ is the hyperbolic excess velocity, μ_{sun} is the gravitational parameter of the Sun, R_{Earth} and R_{D} is the heliocentric orbital radii of the Earth and the destination planet.

Using the V_∞, the characteristic energy required to reach the destination planet can be calculated as:

$$C_3 = V_\infty^2. \tag{4.2}$$

The ΔV needed to for the mission from Earth parking orbit can be calculated as:

$$\Delta V = V_c \left(\sqrt{2 + \left(\frac{V_\infty}{V_c} \right)^2} - 1 \right), \tag{4.3}$$

where V_c is the velocity on the Earth parking orbit which can be calculated as:

$$V_c = \sqrt{\frac{\mu_{\text{Earth}}}{R_{\text{Earth}} + R_{\text{altitude}}}}, \tag{4.4}$$

where R_{Earth} is the radius of the Earth and R_{altitude} is the altitude of the spacecraft's from the surface of the Earth on LEO.

The gravitational loss estimation can be shown in the specific energy equation as:

$$e = \frac{1}{2}V^2 + \int_0^s g_d \, ds, \tag{4.5}$$

where 'd' is the distance along the trajectory:

$$de = V dV + g_d \, ds \tag{4.6}$$

using the trajectory equation, the gravity loss estimation by subtracting the real velocity increase from the ideal velocity increase can be shown as:

$$dG = -I_{sp} g_0 V \frac{dm}{m} \int_0^t g_d \, dt. \tag{4.7}$$

The propellant required for the trans-planetary injection can be calculated as:

$$\frac{\Delta m}{m} = 1 - e^{-\frac{\Delta V}{I_{\mathrm{sp}} \cdot g_0}} \tag{4.8}$$

$$\Delta m = m_0 - m_f, \tag{4.9}$$

where m_0 is the initial mass (wet), m_f is the final mass (dry). The final dry mas includes the NTP system mass and the spacecraft mass.

Finally, the time of flight for the transfer orbit can be calculated as:

$$ToF = \pi \sqrt{\frac{a^3}{\mu_{\mathrm{sun}}}}, \tag{4.10}$$

where ‘a’ is the semi-major axis of the transfer orbit.

Using the described method, the performance of NTP system optimized for deep space mission is determined and compared with the standalone heavy lift and super-heavy lift launch vehicles. The payload vs C_3 data for commercial launchers is referenced from the open literature and the performance of NASA's Space Launch System (SLS) is referenced from the SLS mission planner's guide [93, 94]. Figure 4.1 shows the C_3 curve of the Vulcan Centaur, Vulcan Heavy, SLS Block 1 and NTP using Vulcan Heavy configuration for C_3 energy of 10 to 100 km^2/s^2. Among all the launchers, SLS Block 1 has the highest performance for missions to Mars which requires C_3 energy of about 10 km^2/s^2. However, with increase in the energy requirements for missions to the outer planets the payload delivery capability reduces significantly. Missions to Jupiter and Saturn require C_3 energy of about 80 and 100 km^2/s^2 respectively. The NTP injection stage using Vulcan Heavy configuration is capable of delivering spacecraft mass of 6,237 kg to Jupiter and 4,882 kg to Saturn. Table 4.1 shows the payload delivery capability for rendezvous mission to Mars, Jupiter and Saturn which require C_3 energy in the range of 10, 80 and 100 km^2/s^2 respectively.

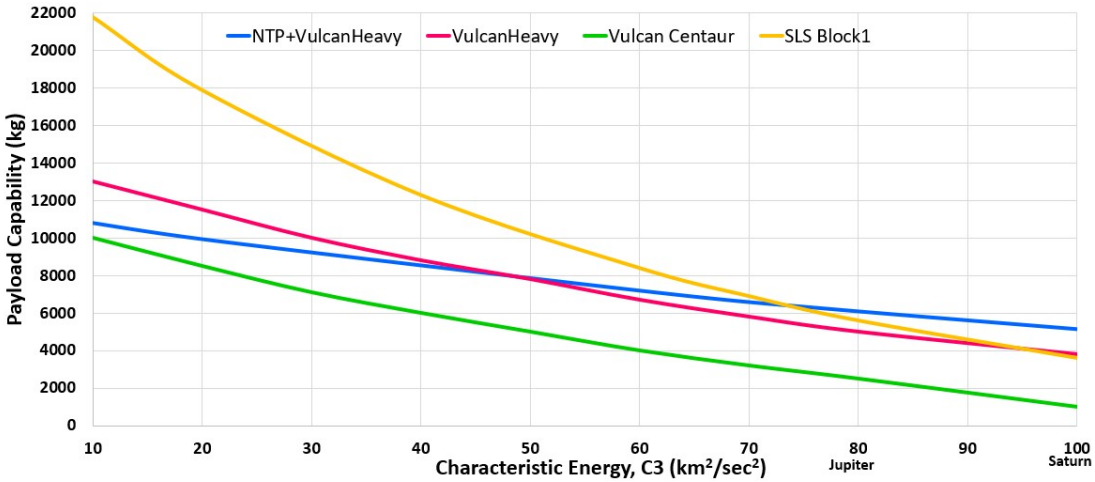

Figure 4.1: Useful payload mass vs characteristic energy of standalone launch vehicle and NTP injection stage.

Table 4.1: Useful payload system mass for missions to Mars and beyond.

Destination	**SLS Block 1**	**NTP + Vulcan Heavy Configuration**
Mars	21,800 kg	10,909 kg
Jupiter	5,600 kg	6,237 kg
Saturn	3,600 kg	4,882 kg

4.2 Mission Concept of Operations

The mission design objectives for the point design study were to enable a flagship or a new frontiers class mission to the Gas and Ice giant planets in a direct transfer trajectory. The analysis addresses the mass and launch vehicle challenges for NTP-powered robotic missions. The high level mission design guidelines are:

- Trajectory search for launch between 2025-2034.
- Total trip time of no more than 6 years for Gas giant missions and 13 years for Ice giant missions.
- NTP system and spacecraft to be launched using a single commercial launch vehicle.
- Use of a single NTP engine with baseline thrust of 15 klbf and an I_{sp} of 900 s.
- Comply with the nuclear safe orbit requirements in the LEO.

The vehicle design is based on expendable mission mode, which consists of a spacecraft and an NTP injection stage as illustrated in Figure 4.2. The NTP injection stage consists of an NTP engine system and $LH2$ propellant tank. The NTP injection stage is used for spacecraft injection with sufficient C_3 energy and plane change for direct transfer to the destination planet.

The NTP engine baseline for this study has the capability to produce 15 klbf of thrust and a steady-state vacuum specific impulse of 900 s. To produce

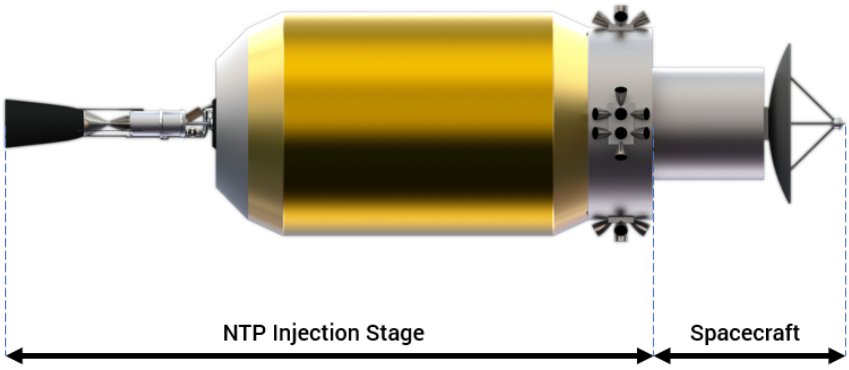

Figure 4.2: NTP injection stage and spacecraft configuration.

these baseline performance parameters, the nozzle area ratio is 300:1, the maximum fuel temperature is 2800 K, and the reactor power is 323 MW. The engine thrust-to-weight (T/W) ratio and nozzle exit diameter are 2.65 and 1.85 m, respectively. These NTP system parameters used in this study are summarized in Table 4.2 and are obtained from NASA's low-enriched uranium NTP project published reports [95, 96, 34]. The dry mass estimates of the propellant tank are performed using the method described in the section 3.3.2.

The payload fairing (PLF) constraints of the commercial launch vehicles considered in the point designs and the NTP spacecraft requirement for Jupiter rendezvous mission is provided in Table 4.3.

The initial parking orbit of the spacecraft is considered to be circular at an altitude of 1000-2000 km with 28.5 deg inclination. The selected parking orbit complies with the minimum required altitude for final end-of-life storage and is also beyond the maximum internationally deployed objects and debris belt in LEO which is between the altitude of 600 km to 900 km [57]. The trajectory

Table 4.2: Nuclear thermal propulsion system parameters [95].

Parameter	Values
Thrust	66723.32 N (15klbf)
Specific impulse (vac.)	900 s
Nozzle area ratio	300:1
NTP engine T/W	2.65
Reactor PWR	323 MW
LH_2 mass flow rate	7.56 kg/s

Table 4.3: Launch vehicle spacecraft encapsulation capability [97, 98].

Vehicle	PLF diameter (m)	PLF length (m)
Vulcan Heavy (ULA)	5.4	21.3
New Glenn (Blue Origin)	7.0	21.9
NTP spacecraft requirement	5.0	20.53

design of the NTP vehicle and spacecraft starting from low Earth parking orbit to the target planet was divided into three phases. The first phase consists of Earth escape phase. During the Earth escape phase, spacecraft departs from low Earth parking orbit using its onboard NTP powered system. The thrust vectors are specified in cartesian axes in order to provide the departure ΔV and plane change with respect to the destination planet. The second phase of the spacecraft

is the coasting phase. During this phase, heliocentric propagator is used without any active propulsion system to determine the spacecraft's expected trajectory. A Deep Space Maneuver (DSM) is utilized during the heliocentric transfer so that the spacecraft's arrival constraints for the Planetary Orbit Insertion (POI) can be converged. The spacecraft is then separated from the NTP injection stage and is discarded after the DSM maneuver. Using the NTP injection stage for only TPI and DSM eliminates the complexities of long term LH2 propellant storage and reduces stage thermal protection system. The last phase consists of planetary capture and orbital insertion phase. During this phase the spacecraft's onboard chemical propulsion system is utilized to reduce the spacecraft's heliocentric velocity and successfully perform the POI to achieve targeted orbit around Jupiter. A high-thrust apogee engine with a thrust capability of 1100 N and I_{sp} of 323 s is used for orbit insertion calculations [99]. High-eccentric near polar orbit around the target planet is targeted during the analysis which is usually preferred for planetary science missions. The summary of each trajectory segment between the maneuver phases is given in Table 4.4 and the graphical Earth to Jupiter trajectory is shown in Figure 4.3.

4.3 Rendezvous Mission to the Gas Giant System

4.3.1 Jupiter Rendezvous Mission

The total wet mass of the spacecraft is for a flagship class Jupiter rendezvous mission is estimated to be at 4,350 kg of which 2,300 kg is allocated for

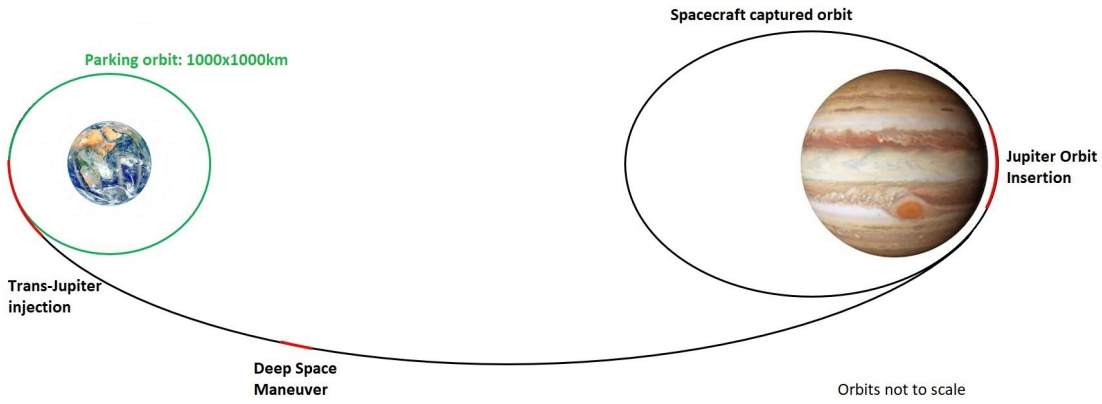

Figure 4.3: Mission concept: NTP powered expendable mission mode Earth to Jupiter rendezvous trajectory.

Table 4.4: Required maneuvers during trajectory segments.

Trajectory phase	Maneuvers
Low Earth parking orbit	Trans-planetary injection
Heliocentric phase	Deep Space Maneuver
Planetary capture	Planetary orbit insertion
Captured orbit	Period reduction maneuver

the spacecraft flight system bus and science payloads, and 2,050 kg of storable propellant is used for planetary orbit insertion and trajectory correction maneuvers during the science phases. The dry mass estimates of the orbiter are derived from the Jet Propulsion Laboratory (JPL) mission concept studies to the gas giant planet system [100, 101]. The propellant tank sizing is cylindrical, which has a length of 9.4 m and diameter of 5.0 m. Based on the spacecraft mass esti-

mates and required $LH2$ propellant calculation, the total initial wet mass of the NTP injection stage and the spacecraft in LEO is estimated to be 21.76 metric tons. The total NTP injection stage length is 16.53 m, which includes a 6.63 m long NTP engine, 9.4 m long $LH2$ tank, and interstage between the NTP engine and $LH2$ tank of 0.5 m. The dimensions of the orbiter are estimated to be 3.5 m in length and 3.5 m in width along with a 0.5-m-long interstage between the $LH2$ tank and payload. This makes the total length of the spacecraft to be 20.53 m, which is within the payload fairing limits of future commercial launchers in development such as United Launch Alliance's (ULA's) Vulcan Heavy and Blue Origin's New Glenn.

Table 4.5: NTP vehicle mass breakdown for the Jupiter rendezvous mission.

Vehicle	Mass (kg)
NTP engine	2,560
Tank dry mass	2,200
Spacecraft flight system bus and payload	2,300
Spacecraft onboard chemical propellant	2,050
LH_2 propellant (with 3% ullage volume)	12,650
Total 'wet' mass at launch	21,760

- **Earth Escape Phase**

  The duration of the NTP engine burn for trans-Jupiter injection (TJI) maneuver is 26.2 min, which provides a ΔV of 7 km/s and uses 11,904 kg of $LH2$ fuel. The thrust vectors are along the velocity vector in Velocity-Normal-Co-normal (VNC) (Earth) reference frame, and the maneuver direction is updated during the burn. The spacecraft orbital parameters at the beginning and end of the TJI are provided in Table 6. Figure 5 shows the spacecraft C3 energy during the TJI maneuver.

Table 4.6: Spacecraft orbital parameters during the TJI maneuver.

Parameters	Beginning of maneuver	End of maneuver
Ephimeris	08 Sept 2025 10:00:00	08 Sept 2025 10:26:14 UTCG
Right Asc. (deg.)	295	32.34
Decl. (deg.)	0	28.28
$\|R\|$ Earth inertial (km)	7,378.13	11,992.64
Inc. (deg.)	28.5	28.5
C_3 (km^2/sec^2)	-54.02	86.45

- **Coasting Phase and DSM**

  The coasting phase of the spacecraft begins after the TJI maneuver and is during the heliocentric transfer of the spacecraft. The only maneuver needed during this phase is the DSM, which is used to perform the plane change of

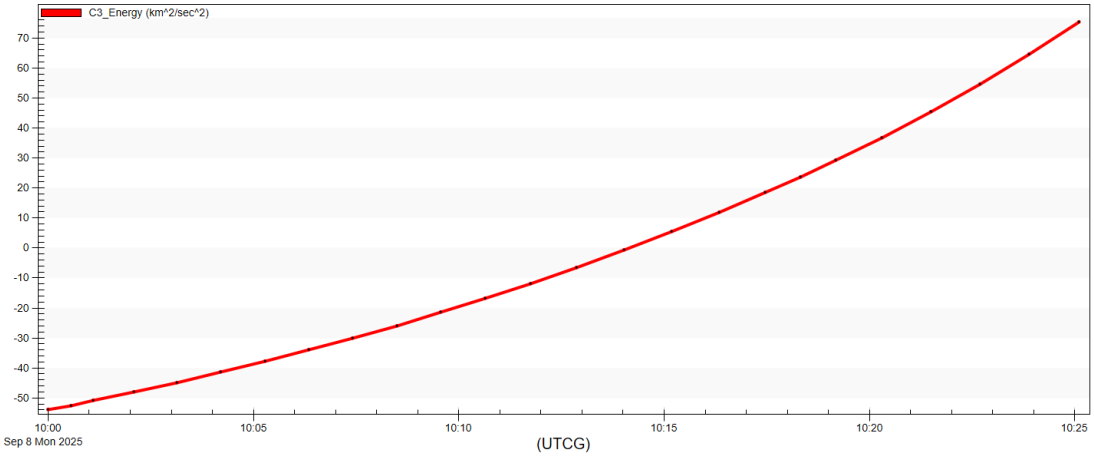

Figure 4.4: Spacecraft C_3 energy during the TJI maneuver.

the spacecraft with respect to the arrival conditions at Jupiter. The DSM is separated between two coasting phases. The first coasting phase before the DSM has a duration of 100 days, and the second coasting phase after the DSM is 665.5 days. The NTP burn duration for the DSM is 98 s, which uses 741 kg of $LH2$ fuel. The thrust vectors during the maneuver are defined with respect to VNC Earth axes, which are defined to be at -0.17 (velocity), -0.98 (normal), and -0.08 (conormal), respectively. After the completion of the DSM, the NTP injection stage is separated from the spacecraft, which continues on to Jupiter. The stopping conditions were defined based on the equality constraints of declination and right ascension at the perijove.

- **Planetary Capture and Orbit Insertion Phase**

  The planetary capture and orbital insertion phase of the spacecraft is the Jupiter orbit insertion (JOI) maneuver, using the orbiter's onboard chemical propulsion system. The ΔV magnitude needed for targeted capture orbit

is 1 km/s and is achieved by having a burn duration of 56.7 min using a chemical propulsion system. The spacecraft thrust vectors are aligned along the anti-velocity vector, and the direction is updated during the maneuver. The total fuel used during the burn is 1200 kg. The spacecraft orbital parameters during the JOI are mentioned in Table 7. At the completion of the JOI maneuver, the final captured orbit around Jupiter has a period of 48.5 days with an eccentricity of 0.96. The final spacecraft mass delivered to Jupiter is 3,169 kg, which includes 900 kg of fuel for orbit corrections during the science phase of the mission, which has been estimated based on the tour design of NASA's Juno mission [102]. Figures 4.5 and 4.6 show the spacecraft heliocentric and captured orbit trajectories.

Table 4.7: Spacecraft orbital parameters during JOI maneuver.

Parameters	Beginning of maneuver	End of maneuver
Ephemeris	12 Oct 2027 05:00:00 UTCG	12 Oct 2025 05:56:40 UTCG
Right Asc. (deg.)	123.9	106.7
Decl. (deg.)	-11.25	36.38
$\|R\|$ Jupiter inertial (km)	156,551.3	164,220.2
Inc. (deg.)	107.5	107.8

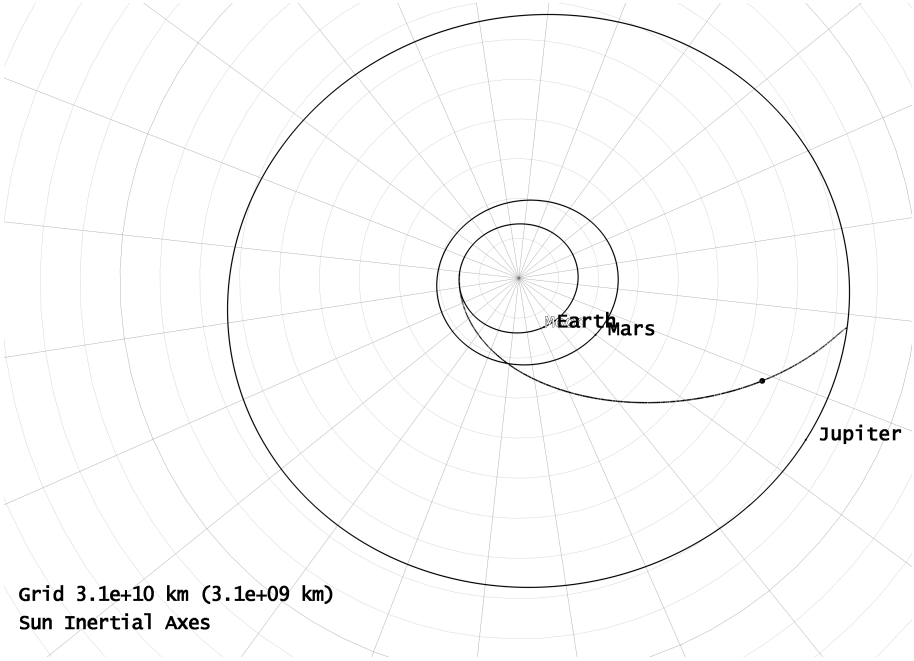

Figure 4.5: Spacecraft E-J heliocentric trajectory.

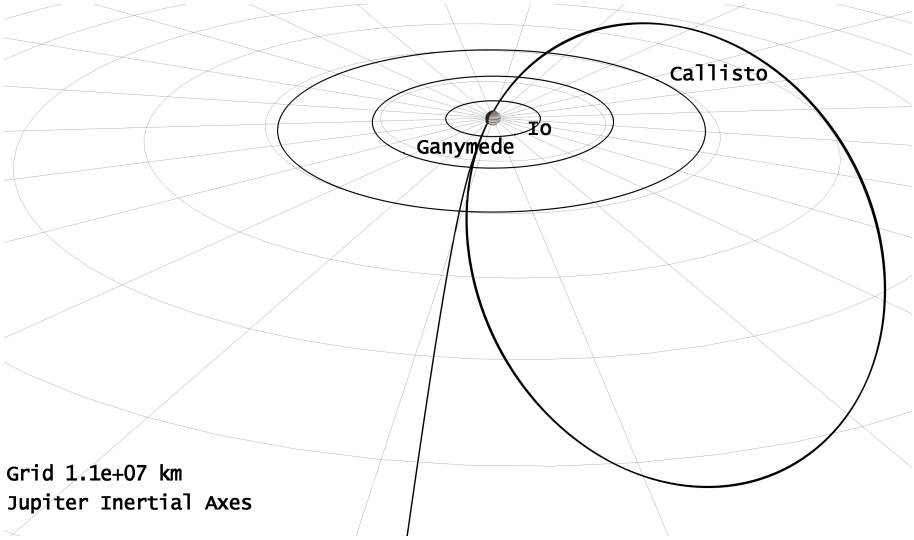

Figure 4.6: Spacecraft captured orbit around Jupiter.

4.3.2 Saturn Rendezvous Mission

For the Saturn rendezvous mission in order to deliver the spacecraft at a distance of 9.5 AU the spacecraft dry mass and onboard chemical propellant for orbit insertion are optimized. The total spacecraft mass is constrained to 3,900 kg, which includes 2,100 kg of dry mass. The NTP injection stage and spacecraft mass breakdown are described in Table 4.8.

Table 4.8: NTP vehicle mass breakdown for the Saturn rendezvous mission.

Vehicle	Mass (kg)
NTP engine	2,560
Tank dry mass	2,200
Spacecraft flight system bus and payload	2,100
Spacecraft onboard chemical propellant	1,800
LH_2 propellant (with 3% ullage volume)	12,650
Total 'wet' mass at launch	21,310

- **Earth Escape Phase**

  The duration of the NTP engine burn for the trans-Saturn injection (TSI) maneuver is 27.34 min, which provides a ΔV of 7.7 km/s and uses $LH2$ fuel of 12,404 kg. The spacecraft orbital parameters at the beginning and end of the TSI are provided in Table 4.9. Figure 4.7 shows the spacecraft C_3 energy during the TSI maneuver.

Table 4.9: Spacecraft orbital parameters during the TSI maneuver.

Parameters	Beginning of maneuver	End of maneuver
Ephemeris	20 Jul 2029 09:00:00 UTCG	20 Jul 2029 19:27:20 UTCG
Right Asc. (deg.)	232.84	334
Decl. (deg.)	-12.05	-6.67
$\|R\|$ Earth inertial (km)	7,378.13	12,708.20
Inc. (deg.)	15	15
C_3 (km^2/sec^2)	-54.02	104.78

- **Coasting Phase and DSM**

  The total coasting phase of the spacecraft is 4.67 years. The DSM is performed three months after the TSI maneuver. An NTP injection stage is used for the DSM burn. The stopping conditions for the burn were defined based on the equality constraints of declination and right ascension at the perikrone. The NTP burn duration for DSM is 32 s, which uses about 243 kg of $LH2$ fuel. The thrust vectors during the maneuver are defined with respect to VNC Earth axes, which are defined to be at -3.15 (velocity), -0.78 (normal), and -0.62 (conormal), respectively.

- **Planetary Capture and Orbit Insertion Phase**

  The Saturn orbit insertion (SOI) maneuver is performed using the spacecraft onboard chemical propulsion system. The ΔV needed for the targeted

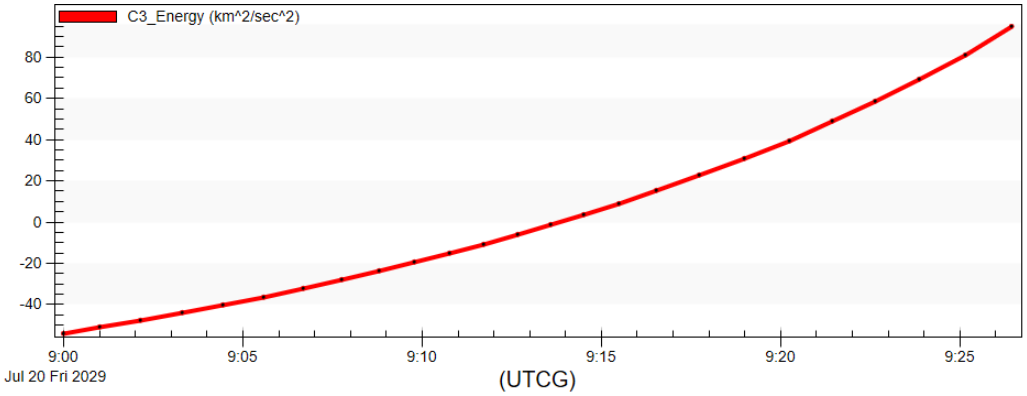

Figure 4.7: Spacecraft C_3 energy during the TSI maneuver.

captured orbit is 0.93 km/s and is achieved by having a burn duration of 48 min using a chemical propulsion system. The spacecraft thrust vectors are aligned along the anti-velocity vector, and the direction is updated during the maneuver. The total fuel used during the burn is about 1,000 kg. The spacecraft orbital parameters during the SOI are summarized in Table 4.10.

Table 4.10: Spacecraft orbital parameters during SOI maneuver.

Parameters	Beginning of maneuver	End of maneuver
Ephemeris	23 Mar 2034 12:45:53 UTCG	23 Mar 2034 13:33:53 UTCG
Right Asc. (deg.)	16.47	73.2
Decl. (deg.)	18.64	-5.13
$\|R\|$ Saturn inertial (km)	72,092.74	96,666.10
Inc. (deg.)	25.23	25.28

At the completion of SOI maneuver, the spacecraft is captured in a highly eccentric orbit with an orbital period of 31.6 days and has final wet mass of 2,900 kg. The spacecraft mass includes about 800 kg of onboard chemical propellant for orbit correction during the science phase of the mission. Figures 4.8 and 4.9 show the spacecraft heliocentric and captured orbit trajectories.

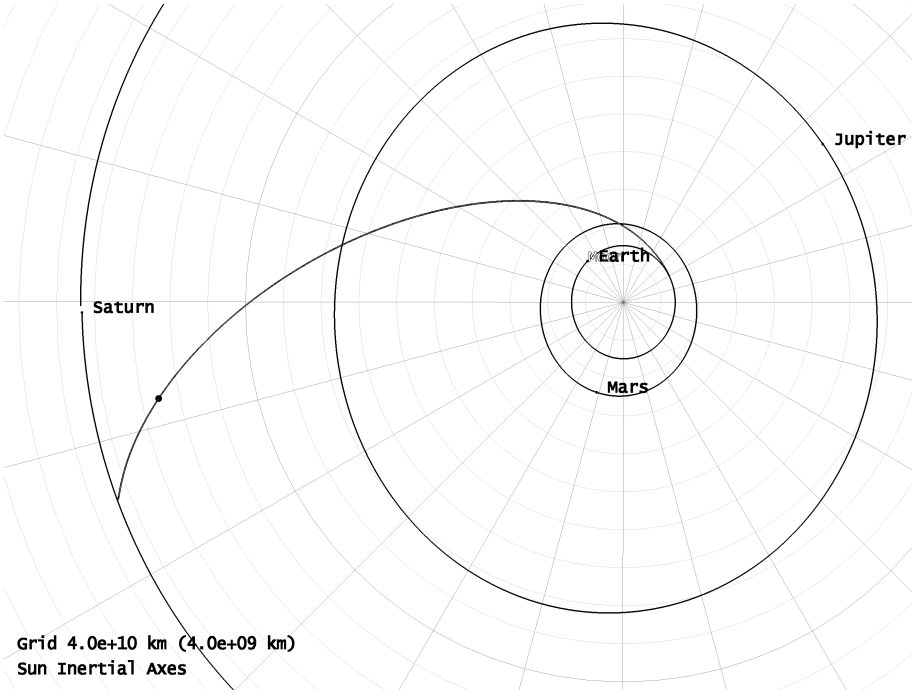

Figure 4.8: Spacecraft E-S heliocentric trajectory.

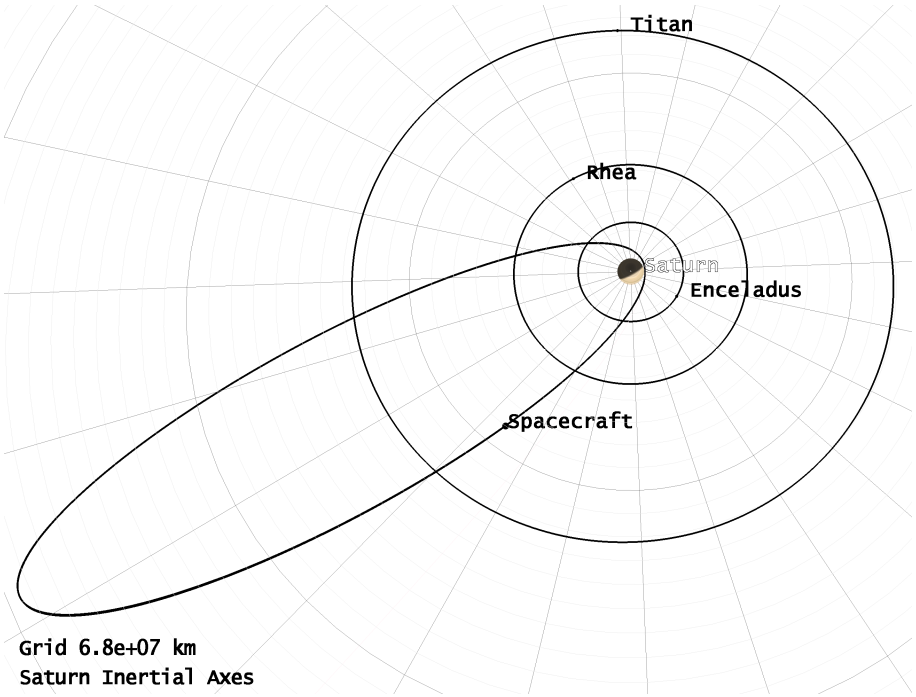

Figure 4.9: Spacecraft captured orbit around Saturn.

4.4 Rendezvous Mission to the Ice Giant System

The high energy requirements for missions to the Ice giant planets required optimization in NTP system and spacecraft design. The goal is to deliver a spacecraft with a minimum dry mass of over 1,000 kg in order to meet the planetary science missions program. The point design required the utilization of mass and volume capability of the commercial launcher down to the last kilo and cubic meter therefore the NTP system is designed to have the maximum propellant capability. The parking orbit of the vehicle was also raised to an altitude of 2,000 km which is within the capability of the launch vehicle considered. The higher parking orbit allows the spacecraft to be further away from the Earth's gravity well thereby reducing the trans-planetary injection ΔV requirements when compared with the lower parking orbit. Multiple point designs were completed to the Ice giant planets and the one presented in this section distinctly demonstrates the capability of the NTP system when compared with the traditional propulsion system in order to answer the Research Question #1.

4.4.1 Uranus Rendezvous Mission

Using the expendable configuration of the NTP system, the total spacecraft wet mass for Uranus rendezvous mission is 2,500 kg. Table 4.11 mentions the NTP injection stage and spacecraft mass breakdown which shows the maximum possible $LH2$ propellant mass which can be used for the designed NTP system is at 14 mT thereby having a total 'wet' mass of 21.26 mT at launch .

Table 4.11: NTP vehicle mass breakdown for the Uranus rendezvous mission.

Vehicle	Mass (kg)
NTP engine	2,560
Tank dry mass	2,200
Spacecraft flight system bus and payload	1,100
Spacecraft onboard chemical propellant	1,400
LH_2 propellant (with 3% ullage volume)	14,000
Total 'wet' mass at launch	21,260

- **Earth Escape Phase**

  The total ΔV requirement for Uranus rendezvous mission is 9.483 km/s if which 9 km/s is imparted during the Trans-Uranus Injection (TNI) maneuver and the remaining at the DSM phase. The NTP engine run duration during the TNI maneuver is at 30 min and during the burn the total $LH2$ propellant requirement is at 13.6 mT. Table 4.12 mentions the spacecraft orbital parameters during the TNI manuever with Figure 4.10 displaying the the required C_3 energy achieved during the finite maneuver analysis.

- **Coasting Phase and DSM**

  The coasting phase of the spacecraft during the heliocentric transfer is for the duration of 7.97 years which also includes a TCM burn to point the spacecraft according to the planetary arrival constraints. The total ΔV

Table 4.12: Spacecraft orbital parameters during the TUI maneuver.

Parameters	Beginning of maneuver	End of maneuver
Ephemeris	20 Aug 2032 18:00:00 UTCG	20 Aug 2032 18:29:57 UTCG
Right Asc. (deg.)	255.77	350.7
Decl. (deg.)	0	28.4
$\|R\|$ Earth inertial (km)	8,378.13	14,763.1
Inc. (deg.)	28.5	28.5
C_3 (km^2/sec^2)	-47.57	142.8

during the TCM is 483 m/s which uses $LH2$ propellant of 408 kg. The thrust vectors during the maneuver are defined with respect to Earth inertial axes, which are defined to be at -0.72 (velocity), 0.47 (normal), and 0.50 (conormal), respectively. Figure 4.11shows the spacecraft's Earth- Uranus type-1 heliocentric transfer trajectory.

- **Planetary Capture and Orbit Insertion Phase**

  The Uranus Orbit Insertion (UOI) maneuver is performed using the 1,100 N LEROS-4 chemical engines. The total ΔV needed to capture the spacecraft to the required orbit is 2.25 km/s. The higher capture ΔV requirement is due to the type-1 fast transfer trajectory which in this case has a heliocentric transfer of under 8 years. The engine burn duration during the UOI is at 61 min and uses 1271 kg of propellant. The thrust vector during the UOI are

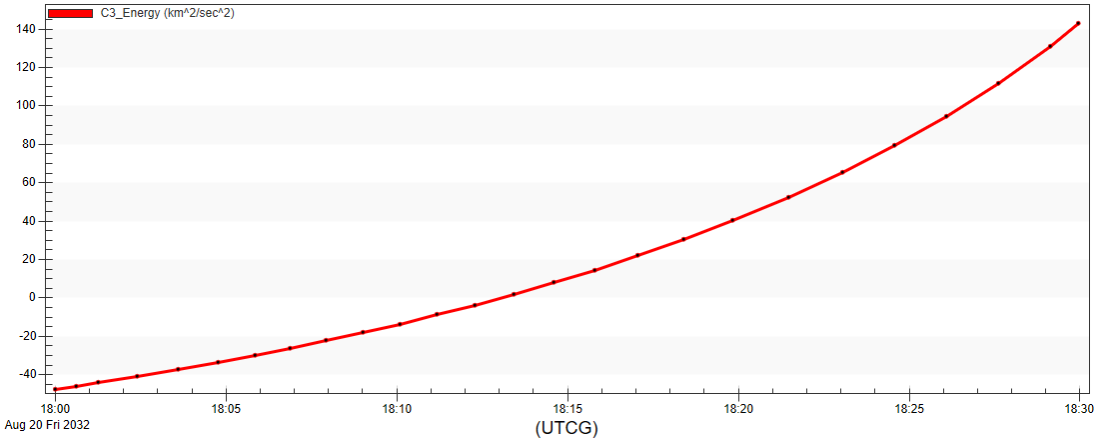

Figure 4.10: Spacecraft C_3 energy during the TUI maneuver.

actively controlled in order to achieve the net negative velocity vector. Table 4.13 mentions the spacecraft orbital parameters during the UOI maneuver.

Table 4.13: Spacecraft orbital parameters during UOI maneuver.

Parameters	Beginning of maneuver	End of maneuver
Ephemeris	12 Aug 2040 01:30:52 UTCG	12 Aug 2040 02:31:52 UTCG
Right Asc. (deg.)	198.4	197.1
Decl. (deg.)	-7.46	-5.97
$\|R\|$ Uranus inertial (km)	1.312e+6	1.271e+6
Inc. (deg.)	25.23	25.28

The final spacecraft wet mass post UOI is 1,229 kg and the spacecraft is at an eccentric orbit (eccentricity: 0.985) around Uranus with orbit period of 55 days at an inclination of 111 degrees. The captured orbit radius of

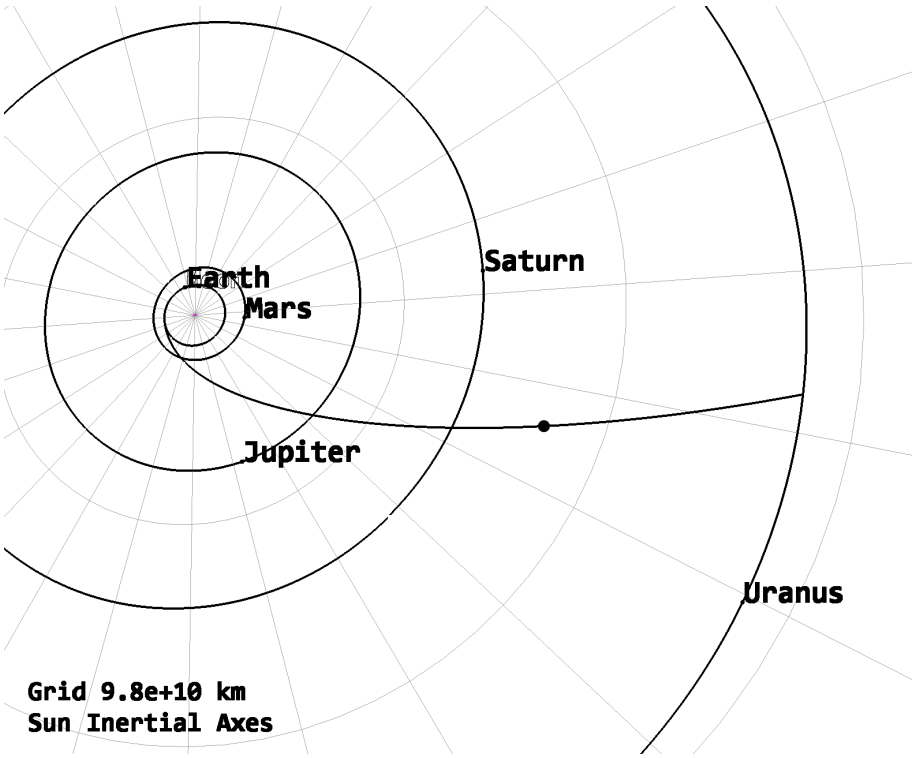

Figure 4.11: Spacecraft E-U type-1 trajectory.

periapsis and apoapsis are 22,090 km and 2.961×10^6 km respectively. Figure 4.12 shows the spacecraft captured orbit around Uranus post UOI.

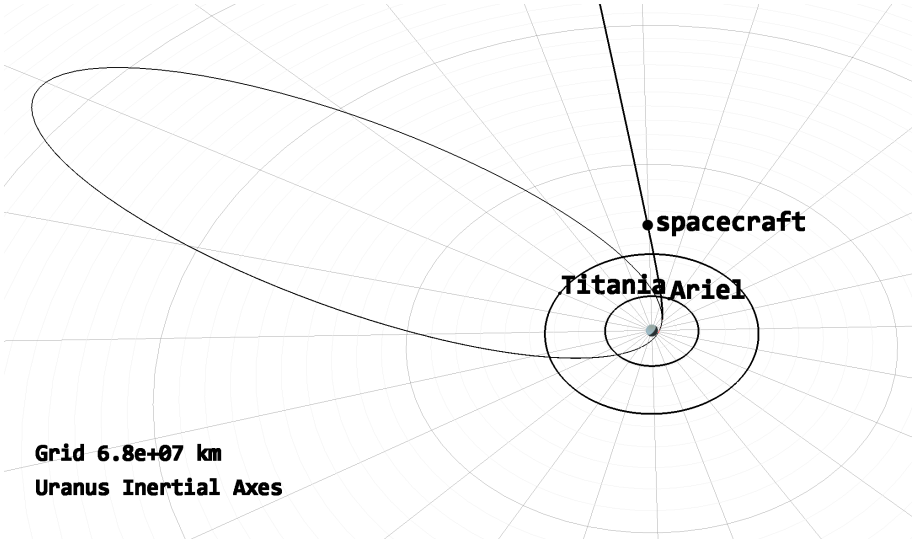

Figure 4.12: Spacecraft captured orbit around Uranus.

4.4.2 Neptune Rendezvous Mission

A mission concept to the Neptune which is the farthest planet in our solar system at a distance of about 30 AU required a trade-off between trip time and spacecraft mass. The total trip time was constrained at 13 years due to the flight design life of RPS of 14 years [27]. A 13 year cap on trip time would allow for a minimum of one year of science operations within the RPS design life. The NTP injection stage length is 16.73 m, which includes a 6.63-m-long NTP engine and a 9.6 m long $LH2$ tank and an interstage between the NTP engine and the LH2 tank of about 0.5 m. The total spacecraft 'wet' mass is 1,957 kg which includes dry mass of 1,583 kg. Table 4.14 shows the mass breakdown of the NTP injection stage and spacecraft for Neptune rendezvous mission.

Table 4.14: NTP vehicle mass breakdown for the Neptune rendezvous mission.

Vehicle	Mass (kg)
NTP engine	2,560
Tank dry mass	2,200
Spacecraft flight system bus and payload	1,583
Spacecraft onboard chemical propellant	374
LH_2 propellant (with 3% ullage volume)	14,000
Total 'wet' mass at launch	20,717

- **Earth Escape Phase** Trans-Neptune Injection (TNI) maneuver at the LEO parking orbit is used to inject the spacecraft in a direct transfer orbit. The total ΔV required for the type-1 trajectory is 9.76 km/s. The total NTP engine run duration of 30.3 min and $LH2$ propellant of 13.76 mT is needed to impart the required change in velocity. The spacecraft orbital parameters during the TNI maeuver are mentioned in the Table 4.15. At the end of the maneuver, the total C_3 energy achieved by the spacecraft is 157.5 (km^2/sec^2) which is required for the selected rendezvous mission. Figure 4.13 shows the C_3 energy plot during the Earth escape phase.

Table 4.15: Spacecraft orbital parameters during the TNI maneuver.

Parameters	Beginning of maneuver	End of maneuver
Ephemeris	01 Jun 2033 12:00:00 UTCG	01 Jun 2033 12:30:20 UTCG
Right Asc. (deg.)	205.6	297.8
Decl. (deg.)	26.9	-7.31
$\|R\|$ Earth inertial (km)	8,378.1	15,166.5
Inc. (deg.)	28.5	22.23
C_3 (km^2/sec^2)	-47.57	157.3

- **Coasting Phase and DSM** The coasting phase for the mission is for the duration of 13 years post TNI manuver. During the heliocentric phase, DSM is utilized for trajectory correction and requires a total ΔV magnitude of

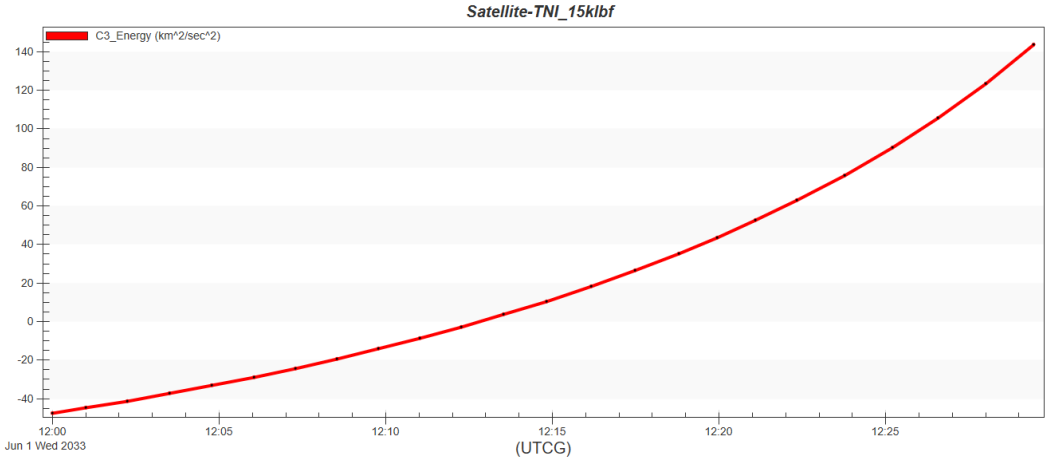

Figure 4.13: Spacecraft C_3 energy during the TNI maneuver.

182 m/s. Earth-Neptune heliocentric trajectory for the rendezvous mission is shown in the Figure 4.14.

- **Planetary Capture and Orbit Insertion Phase** The total ΔV needed for planetary capture during the Neptune Orbit Insertion (NOI) is 800 m/s and is imparted using the chemical propulsion system. The maneuver duration is for 16.8 min and utilizes 351 kg of propellant. The spacecraft orbital parameters during the NOI phase are presented in the Table 4.16. The spacecraft's captured orbital period around Neptune is of 45.7 days with an inclination of 152.4 degrees as illustrated in the Figure 4.15.

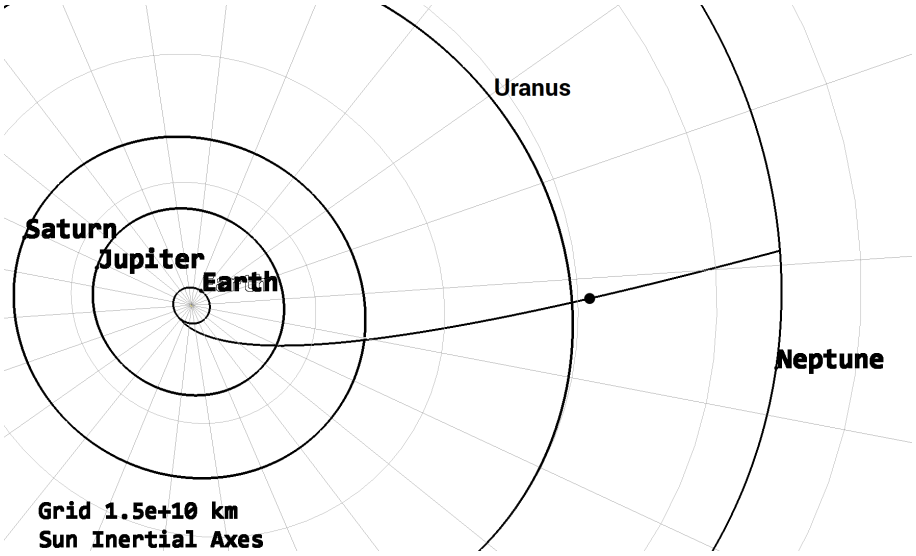

Figure 4.14: Spacecraft E-N type-1 trajectory.

Table 4.16: Spacecraft orbital parameters during NOI maneuver.

Parameters	Beginning of maneuver	End of maneuver
Ephemeris	27 May 2046 23:28:31 UTCG	27 May 2046 23:45:22 UTCG
Right Asc. (deg.)	93.4	90.7
Decl. (deg.)	23.3	23.2
$\|R\|$ Neptune inertial (km)	729000	716152
Inc. (deg.)	156.6	156.5

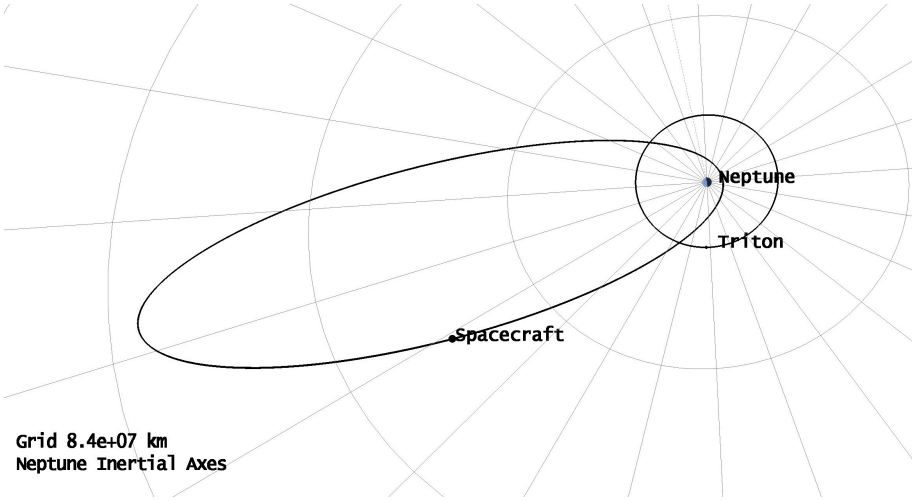

Figure 4.15: Spacecraft captured orbit around Neptune.

4.5 Chapter Summary and Answering Research Question #1

This chapter discusses the performance of NTP system for robotic missions to the Gas and Ice giant planets. The direct spacecraft injection analysis and its performance comparison with the standalone launch vehicles establishes the NTP's higher payload delivery capability in a direct transfer trajectory. The NTP system using commercial launcher was able to deliver over 12% to Jupiter and over 30% to Saturn when compared with the super heavy lift SLS Block 1 launch vehicle.

The chapter also presented the point design studies to the outer planets Jupiter, Saturn, Uranus and Neptune. The end-to-end mission analysis for an expendable NTP configuration discussed the capability to deliver flagship and new-frontiers class spacecrafts. Although there can be numerous point design studies with trade-offs in spacecraft mass and trip times, the goal of the mission analysis discussed in the chapter was to answer Research Question #1 *What us the potential difference in performance parameters for NTP systems in comparison to traditional propulsion systems towards enabling ambitious missions to the outer solar system exploration?*

For the Gas giant rendezvous missions using the NTP system in an expendable configuration can deliver the flagship class spacecraft with total 'wet' mass of over 4 mT to Jupiter and Saturn in 2.1 years and 4.68 years respectively. Figures 4.16 and 4.17 shows the spacecraft dry mass versus trip time of the NTP system and compares them with some of the past and present missions using

chemical propulsion system to Jupiter and Saturn. The comparison in the figures illustrates that the NTP system can reduce the trip times by a factor of two or more along with delivering higher spacecraft mass.

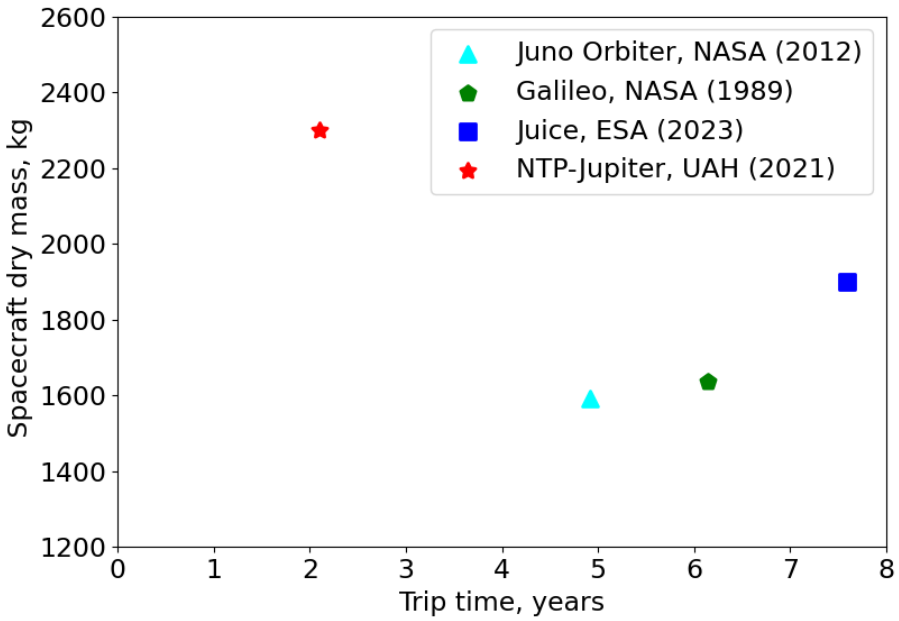

Figure 4.16: Spacecraft dry mass vs trip time for Jupiter rendezvous mission.

The point designs to the Ice giant planets Uranus and Neptune have also demonstrated the enhanced performance using NTP system. Planning a rendezvous mission to the Ice giants has been a major challenge by the space agencies over the last many decades. Mission concepts to Neptune using chemical propulsion system require the use of Jupiter Gravity Assist (JGA) due to its low efficiency. The synodic period of Neptune with respect to Jupiter is about 12.8 years which means that the optimal trajectory design using JGA occurs only every 13 years. The presented point design enables direct transfer to Ice giants with trip time of 7.97 and 13 years to Uranus and Neptune respectively. Figure

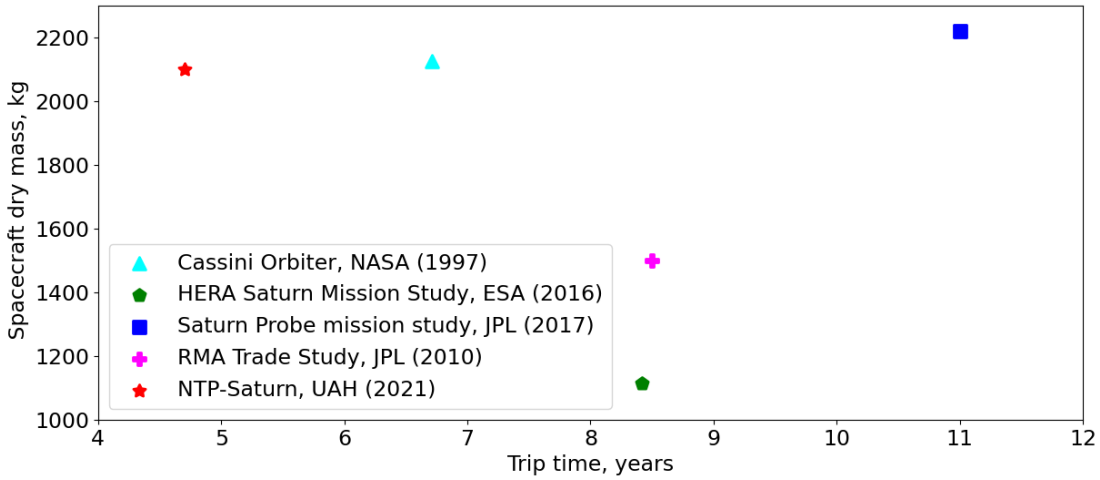

Figure 4.17: Spacecraft dry mass vs trip time for Saturn rendezvous mission.

4.18 show the comparison of NTP powered mission with some of the conceptual missions for Neptune rendezvous using chemical propulsion system. The studies using chemical propulsion system depended on the use of super heavy lift launch vehicle such as SLS Block 2 to close the mission as none of the available commercial launchers could meet the mission requirements of delivering a flagship class missions under the 16-year trip time in a direct transfer trajectory. The NTP point design study was optimized in order to have a maximum trip time of no more than 13 years using commercial launch vehicle with capability to deliver a minimum spacecraft dry mass of 1500 kg as applicable for the flagship class missions.

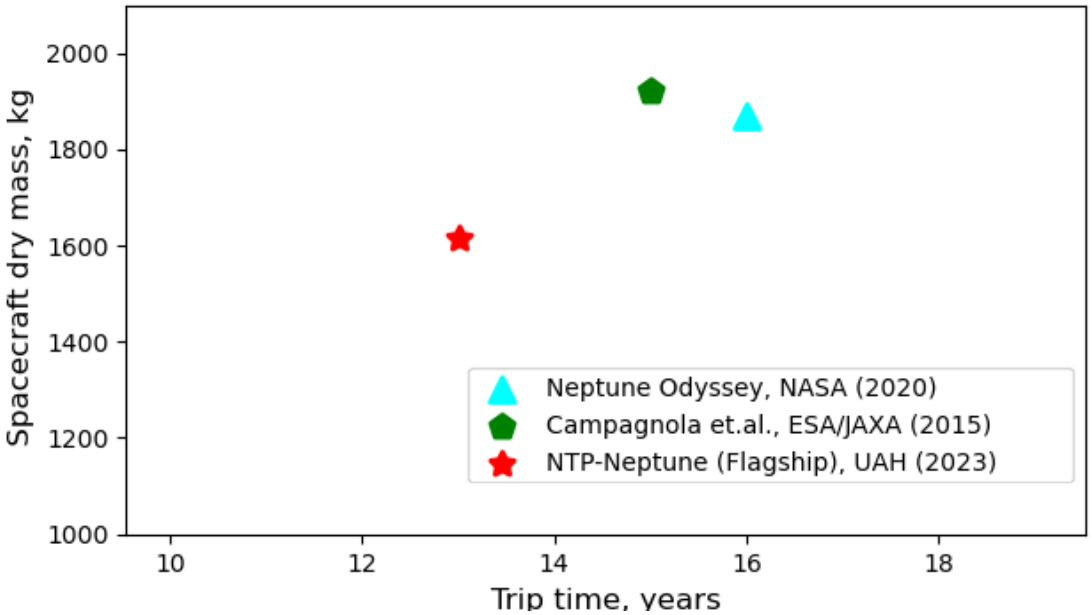

Figure 4.18: Spacecraft dry mass vs trip time for Neptune rendezvous mission.

Chapter 5. Engine System Trades for Robotic Missions

The DRM trade tree and the quantifiable FoM's in the Chapter 3, filtered out key variables in the integrated modeling environment using MBSE. The DRM trade tree provided the manageable number of architectures for the Jupiter and Neptune mission simulations for the complete tradespace exploration of the NTP for robotic missions to the outer solar system. Using the modeling approach, the point design studies in Chapter 4 confirmed that the selected mission architecture for the NTP system can enable ambitious robotic missions to the Gas and Ice giant systems envisioned by the decadal studies.

This chapter will leverage the results from the Chapter 4 and expand the tradespace to answer Research Questions #2 and #3. Using the insights gained from the literature reivew (Chapter 2) and the mission model along with the DRM discussion (Chapter 3), the engine trades are evaluated for the rendezvous mission to Jupiter and Neptune in section 5.1 and 5.2 respectively. The NTP engine thrust to weight parameters used in the analysis has been referred from the LEU cermet paramodel design data for engine thrust class ranging from 5 klbf to 30 klbf which is also shown as a plot in Figure 5.1 [103]. The propellant tank is sized for every mission analysis with different engine thrust class and the total $LH2$ propellant requirement depending on the departure ΔV requirement. The

mission architecture feasibility for expendable and non-expendable missions is presented in section 5.3. Finally, section 5.4 summarizes the chapter and answers the remaining research questions.

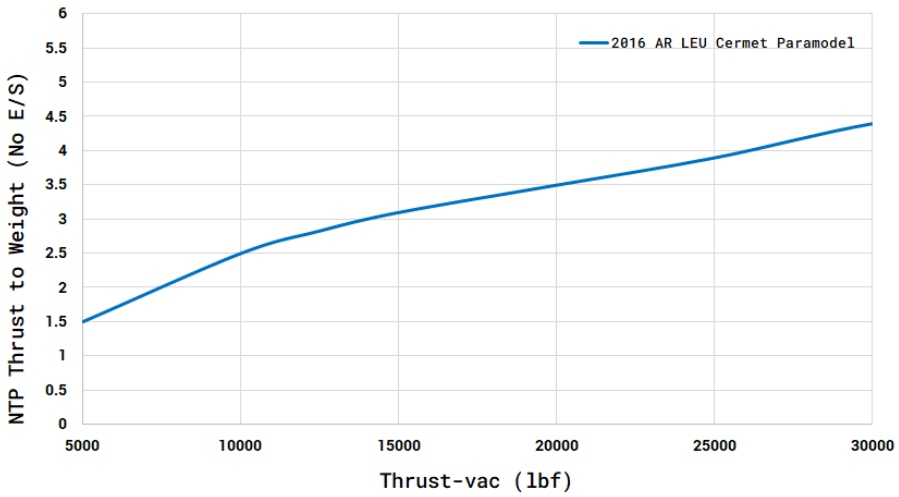

Figure 5.1: LEU NTP cermet paramodel thrust to weight without external shield curve [103].

5.1 Engine System Trades for Missions to Jupiter

For an exhaustive tradespace exploration for NTP system for missions to Jupiter there are four mission classifications inclusive of spacecraft class and trajectory types are considered in the analysis *i.e.,* Flagship class, New Frontiers class, Type-I and Hohmann trajectory missions using expendable NTP configuration. The flagship and new frontiers class missions are initially analysed for most efficient Hohmann transfer trajectories for maximum payload delivery. The direct transfer trip time is also within the maximum trip-time requirement as per the described DRM trade tree and requires lower Jupiter orbit insertion ΔV of

400 m/s. The fast transfer Type-I trajectory missions are also analyzed which can be implemented for time critical missions.

5.1.1 Results for Flagship Class Missions

The mission analysis using engine thrust class from 05 klbf to 30 klbf is performed in an increment of every 1 klbf therefore requiring a total of twenty six mission designs for every distinct Earth departure orbit. The departure orbit considered in the analysis is from 1000 km to 2000 km in altitude with increment of every 200 km. Thus, a total of 156 mission designs were closed to determine the engine performance towards enabling a flagship class mission. The following NTP system analysis is presented for Earth departure circular orbit of 2000 km to inject a spacecraft mass of 4.35 mT to the Jupiter's orbit. The IMLEO for the range of engine thrust class is shown in Figure 5.2 along with the departure ΔV requirements in Figure 5.3 and engine run time in Figure 5.4. Although, the analysis was performed for engine thrust starting with 5 klbf however, in the mentioned plots the lowest data point is from 8 klbf is due to the reason that for 5 klbf to 7 klbf the mission did not close within the required constraints and would have required prohibitively large IMLEO which will be beyond the lift off carrying capacity of the launch vehicle to the destination orbit.

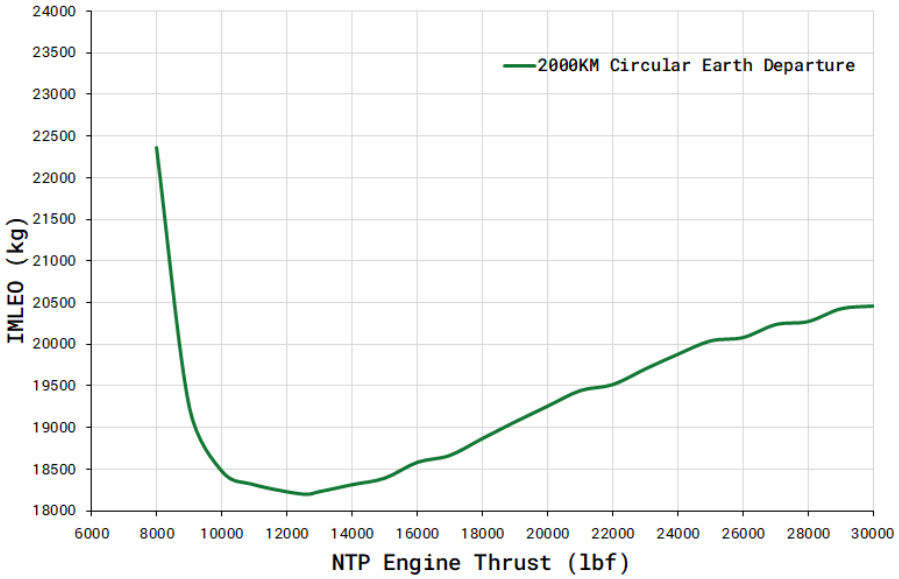

Figure 5.2: IMLEO vs engine thrust for 2000 km circular departure orbit.

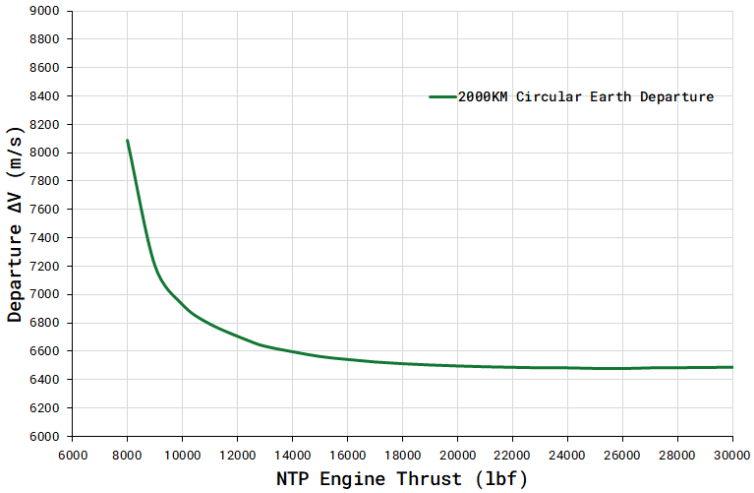

Figure 5.3: Departure ΔV vs engine thrust for 2000 km circular departure orbit.

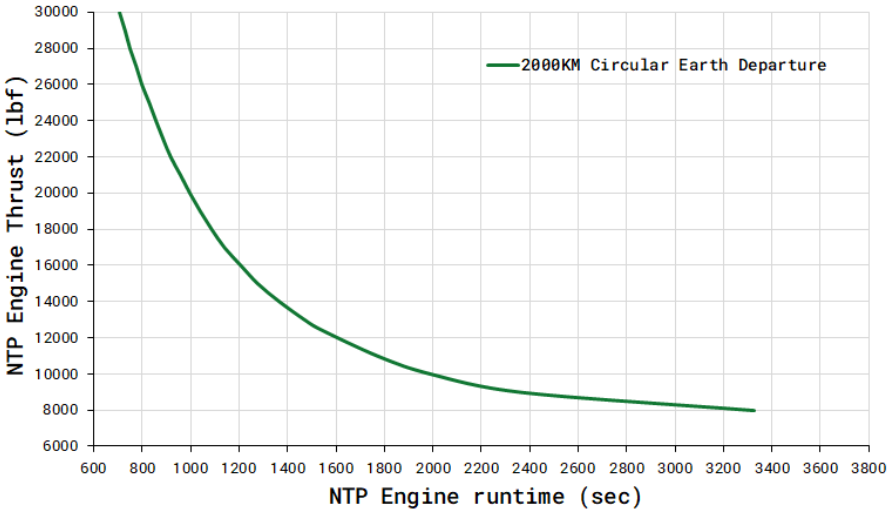

Figure 5.4: NTP engine run time vs thrust for 2000 km circular departure orbit.

All the above three plots are interlinked to each other. Firstly, the finite maneuver analysis to determine the engine run time shows that the lower thrust engines require significantly longer duration to achieve the required departure ΔV. This increase in run time also incorporates gravity losses and thrust vector control losses with majority of the ΔV losses among the two being from the gravity losses. The ΔV loss for the engine thrust can be seen in Figure 5.5 where for the lower thrust engines the gravity losses can be up to 20 percent of the total departure ΔV and almost negligible for the higher end thrust engines. This departure ΔV requirement is then needs to be compensated for the losses and therefore it can be noticed that the lower thrust engine have a much higher run time. The engine run time for the lowest 8 klbf engine is at 55.5 min and for the highest thrust of 30 klbf at 12 min during the TJI maneuver.

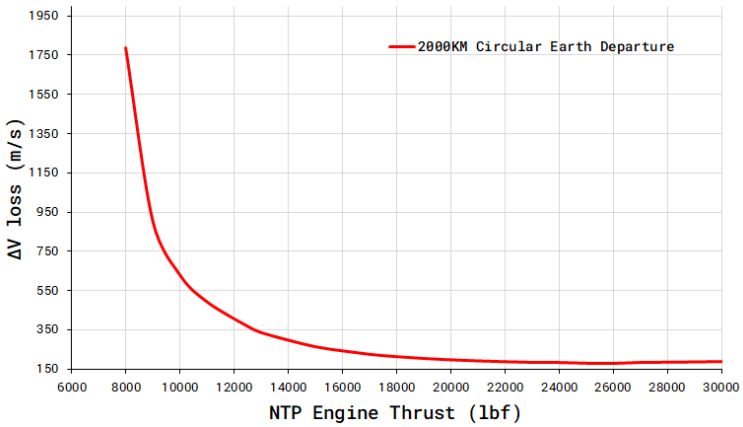

Figure 5.5: ΔV vs Thrust during the TJI maneuver.

The higher ΔV requirement for the lower thrust engines also has cascading impact on the IMLEO due to higher propellant requirement. This impacts the tank re-sizing and therefore the redesign of the NTP injection stage. Therefore,

it can be noticed in the Figure 5.2 that the lowest thrust engines have the highest IMLEO of over 22 mT. With the increase in engine thrust, the engine run time decreases and so does the required departure ΔV due to reduced gravity loss. This reduces the IMLEO requirement and it can be seen until the minima at 12.5 klbf engine thrust. The IMLEO using the 12.5 klbf engine is at 18.205 mT which includes 9.9 mT of $LH2$ propellant required to impart 6.66 km/s of departure ΔV and has engine run duration of 25.5 min. Post the minima at 12.5 klbf, the IMLEO increases due to the increase in engine mass. This increase in engine mass is greater than the mass reduction resulting from reduced $LH2$ propellant and the smaller $LH2$ tank, such that the net IMLEO increases, reaching 20.458 mT for the 30 klbf engine.

Similarly, the engine performance for difference LEO departure orbits was analyzed with Figure 5.6, 5.7 and 5.8 showing the impact on TJI ΔV, engine run time and IMLEO respectively.

The TJI ΔV requirement for multiple LEO departure orbits shows that at the lower altitude orbits for lower thrust engine require higher ΔV in comparison to the higher orbit and higher thrust engines. The minimum thrust at 1000 km altitude needed to close the mission and achieve TJI ΔV is at 10 klbf. With the increase in thrust irrespective of the departure orbit the required TJI ΔV is almost the same at 6.5 km/s. Accordingly, the engine run time is proportional to the TJI ΔV with lower thrust engines requiring the higher run time. The maximum run time as shown in Figure 5.7 is for 8 klbf engine for departure orbit at 1800 km altitude and with minimum for 30 klbf engine at 12 min. The IMLEO

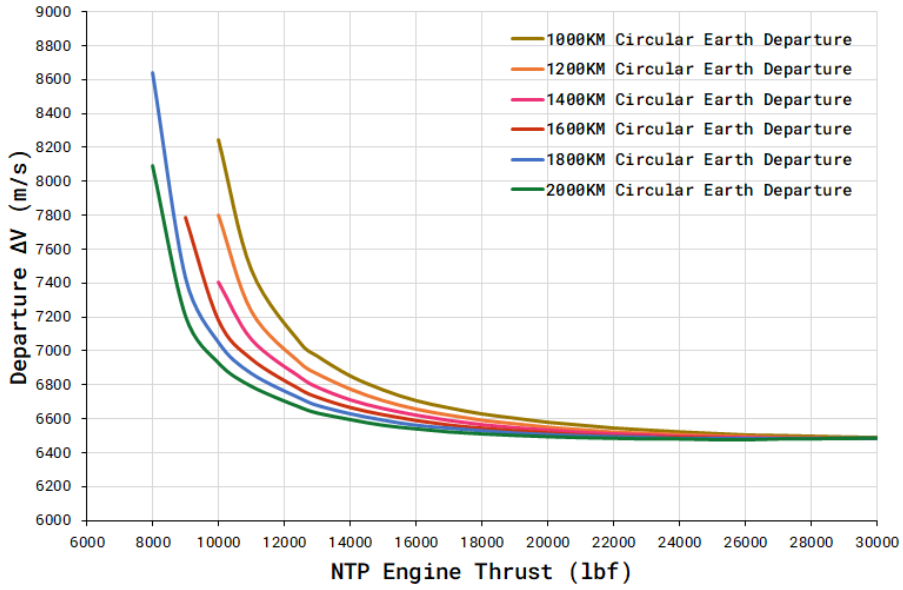

Figure 5.6: Departure ΔV vs engine thrust for multiple LEO circular departure orbits.

curve for different departure orbits is similar to the one shown in Figure 5.2 but with change in minima for each distinct altitude. From the Figure 5.8 it can be noticed that with the decrease in the departure orbit altitude, the IMLEO for the same thrust increases *i.e.,* at 2000 km altitude departure orbit the IMLEO is lowest for 12.5 klbf thrust engine and at 1000 km altitude the lowest IMLEO is for 16 klbf thrust engine. For the lowest 1000 km departure orbit, minimum engine thrust needed to close the mission is at 10 klbf. Table 5.1 shows the minimum IMLEO and its respective thrust class for different departure orbits.

The total trip for all the missions is fixed at 2.74 years and requires a JOI ΔV of 400 m/s. The JOI maneuver is performed using the spacecraft's onboard chemical propulsion system which requires 516 kg of propellant. The

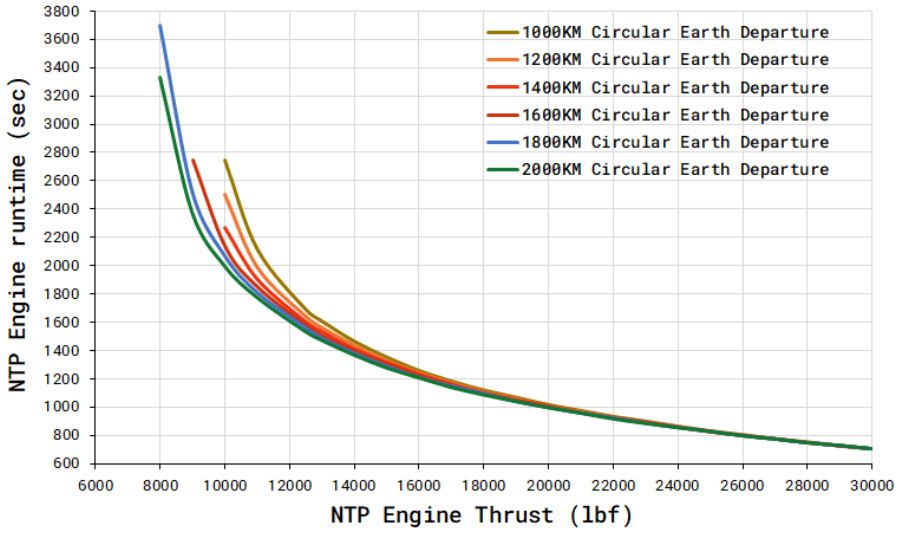

Figure 5.7: NTP engine run time vs thrust for multiple LEO circular departure orbits.

Table 5.1: Minimum IMLEO and its respective thrust class for multiple departure orbits.

LEO Altitude (km)	IMLEO (kg)	NTP Engine Thrust (klbf)
1000	19,051	16 klbf
1200	18,861	15 klbf
1400	18,667	14 klbf
1600	18,467	13 klbf
1800	18,351	13 klbf
2000	18,204	12.5 klbf

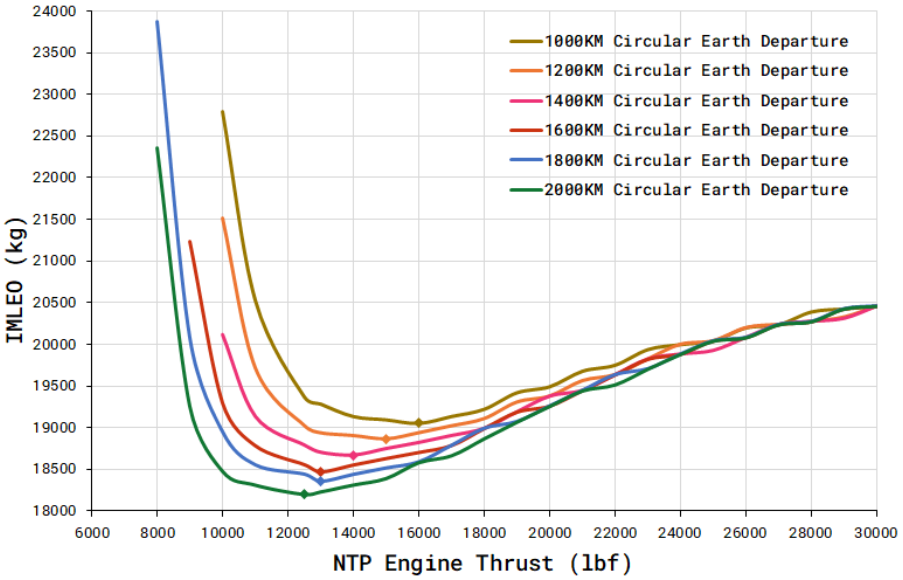

Figure 5.8: IMLEO vs engine thrust for multiple circular LEO departure orbits.

final spacecraft wet mass post JOI maneuver is at 3.83 mT which includes 2.3 mT of spacecraft dry mass.

5.1.2 Results for New Frontiers Class Missions

Spacecraft wet mass of 3,100 kg is used to determine the engine trades for a New Frontiers class mission to Jupiter. The IMLEO as a function of engine thrust for NF class mission is shown in Figure 5.9. When comparing the performance with a Flagship class mission presented in section 5.1.1, it can be noticed that the engine thrust for a minima IMLEO is reduced and is at 10 klbf in this case in comparison to 12.5 klbf for flagship class mission. The maximum IMLEO of 17.3 mT is for the mission using a 30 klbf engine thrust. The Similarly, engine trades were performed for multiple LEO departure orbits with Figure 5.10 and 5.11 demonstrating departure ΔV and engine run time as a function of engine thrust. The lowest engine thrust of 9 klbf is needed for the 1000 km departure orbit and minimum engine thrust of 7 klbf for higher departure orbit at 2000 km altitude. The mission did not close for 5 klbf and 6 klbf engine thrust within the constrained mentioned in the DRM trade tree.

Among the closed missions, the highest departure ΔV needed is for 7 klbf engine thrust departing at 1600 km circular orbit. The total engine run time to achieve the departure ΔV in the analysis ranges from 51.2 min to lower thrust engine and 10 min for higher thrust engines. Figure 5.12 shows the IMLEO as a function of engine thrust ranging from 7 klbf to 30 klbf for multiple LEO departure orbits. The highest IMLEO requirement is of 18.02 mT for 7 klbf engine with departure orbit altitude of 1,600 km. For the missions using higher thrust engines the IMLEO is at 17.3 mT irrespective of the departure orbit constraints.

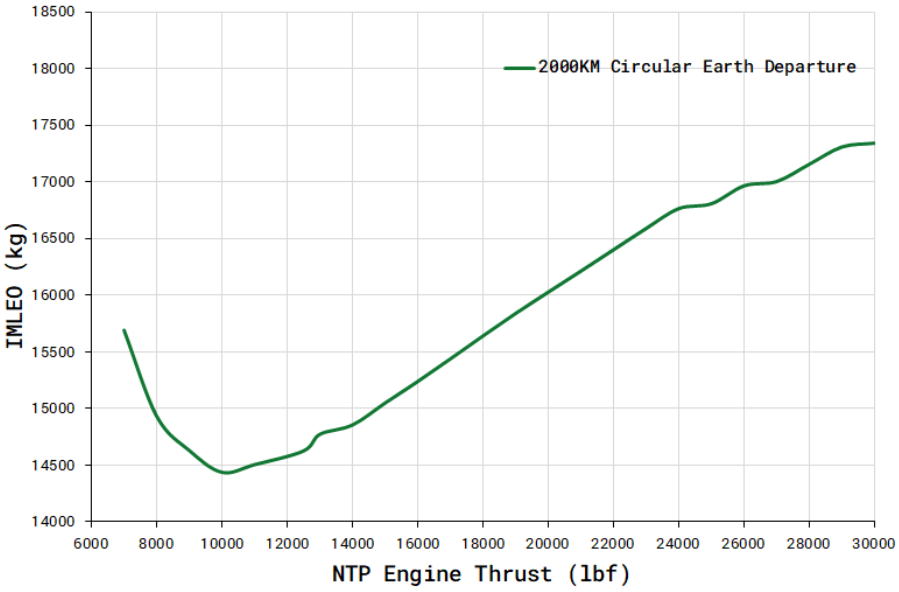

Figure 5.9: IMLEO as a function of engine thrust for NF class mission departing at 2000 km circular LEO orbit.

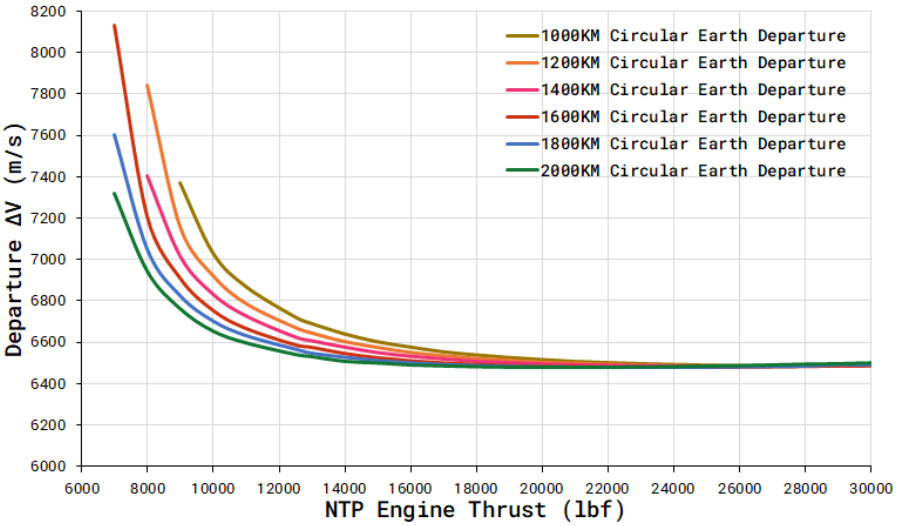

Figure 5.10: Departure ΔV as a function of engine thrust for NF class mission for multiple LEO circular departure orbits.

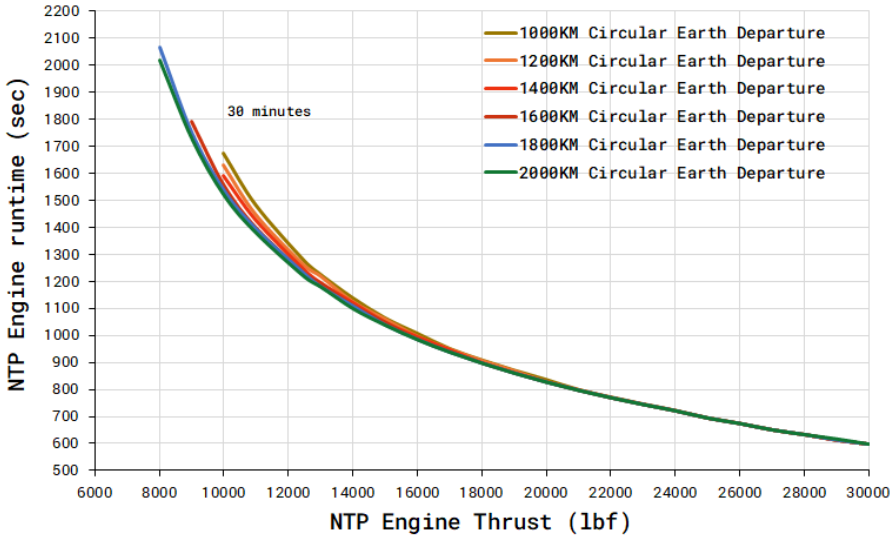

Figure 5.11: Engine run time as a function of engine thrust for NF class mission for multiple LEO circular departure orbits.

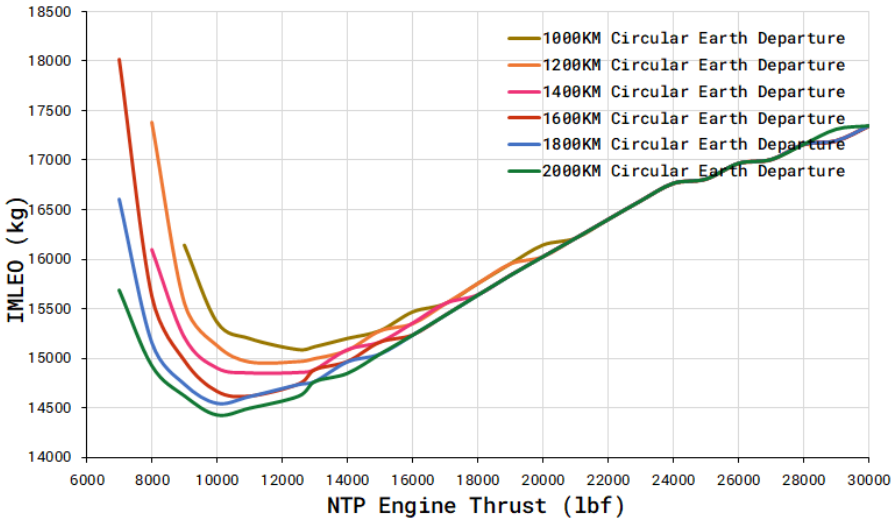

Figure 5.12: IMLEO vs engine thrust for NF class missions for multiple circular LEO departure orbits.

As expected, Figure 5.12 shows that the minima in IMLEO is is different for each departure orbit with respect to the engine thrust. To achieve the lowest IMLEO the engine thrust is inversely proportional to the departure orbit altitude. Table 5.2 shows the minimum IMLEO and its respective thrust class for different departure orbits to enable a NF class mission to Jupiter.

Table 5.2: Minimum IMLEO and its respective thrust class for multiple departure orbits to enable NF class mission.

LEO Altitude (km)	**IMLEO (kg)**	**NTP Engine Thrust (klbf)**
1000	15,090	12.5 klbf
1200	14,969	11 klbf
1400	14,852	11 klbf
1600	14,619	11 klbf
1800	14,551	10 klbf
2000	14,434	10 klbf

In the expendable configuration, the JOI maneuver is performed usign the chemical propulsion system. The final spacecraft mass post JOI is at 2.58 mT which includes 1.8 mT of spacecraft dry mass.

5.1.3 Results for Type-I Trajectory Missions

The fast transfer using Type-I trajectory missions were also evaluated for the Jupiter rendezvous missions. The circular departure orbit constrained in the analysis was at an 2,000 km altitude to maximize the use of launch vehicle payload delivery capability for the highest possible parking orbit. The purpose of this analysis was to understand the impact on IMLEO for a mission trip times under 2.74 years considered previously for Hohmann transfers. Figure 5.13 shows the selected Earth to Jupiter type-I trajectories for missions using NTP engine thrust ranging from 10 klbf to 30 klbf and the Table 5.3 shows the IMLEO and trip time for the thrust engines.

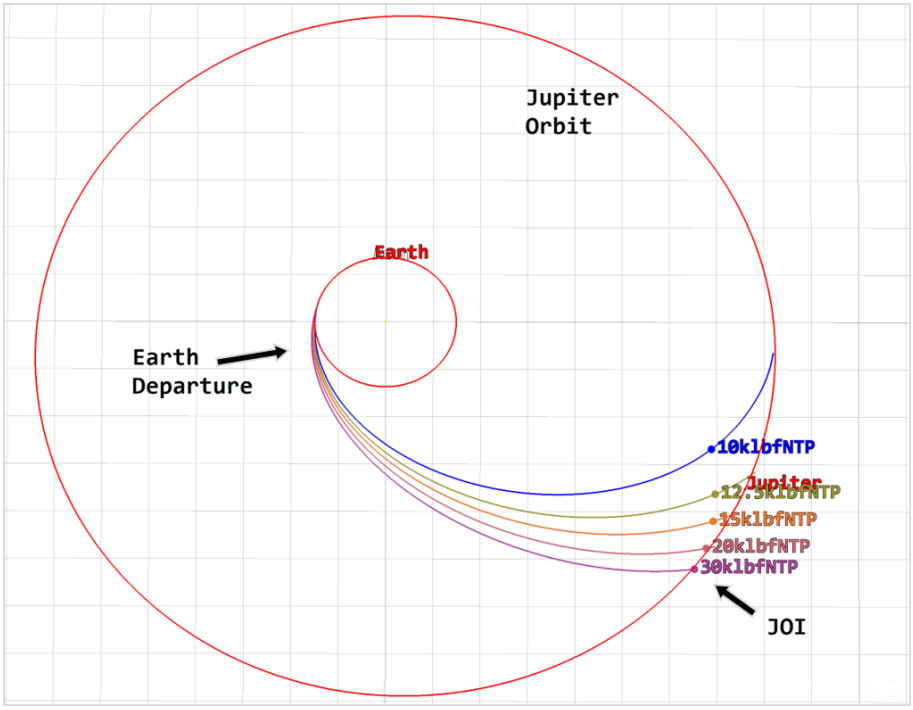

Figure 5.13: Selected Earth-Jupiter type-I transfer trajectories.

Table 5.3: IMLEO and trip time for the NTP engine class using type-I trajectory missions.

NTP Engine Class (klbf)	**IMLEO (kg)**	**Trip Time (years)**
12.5 klbf	18,903	2.15
15 klbf	19,327	1.96
20 klbf	20,423	1.87
30 klbf	21,857	1.82

Mission analysis has demonstrated that for the given configuration the trip time for Jupiter rendezvous can be as low as 1.82 years with maximum IMLEO of 21.8 mT. The type-I trajectory mission is possible but will not be recommended for the traditional planetary science missions unless the mission is time critical. This is due to the fact that the higher departure velocity also necessitates a higher arrival ΔV for about 400 m/s for Hohmann transfers to up to 2.5 km/s for type-I fast transfer missions. This has an impact on the overall vehicle IMLEO with an increase of over 20% for Type-I mission using a 30 klbf engine when compared with the IMLEO required for a Hohmann transfer mission mainly due to higher propellant requirement to achieve the JOI ΔV requirement.

5.1.4 Specific Impulse Sensitivity

The mission performance for a flagship class mission to Jupiter was analysed for the change in I_{sp} and its impact on mission parameters. Specific impulse ranging from 850 seconds to 900 seconds was used to perform the mission analysis. Figure 5.14 shows the departure ΔV as a function of engine thrust for different I_{sp} of 850, 875 and 900 s. The impact of change in I_{sp} is largely seen for missions using lower thrust engines from 8 klbf to 15 klbf. Missions using lower I_{sp} have higher ΔV losses due to decrease in the efficiency thereby requiring longer engine run duration. Higher I_{sp} also enables missions with lower thrust engines which can be seen from the Figure 5.14 that missions using 900 s of I_{sp} can enable TJI maneuver using an 8 klbf engine in comparison to the 9 klbf thrust for lower I_{sp} NTP engines.

Figure 5.15 shows the impact of I_{sp} on IMLEO for multiple engine thrusts class. The higher I_{sp} engines have a lower IMLEO requirement when compared with lower I_{sp} NTP engines. The minimum IMLEO for the Jupiter rendezvous mission using a 12.5 klbf engine with specific impulses of 900 s, 875 s and 850 s are 18.2 mT, 18.9 mT and 19.6 mT respectively thus having a difference of 0.7 mT for every 25 s of change in I_{sp}.

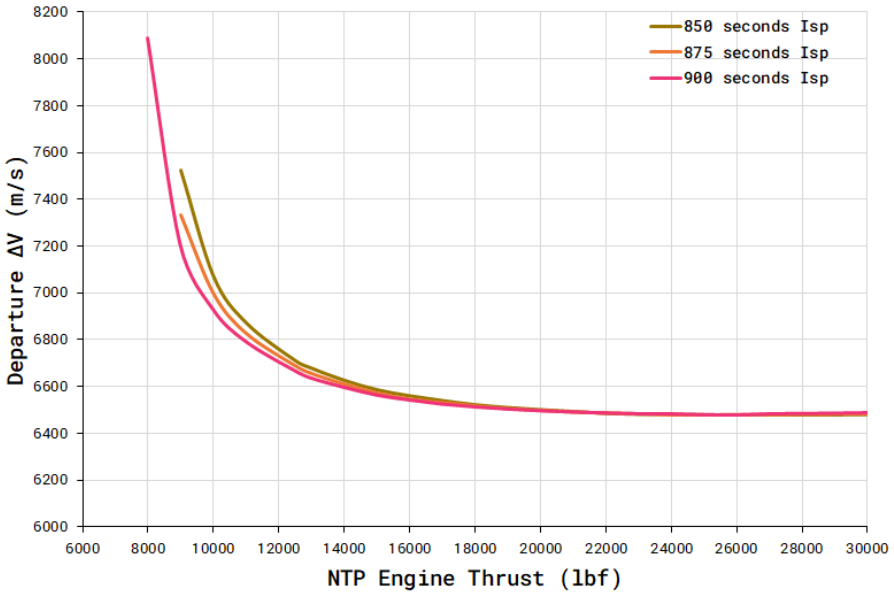

Figure 5.14: I_{sp} sensitivity on departure ΔV vs engine thrust.

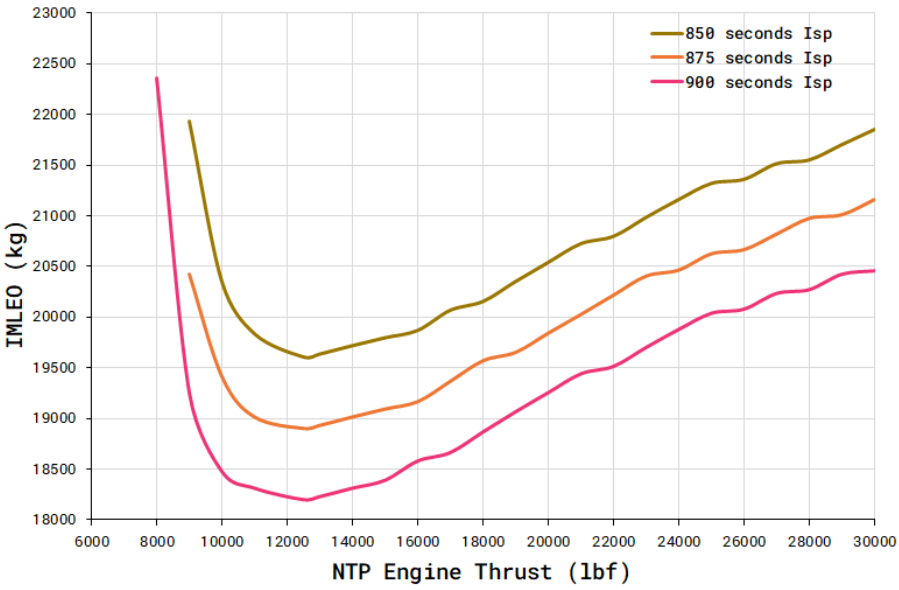

Figure 5.15: I_{sp} sensitivity on IMLEO vs engine thrust.

5.2 Engine System Trades for Missions to Neptune

In order to identify the enabling NTP engine thrust for rendezvous mission to the Ice giant planet Neptune, flagship and new frontiers class missions using type-I and type-II trajectories were considered. The Hohmann transfer between Earth and Neptune is at just over 30 years and with the total trip time constrained in the analysis of no more than 14 years the mission analysis did not include Hohmann transfers. Due to the high energy mission, the highest circular departure orbit at an altitude of 2000 km was considered to maximize the payload delivery capability of the commercial launch vehicle. The mission goal for engine trades to Neptune is to maximize the spacecraft delivery capability for a fixed trip time (13 years for flagship class mission and 10 years for New Frontiers class mission) with IMLEO and NTP injection stage and spacecraft configuration within the requirements of the Vulcan Heavy and New Glen launch vehicles.

5.2.1 Results for Type-I Trajectory Missions

The direct Earth-Neptune transfer mission focused on delivering a spacecraft mass of over 1.5 mT to the Neptune orbit using an expendable NTP configuration with maximum trip time of 14 years. The departure ΔV for the engines performance evaluation ranges from 10.74 km /s to 9.26 km/s for 5 klbf to 30 klbf. The NTP injection configuration used the maximum possible $LH2$ propellant for the mission which is at 14 mT to achieve the departure ΔV. The spacecraft mass post NOI vs the engine thrust during the TNI maneuver is shown in Figure 5.16.

The spacecraft delivery mass is in the range of 1,033 kg to 1,614 kg with lowest mass delivered by 5 klbf engine and maximum by 13 klbf engine. The engine thrust range which could deliver the spacecraft mass of over 1.5 mT are 10 klbf to 17 klbf. Figure 5.17 shows the IMLEO vs engine thrust at the TNI maneuver with IMLEO range of 19.5 mT to 21.1 mT.

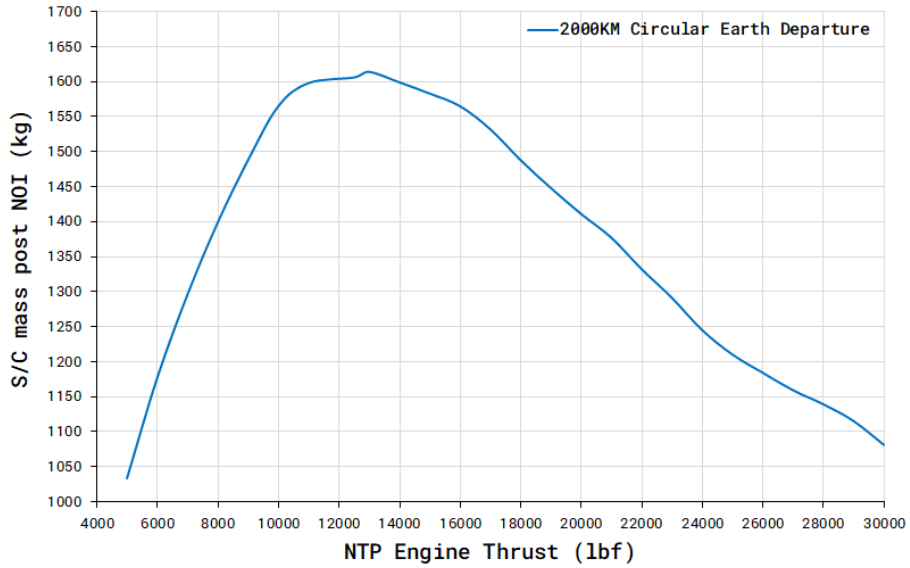

Figure 5.16: Spacecraft mass post NOI vs NTP engine thrust during the TNI maneuver.

The NTP engine run time during the TNI maneuver analysis for engine thrust of 8 klbf and under was determined to be significantly higher with total run time during the Earth departure maneuver to be at 91 min for 5 klbf engine. This longer during run time of the engine might not be desirable due to the limits with the turbo-machinery. The run time for the engine thrust which could deliver the spacecraft mass of over 1.5 mT was in the range of 27 min to 45.5 min as seen in Figure 5.18.

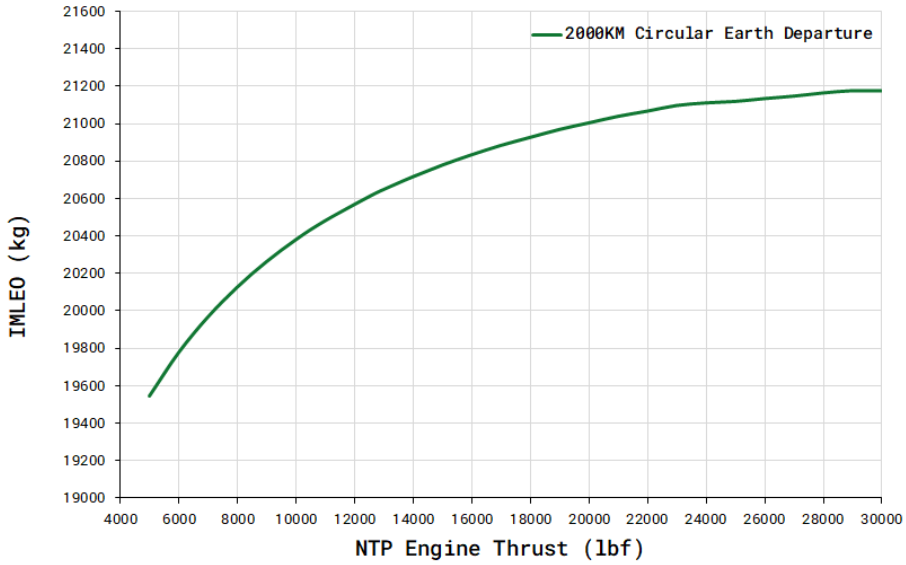

Figure 5.17: IMLEO vs engine thrust for Neptune rendezvous mission using type-I trajectory.

The spacecraft heliocentric trajectory is shown in Figure 5.19 which has a total trip time of 14 years with TNI ΔV of 9,688 m/s and arrival ΔV for NOI at 860 m/s for the mission using 13 klbf engine.

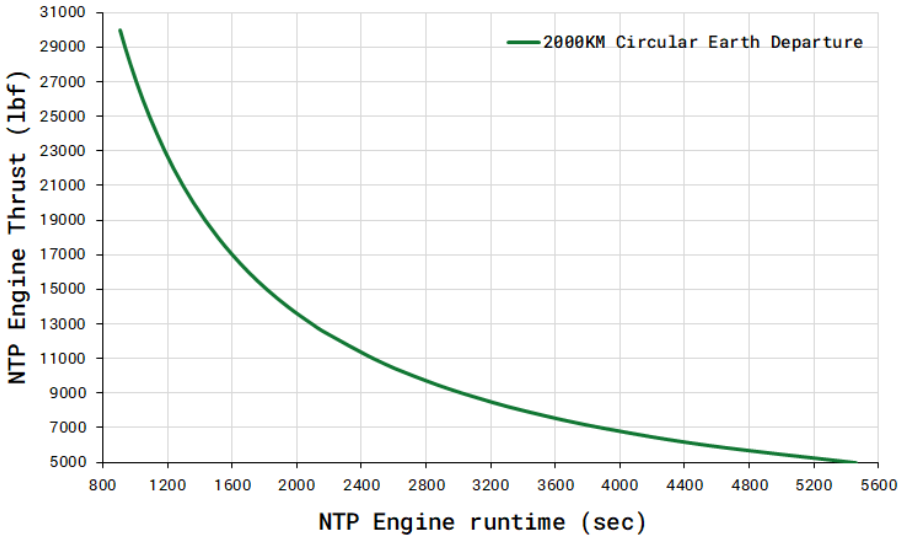

Figure 5.18: Engine run time during Earth departure for Neptune rendezvous mission using type-I trajectory.

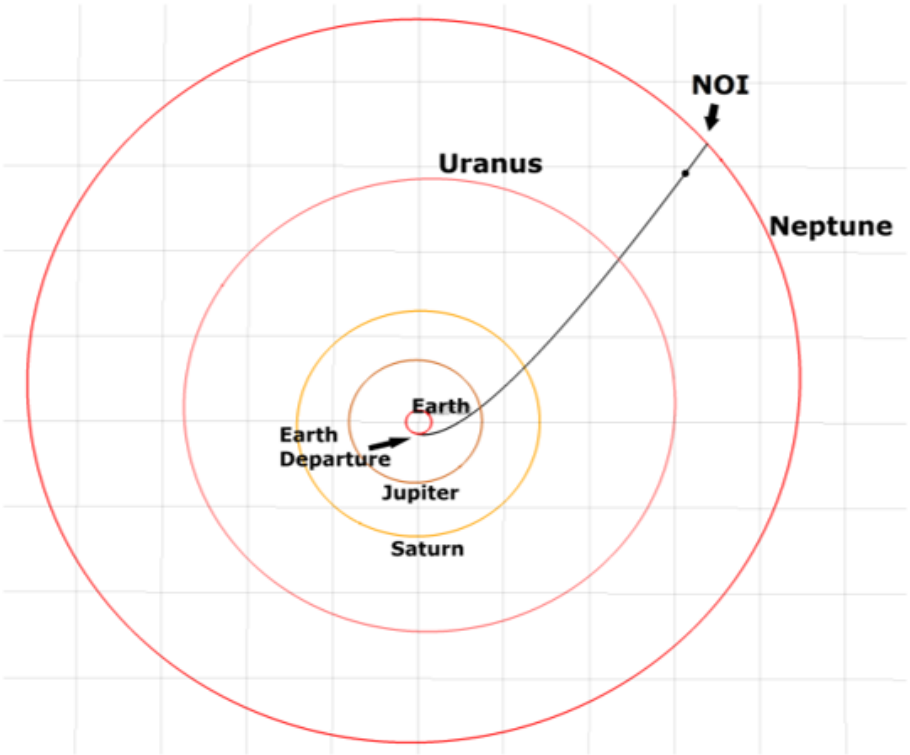

Figure 5.19: Spacecraft E-N type-I trajectory using a 13 klbf NTP engine.

5.2.2 Results for Type-II Trajectory Missions

The engine trades for type-II trajectory missions involved Jupiter gravity assist (EJGA) to Neptune to enable New Frontiers class missions with at least 1 mT of spacecraft mass delivery to Neptune orbit using an expendable NTP configuration. The total trip time in this analysis was constrained to 10 years for medium class missions with trip time being relevant to the longest primary mission of New Frontiers class New Horizons mission. Figure 5.20 and 5.21 shows the spacecraft mass delivered post NOI as a function of engine thrust and engine run time during the TNI maneuver. The spacecraft payload delivery requirement were met for the engine thrusts in the range of 12.5 klbf to 15 klbf with engine run time during the TNI maneuver being 24 min to 30 min in total.

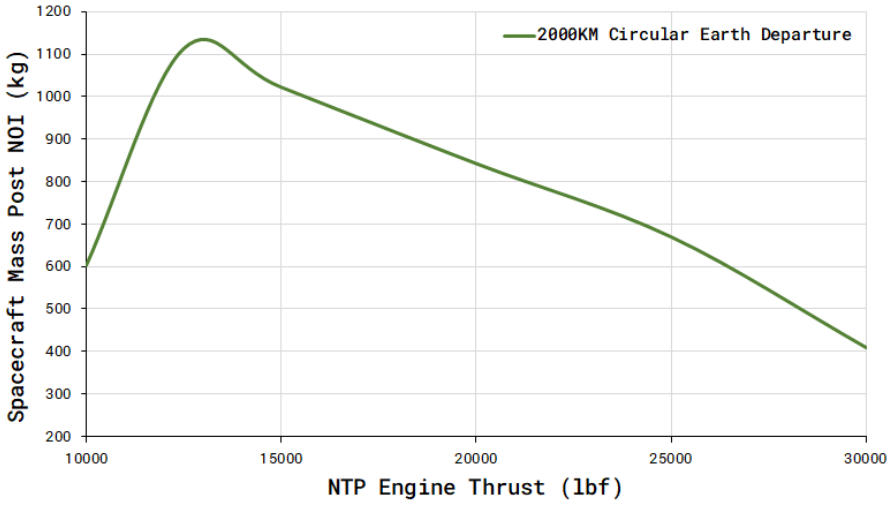

Figure 5.20: Spacecraft mass post NOI vs engine thrust using EJGA trajectory.

Figure 5.22 shows the spacecraft trajectory to Neptune using Jupiter gravity assist using a 12.5 klbf NTP engine. The TNI maneuver ΔV magnitude is

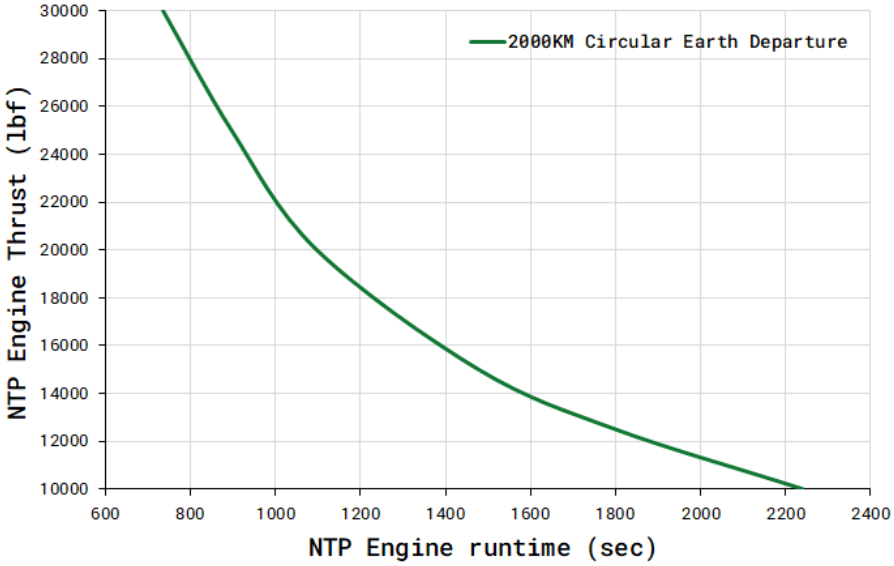

Figure 5.21: Engine run time during Earth departure for Neptune rendezvous mission using EJGA trajectory.

7.2 km/s and has a trip time of 1.6 years between Earth and Jupiter. During the Jupiter gravity assist the spacecraft's heliocentric velocity magnitude is increased by 23 km sec. Figure 5.23 shows the spacecraft's velocity magnitude and radial distance from Sun during the Earth to Neptune transfer.

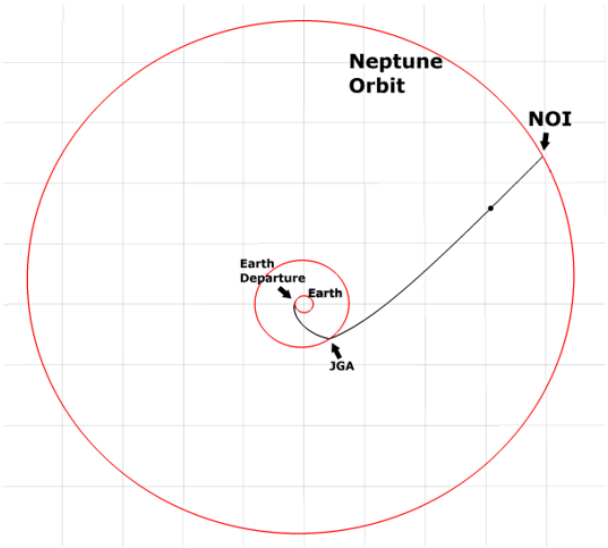

Figure 5.22: Spacecraft EJGA trajectory to Neptune using a 12.5 klbf NTP engine.

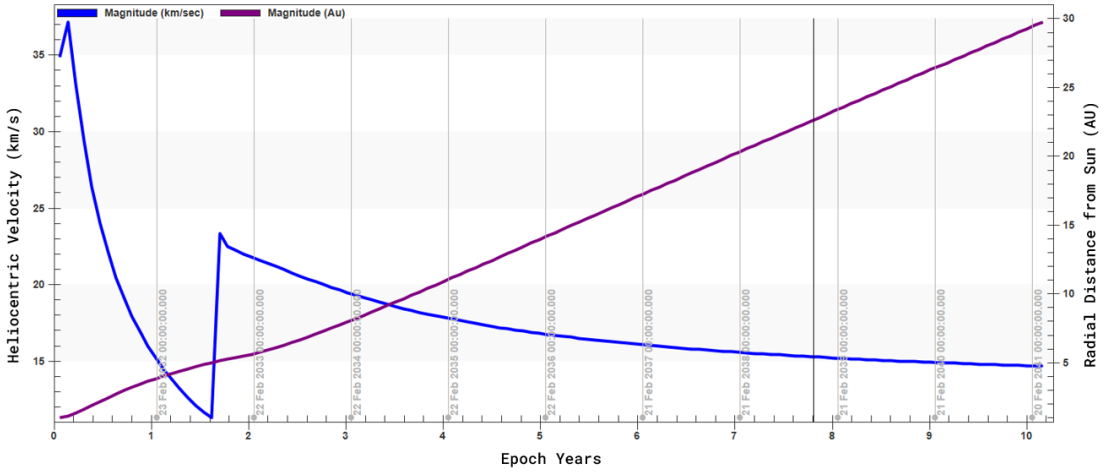

Figure 5.23: Spacecraft heliocentric velocity and radial distance from Sun for Neptune rendezvous mission using a 12.5 klbf NTP Engine.

5.3 Expendable and Non-Expendable Mission Architectures

This section explores the feasibility of non-expendable configuration and compares the performance between the mission architecture using expendable and non-expendable NTP system. In the non-expendable configuration, the NTP system is utilized for both Trans-Planetary Injection (TPI) and Planetary Orbit Insertion (POI) maneuvers. One major challenge for POI maneuver using $LH2$ propellant is the long term storage with Zero Boil-Off (ZBO). The mission analysis presented in this study uses a passive ZBO system to reduce the spacecraft delivered mass penalty when compared with using active cryocoolers. To achieve ZBO for $LH2$ propellant, the propellant tank view is isolated to the deep space and the use of several shades and Multi-Layer Insulation (MLI) to protect the tank from the Sun and spacecraft bus post the TPI maneuver and during the heliocentric cruise phase of the mission.

Figure 5.24 shows the example configurations of the shades which can be used to achieve ZBO storage [104]. The shade geometry used in the three configurations is based on the thermal requirements and the constraints on the spacecraft attitude. The M1 configuration design covers the propellants tank which assumes no attitude constraints. The M3 shade configuration uses the conical shade and constraints the spacecraft attitude from both Sun and planetary albedo.

The JPL's thermal model of a ZBO cryogenic propellant system using MLI blanket for $LH2$ propellant tank in a cone shape to bahve like a "V" grove

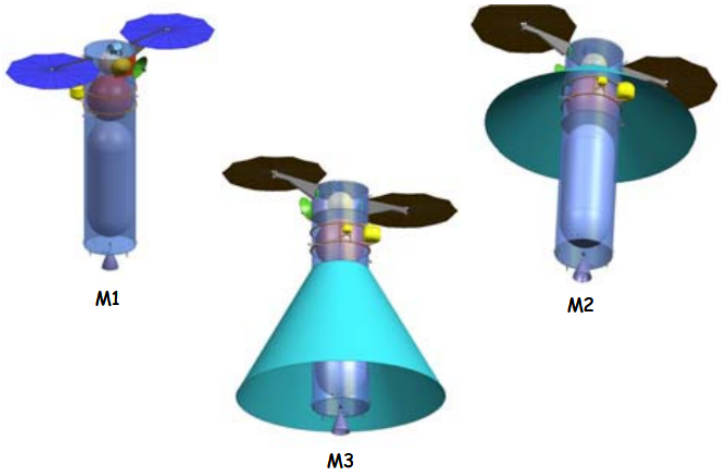

Figure 5.24: Spacecraft configurations using passive thermal protection system [104].

radiator was modeled with an reflective emmisivity of 0.004 [105]. Studies have also demonstrated that the $LH2$ propellant can be stored for longer period of times using an actively cooled inner shield and MLI blanket [106]. However. due to the use of active cooling the total system mass to keep the propellant in cryogenic state will be at 2 mT and will require more than 100 MLI layers. The mass penalty of 2 mT to achieve the ZBO will have significant impact on the overall spacecraft delivery capability of the NTP system therefore an active ZBO system will not be feasible for flagship and new frontiers class robotic missions to the outer planets.

A NASA experimental study on long term storage of cryogenic propellant using passive ZBO system was demonstrated for 1200 days (3.28 years) of simulated mission to the gas giant planets [107]. The passive thermal protection system consisted of 34 layers of MLI blanket supported by 12 fiber-glass struts

and two double alumnized mylar sheeted shadow shields [108]. The test results for the near Earth phase of the mission measured the heat transfer to the hydrogen tank at 22 Watt. To keep the $LH2$ in the cryogenic state for the majority of the mission in deep space the allowable heat transfer rate was 0.21 Watt. The tests for deep space simulation with active attitude control resulted in measured heat transfer rate of 0.11 Watt which is half of the allowable hear transfer rate. The total tank pressure increase at the end of 1200 days mission simulation resulted in 50 psi which was within the limits in order to eliminate the propellant venting. The total passive ZBO system mass in the experimental study is at $1.54kg/m^2$ and has been used in the results presented in this section. The total calculated thermal protection system mass is at 310 kg for the designed $LH2$ propellant tank for the designed NTP system.

The performance comparison between expendable and non-expendable architectures was for the Jupiter rendezvous mission with trip times ranging from 1.49 years to 2.72 years. The simulated missions in the analysis are given in the Table 5.4 with mission timelines ranging from 2028-2035. For the non-expendable configuration a single 12.5 klbf with 900 s I_{sp} NTP engine is used for TJI and JOI maenuvers and for the expendable configuration a single 12.5 klbf engine with 900 s I_{sp} is used for the TJI maneuver and a chemical engine with thrust of 1100 N and I_{sp} of 323 s is used for the JOI maneuver.

Table 5.4: Jupiter rendezvous mission opportunities between 2027-2035 with trip time in range from 2.72 to 1.49 years.

Departure	**Arrival**	**Injection** C_3 (km^2/s^2)	**Abs. DLA** (deg.)	**Trip time** (years)	**TJI** ΔV (m/s)	**JOI** ΔV (m/s)
31-Dec-28	19-Sep-31	79.3	17	2.72	6370	220
27-Nov-27	24-Mar-30	86.2	35	2.32	6640	275
15-Dec-28	22-Jan-31	83.1	22	2.1	6510	381
23-Feb-31	26-Dec-32	81.2	-19	1.84	6440	510
3-May-33	1-Jan-35	87.9	-33	1.66	6680	593
29-Mar-32	24-Sep-33	94.5	-29	1.49	6900	937

Figure 5.25 shows the JOI ΔV requirements for the range of trip times considered in the mission analysis in order to compare the performance of both the mission architectures. The JOI ΔV is lowest for the mission using Hohmann transfer trajectory and maximum for the mission with trip time of 1.49 years using high energy Type-I transfer.

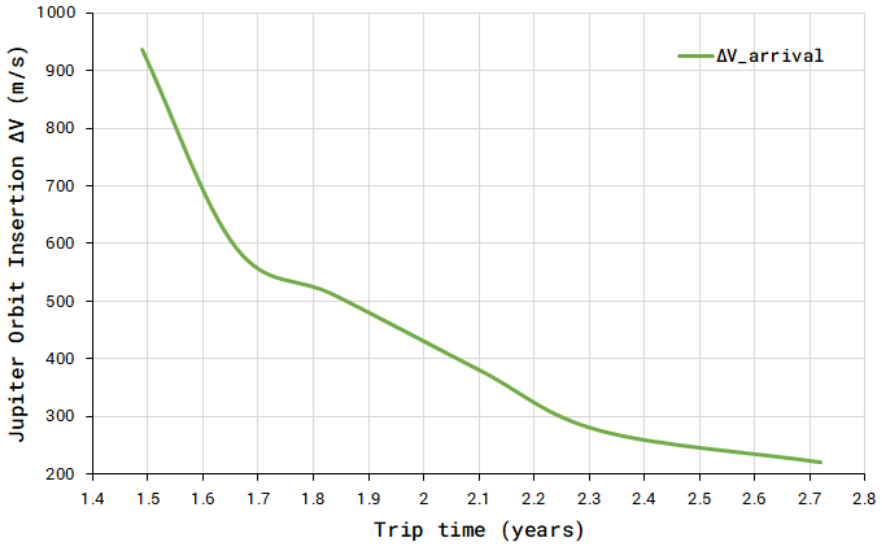

Figure 5.25: Jupiter orbit insertion ΔV requirement for the range of trip times.

To compare the performance of the considered architectures, the figure of merit is to determine the maximum spacecraft mass delivered in the Jupiter's orbit post JOI maneuver. Figure 5.26 shows the comparison of spacecraft mass delivered using the chemical propulsion for JOI maneuver in the expendable configuration and using NTP engine for JOI maneuver in the non-expendable configuration. For lower energy mission using Hohmann transfer trajectory, the expendable configuration has the higher payload delivery capability thus traditional propulsion system outperforms for missions with lower arrival ΔV. The

gap however reduces as the JOI ΔV requirement increases for the type-I transfer missions. For the fastest mission considered in the analysis with trip time of 1.49 years to Jupiter the expendable and non-expendable performance are similar with spacecraft mass of 3200 kg delivered to Jupiter orbit post JOI maneuver..

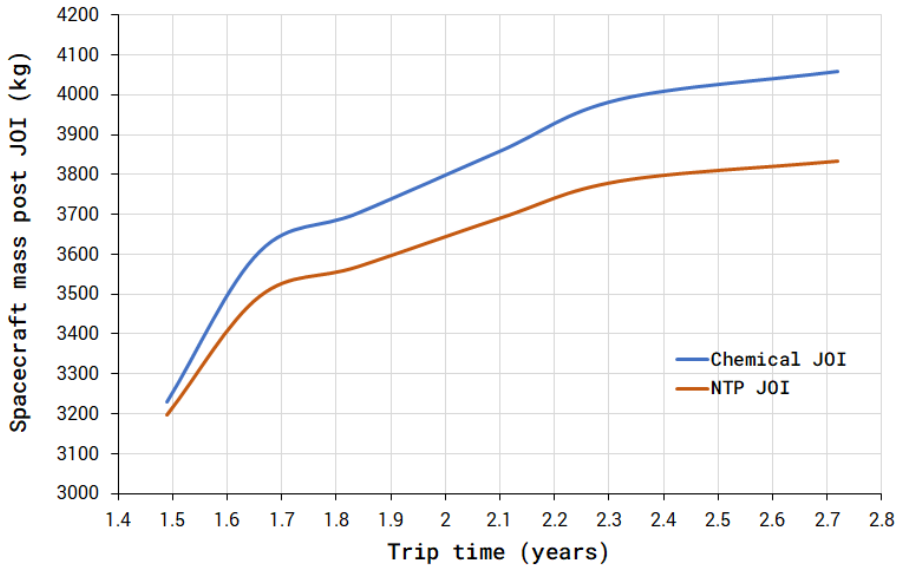

Figure 5.26: Spacecraft mass delivered post JOI using expendable and non-expendable configuration.

5.4 Chapter Summary and Answering Research Questions #2 and #3

This chapter discusses the results of NTP engine trades for robotic missions to the outer planets. As discussed in the DRM trade tree, the missions to Gas giant Jupiter and Ice giant Neptune can provide the solution space of the NTP engine parameters for flagship and New-frontiers class missions. The engine trade for Jupiter are performed for combination of spacecraft class and possible trajectories (Hohmann and type-I). Section 5.1 also discusses the specific impulse

sensitivity for missions to Jupiter and identifies the impact on IMLEO for lower I_{sp} NTP powered missions. The results demonstrated that the NTP engines even with 850 s of I_{sp} can enable flagship missions to the outer planets. Results on engine system trades for missions to Neptune using type-I and type-II trajectories have demonstrated the capability to deliver flagship and new-frontiers missions within the 13 and 10 years of trip times respectively. The trade-offs between the expendable and non-expendable missions architectures are presented in section 5.3 which also discusses the challenges with respect to the ZBO storage of the cryogenic propellants for long duration missions.

The performance comparison of mission architectures for rendezvous mission to Jupiter can be used to answer Research Question #2 *What is an enabling mission architecture for the robotic missions using NTP systems?* The results on spacecraft mass delivery post JOI for the range of trip-times between expendable and non-expendable missions have demonstrated that to enable current planetary science missions an expendable architecture will be preferred due to its higher payload delivery capability. The architecture also eliminates the requirement of long duration $LH2$ storage as NTP system is only used during the TPI maneuver. The non-expendable architecture using the described ZBO storage approach can have significant benefits for missions that share two characteristics:

1. Very large mission ΔV requirement: The planetary missions designs which are highly dependent on short trip times such as missions to the ocean worlds where region of interest to the scientific community could get into seasonal shadow for longer period of time [109] or missions targeting small

celestial bodies in highly elliptical orbit which would require high planetary orbit insertion ΔV.

2. No requirement of $LH2$ storage for extended period of time: The literature studies have demonstrated tht the maximum heat transfer to the propellant tank is from the Sun and planetary albedo and minimum during the cruise phase with active attitude control with respect to the orientation of the spacecraft to the Sun.

The results on engine system trades can be used to answer the Research Question #3 *What is the enabling engine thrust class for targeted robotic missions?* The engine trade results for Jupiter rendezvous mission have demonstrated that the thrust range of 12.5 klbf to 15 klbf can enable flagship and new-frontiers class missions with minimum IMLEO. The IMLEO requirement is also dependent on the departure orbits and are under 1 mT in mass in the 1000 km - 2000 km circular parking orbit which is within the overall mission constraints. For the missions using type-I trajectories, the enabling engine thrust is within the range of 12.5 klbf to 15 klbf. The higher thrust engines (20 klbf - 30 klbf) can enable missions with much shorter trip times but with a requirement off high arrival ΔV thereby significantly reducing the spacecraft dry mass delivery capability. The specific impulse sensitivity analysis showed that using a 13 klbf engine with I_{sp} as low was 850 s can enable missions to the Gas giant. The IMLEO requirements in this case is met by the New Glenn launch vehicle but are outside of the Vulcan Heavy capability. The engine trades for Neptune rendezvous mission using type-I direct transfer trajectory have shown that using a single 9 klbf to 17 klbf engine thrust

can deliver the minimum required 1.5 mT of spacecraft post NOI maneuver. The type-II trajectory missions using JGA have a tighter enabling engine thrust range of 12.5 klbf - 15 klbf which meets the requirement of delivering a minimum of 1 mT of spacecraft mass post NOI.

Chapter 6. Conclusion

6.1 Dissertation Constraints and Limitations

As with the majority of the conceptual space mission design and tradespace exploration studies, the analysis presented in the dissertation are subjected to constraints and limitations. The commercial launch vehicles considered in this study are either operational or have detailed payload performance parameters available. Commercial super heavy lift launch vehicles (*e.g.,* SpaceX Starship) were not included in the study due to limited performance data available. The point design studies and engine trades were limited to the use of liquid Hydrogen as a propellant for the NTP system. Although studies have shown benefits for propellants such a ammonia due to their increased density and ease of long-term storage [110]. There have been limited peer reviewed studies on the long term in-space storage of $LH2$ for duration of five or more years, therefore, the architectures for Ice giant missions is restricted to the expendable mission mode.

6.2 Dissertation Contributions

This dissertation has demonstrated that the use of Nuclear Thermal Propulsion (NTP) can enable flagship and new-frontiers class robotic missions to the outer solar system, as well as the methodology of using the integrated system

model to quantify the enabling mission architectures and the NTP engine parameters. The illustrated point design studies have shown the benefits with respect to the higher spacecraft dry mass delivery capability and reduction in trip times by a factor of two for Gas giant missions in comparison to the missions using traditional propulsion systems and game changing capabilities for ambitious missions to the Ice giant systems.

A more detailed breakdown of the contributions is as follows:

- Identification of the current challenges towards the exploration of the outer solar system and identification of the impact on mission capabilities using NTP for the scientific community towards answering the priority science questions as per the decadal survey 2023-2032.

- Identification of the knowledge gaps in the literature on NTP powered mission concepts and assessing the feasibility of NTP to support current and future planetary science missions within the constraints of the NASA's Planetary Science Division (PSD).

- Development of the systems engineering model driven by the Model Based Systems Engineering (MBSE) coupled with the domain engineering analysis models and systems engineering architectural models. The systems engineering model described as an N2 diagram is used for architecture generation, verification and sizing using the subsystems in the design structure matrix.

- Development of the high-fidelity integrated modeling environment for the Spacecraft Integrated System Model (SISM) using the mission design framework to perform rapid mission analysis and trade space exploration.

- Development of mission architectures and identification of Design Reference Missions (DRM) for the NTP system in order to answer the research questions on engine system trades.

- Mission specific recommendations on NTP powered mission architectures and engine parameters towards enabling missions to the Gas giant and Ice giant systems using the results from the quantifiable figures of merit.

6.3 Dissertation Summary

In this dissertation three research questions based on the knowledge gaps on the application of NTP systems for robotic missions were identified and its solutions were provided. The implementation of MBSE driven systems engineering model for SISM resulted in rapid high-fidelity mission analysis for trade space exploration.

The literature review (Chapter 2) of robotic exploration of the solar system led to the identification of the current challenges in enabling missions to the outer planets. Performance and limitations of the current available in-space propulsion systems (Chemical and SEP systems) were evaluated. The performance of NTP due to its high thrust and high I_{sp} capability has already projected to have higher

payload mass fraction for higher energy missions. However, a detailed literature review of NTP systems led to the identification of following gaps:

- Potential difference in performance parameters for NTP systems in comparison to traditional propulsion system for flagship and new-frontiers class missions.
- Determining the enabling mission architectures due to the complexities of using NTP system (Nuclear safe orbit requirements, use of $LH2$ propellant for long duration missions etc.) and,
- Determining the enabling thrust class for missions to the outer planets.

The performance parameters can be compared using the spacecraft injection analysis and by demonstrating NTP systems enhanced capability in point design studies. Determining enabling mission architectures and engine thrust class will need the development of a comprehensive SISM which tightly couples the domain engineering analysis models and systems engineering architectural models.

The approach and methodology (Chapter 3) is used to design the SISM to run trade studies and requirement analysis on mission designs. The systems engineering model comprises of mission classification, spacecraft and NTP systems for architecture generation and launch vehicle and cost modules for architecture verification and sizing. The mission classification uses the inputs to determine the type of robotic mission which is then used to determine the initial parameters of spacecraft and NTP system module. Once the initial architecture is generated

the designed spacecraft and NTP system are then sized to meet the requirements of launch vehicle and cost with respect to the spacecraft dry mass. The described integrated model is executed through the system descriptive model which then initiates and executes the analytical models to be used to perform the trade studies mission architecture and engine systems. The selected DRMs are defined for point design studies and engine trade study in order to answer the research questions.

The direct spacecraft injection performance and point design studies (Chapter 4) to the outer planets Jupiter, Saturn, Uranus and Neptune are presented. The direct injection analysis demonstrated that using NTP system on a commercial launch vehicle can deliver over 12% and 30% of payload mass to Jupiter and Saturn respectively when compared with SLS Block 1 standalone launch vehicle. The end-to-end mission analysis demonstrated the performance of expendable architecture towards enabling flagship and new-frontiers class missions. The point design also demonstrated the capability to reduce the trip times by a factor of two or more for missions to the gas giants when compared with chemical propulsion systems. A large strategic class spacecraft for a rendezvous mission has a trip time to Jupiter of 2.1 years and to Saturn in 4.68 years versus 5.5 years and 8.5 years using chemical propulsion system respectively. The point design also analyzed direct transfer (Type-I) mission to Uranus and Neptune which demonstrated a trip time of 7.97 and 13 years respectively.

Finally, the results on engine system trades and expendable and non-expendable mission architectures (Chapter 5) are discussed to answer the final two research questions. The engine trades based on the DRM trade tree concludes that the thrust range of 12.5 klbf to 15 klbf can enable flagship and new-frontiers class missions to the outer planets. For mission architectures, expendable configuration demonstrated to have higher performance in terms of spacecraft mass delivery for traditional robotic missions. Non-expendable configuration can have significant benefits for missions requiring very large ΔV for TPI and POI maneuvers.

In conclusion, the answers to the three research questions are:

Research Question #1: *What is the potential difference in performance parameters for NTP systems in comparison to traditional propulsion systems towards enabling ambitious missions to the outer solar system exploration?*

Answer: The NTP powered mission can deliver large strategic class missions to the outer planets with trip time reduction by more than a factor of two using a single launch of a commercial launch vehicle when compared with the similar chemical powered missions. The point design study analysis shows that using NTP system, a flagship class spacecraft can be delivered to Jupiter in 2.1 years, Saturn in 4.68 years, Uranus in 7.97 and Neptune in 13 years vs 5.5 years, 8.5 years, 13.4 years and 16 years respectively using chemical propulsion system. The payload delivery of NTP system

using a single launch of a commercial launcher is 12 to 30 percent higher to the outer planets when compared with super heavy lift launch vehicle SLS Block 1 for a chemical powered mission.

Research Question #2: *What is an enabling mission architecture for the robotic missions using NTP systems?*

Answer: The results on spacecraft mass delivery post planetary orbit insertion for the range of trip-times between expendable and non-expendable mission configurations have demonstrated that to enable current planetary science missions an expendable architecture will be preferred due to its higher payload delivery capability of over 5%. The non-expendable architecture using the described ZBO storage approach can be preferred for missions that share two characteristics: (1) Very large ΔV requirement and (2) No requirement of long duration $LH2$ storage around a celestial body.

Research Question #3: *What is the enabling engine thrust class for targeted robotic missions?*

Answer: The NTP engine thrust range of 12.5 klbf to 15 klbf is recommended for robotic missions. The recommended thrust range can enable a host of flagship and new frontiers class missions to the Gas giant and Ice giant planets which meets the requirements of the NASA's planetary science missions.

6.4 Looking Forward and Skyward

"Dans ses écrits, un sage Italien Dit que le mieux est l'ennemi du bien."

("In his writings, a wise Italian says that the perfect is the enemy of the good.")

- Elements of the Philosophy of Right by Georg Hegel, 1820 [111]

There can be endless details to which an NTP powered mission can be designed, the spacecraft class at its subsystem level, target destinations, engine performance, dependencies on mission architectures and operations can be optimized. This dissertation starts by answering the high level architectural decisions in place and demonstrating NTP system capability by performing high-fidelity end-to-end mission analysis. Some of the suggested leads on future work which can be used to expand the understanding of NTP system for robotic missions are:

- Engine trades using alternative propellants such as ammonia and water which reduces the propellant tank volume by up to 69% and 75% respectively.
- Architecture evaluation for point design studies for mission to ocean worlds which require higher arrival ΔV for planetary orbit insertion.
- Use of bimodal NTP concept which will eliminate the need for a separate power system.

References

[1] National Academies of Sciences, Engineering, and Medicine and others. *Space nuclear propulsion for human mars exploration*. National Academies Press, 2021.

[2] Bret G Drake, Stephen J Hoffman, and David W Beaty. Human exploration of mars, design reference architecture 5.0. In *2010 IEEE Aerospace Conference*, pages 1–24. IEEE, 2010.

[3] Asif A Siddiqi. *Beyond Earth: A chronicle of deep space exploration, 1958-2016*, volume 4041. National Aeronautics & Space Administration, 2018.

[4] Brian Harvey. *Russian planetary exploration: history, development, legacy and prospects*. Springer Science & Business Media, 2007.

[5] Space Studies Board, National Research Council, et al. *Assessment of Mission Size Trade-offs for NASA's Earth and Space Science Missions*. National Academies Press, 2000.

[6] Space Studies Board, Engineering National Academies of Sciences, Medicine, et al. *Powering Science: NASA's Large Strategic Science Missions*. National Academies Press, 2017.

[7] Space Studies Board, Engineering National Academies of Sciences, Medicine, et al. *Powering Science: NASA's Large Strategic Science Missions*, chapter Risks and Realities of Cost Overruns for Large Strategic Missions. National Academies Press, 2017.

[8] Government Accountability Office. Assessments of major nasa projects, GAO-22-105212. Technical report, United States Government Accountability Office, 2022.

[9] Space Studies Board, National Research Council, et al. *Vision and voyages for planetary science in the decade 2013-2022*. National Academies Press, 2012.

[10] New frontiers program, NASA. `https://science.nasa.gov/solar-system/programs/new-frontiers`. Accessed: 08.03.2023.

[11] Ralph D Lorenz, Elizabeth P Turtle, et al. Dragonfly: A rotorcraft lander concept for scientific exploration at titan. *Johns Hopkins APL Technical Digest*, 34(3):14, 2018.

[12] NASA HQ. Dawn at ceres. Press kit, National Aeronautics and Space Administration, March 2015.

[13] NASA HQ. Juno launch. Press kit, National Aeronautics and Space Administration, August 2011.

[14] NASA HQ. Cassini launch. Press kit, National Aeronautics and Space Administration, October 1997.

[15] MG Houts, SK Borowski, JA George, T Kim, WJ Emrich, RR Hickman, JW Broadway, HP Gerrish, and M12-1753 Adams, RB. Nuclear thermal propulsion for advanced space exploration. Technical report, NASA, 2012.

[16] Steven D Howe. Assessment of the advantages and feasibility of a nuclear rocket for a manned mars mission. *NASA. Marshall Space Flight Center Manned Mars Mission. Working Group Papers, V. 2, Sect. 5, App.*, 1986.

[17] George P Sutton and Oscar Biblarz. *Rocket propulsion elements*. John Wiley & Sons, 2016.

[18] Harold P Gerrish Jr. Raising nuclear thermal propulsion (ntp) technology readiness above 3. In *Advanced Space Propulsion Workshop*, number M15-4254, 2014.

[19] Seung Hyun Nam, Paolo Venneri, Yonghee Kim, Jeong Ik Lee, Soon Heung Chang, and Yong Hoon Jeong. Innovative concept for an ultra-small nuclear thermal rocket utilizing a new moderated reactor. *Nuclear Engineering and Technology*, 47(6):678–699, 2015.

[20] Claudio Bruno. *Nuclear Space Power and Propulsion Systems*. American Institute of Aeronautics and Astronautics, 2008.

[21] PW Garrison. Advanced propulsion for future planetary spacecraft. *Journal of Spacecraft and Rockets*, 19(6):534–538, 1982.

[22] Roland Antonius Gabrielli and Georg Herdrich. Review of nuclear thermal propulsion systems. *Progress in Aerospace Sciences*, 79:92–113, 2015.

[23] H Shulman, WS Ginell, et al. Nuclear and space radiation effects on materials. *NASA SP-8053, June*, 15, 1970.

[24] Frank E Rom. Nuclear-rocket propulsion. In *Conference on Non-Chemical Space Propulsion*, number NASA-TM-X-1685, 1968.

[25] Robert G Ragsdale. Performance potential of a radiant-heat-transfer liquid-core nuclear rocket engine. Technical report, NASA Lewis Research Center, 1967.

[26] NASA STI. State of the art in-space propulsion, NASA/TP-2022-0018058. Technical report, NASA Ames Research Center, 2022.

[27] June F. Zakrajsek. Radioisotope power systems program. In *Outer Planet Assessment Group (OPAG) Technology Forum*. NASA, 2018.

[28] Fernando Peralta and Steve Flanagan. Cassini interplanetary trajectory design. *Control Engineering Practice*, 3(11):1603–1610, 1995.

[29] ROBERT G. JAHN. Electric propulsion. *American Scientist*, 52(2):207–217, 1964.

[30] Edgar Y Choueiri. New dawn for electric rockets. *Scientific American*, 300(2):58–65, 2009.

[31] RS Cooper. Nuclear propulsion for space vehicles. *Annual Review of Nuclear Science*, 18(1):203–228, 1968.

[32] James R Powell, John Paniagua, George Maise, Hans Ludewig, and Michael Todosow. High performance nuclear thermal propulsion system for near term exploration missions to 100 au and beyond. *Acta astronautica*, 44(2-4):159–166, 1999.

[33] Stanley K Borowski, David R McCurdy, and Thomas W Packard. Nuclear Thermal Propulsion (NTP): A proven growth technology for human NEO/-Mars exploration missions. In *2012 IEEE Aerospace Conference*, pages 1–20. IEEE, 2012.

[34] Claude Joyner, Daniel Levack, and Stanley Borowski. Development of a small nuclear thermal propulsion flight demonstrator concept that is scalable to human missions. In *48th AIAA/ASME/SAE/ASEE Joint Propulsion Conference & Exhibit*, page 4207, 2012.

[35] Benjamin Donahue. Solar electric and nuclear thermal propulsion architectures for human mars missions beginning in 2033. In *46th AIAA/ASME/SAE/ASEE Joint Propulsion Conference & Exhibit*, page 6819, 2010.

[36] Benjamin Donahue. Nuclear thermal propulsion vehicle design for the mars flyby with surface exploration mission. In *27th Joint Propulsion Conference*, page 2561, 1991.

[37] Stanley K Borowski, David R McCurdy, and Laura M Burke. The Nuclear Thermal Propulsion Stage (NTPS): A Key Space Asset for Human Exploration and Commercial Missions to the Moon. In *AIAA SPACE 2013 Conference and Exposition*, page 5465, 2013.

[38] James Powell, John C Paniagua, Hans Ludewig, and Michael Todosowp. The role of compact nuclear rockets in expanding the capability for solar system science and explorationp. Technical report, Stony Brook, NY: State University of New York at Stony Brook, College of . . . , 1997.

[39] Kurt A Polzin, C Russell Joyner, Timothy Kokan, Stephen Edwards, Adam Irvine, Mitchell Rodriguez, and Michael Houts. Enabling deep space science missions with nuclear thermal propulsion. *White Paper*, 2020.

[40] Charles L Johnson, Michael G Houts, Mitchell A Rodriguez, and Harold P Gerrish. Nuclear Thermal Propulsion (NTP) and Power A New Capability for Outer Planet Science and Exploration. Technical report, NASA MSFC, 2018.

[41] Jesse Powell, James Powell, George Maise, and John Paniagua. NEMO: A mission to search for and return to Earth possible life forms on Europa. *Acta Astronautica*, 57(2-8):579–593, 2005.

[42] Bob Greene. Getting around the solar system quickly: A design study for a high speed, highly reusable nuclear fission rocket engine for use on deep

space missions. In *53rd AIAA/SAE/ASEE Joint Propulsion Conference*, page 4936, 2017.

[43] John Paniagua, James R Powell, and George Maise. Europa sample return mission utilizing high specific impulse propulsion refueled with indigenous resources. *IAF Abstracts, 34th COSPAR Scientific Assembly*, page 677, 2002.

[44] Muriel Noca, Robert Frisbee, Les Johnson, Larry Kos, Leon Gefert, and Len Dudzinski. Evaluating advanced propulsion systems for the Titan explorer mission. In *27th International Electric Propulsion Conference*, pages 15–19, 2001.

[45] C Russell Joyner, Michael Eades, James Horton, Tyler Jennings, Timothy Kokan, Daniel JH Levack, Brian J Muzek, and Christopher B Reynolds. LEU NTP engine system trades and mission options. *Nuclear Technology*, 206(8):1140–1154, 2020.

[46] Stanley K Borowski. Robotic planetary science missions enabled with small NTR engine/stage technologies. In *AIP Conference Proceedings*, volume 324, pages 311–320. American Institute of Physics, 1995.

[47] Peter S Venetoklis, Caroline V Nelson, and Eric R Gustafson. Application of a SNTP-Based propulsion/power system to solar system exploration missions. In *AIP Conference Proceedings*, volume 301, pages 45–53. American Institute of Physics, 1994.

[48] Daniel J Levack, James F Horton, Tyler Jennings, Claude R Joyner, Timothy Kokan, Johnny L Mandel, Brian J Muzek, Christopher Reynolds, and Frederick W Widman Jr. Evolution of low enriched uranium nuclear thermal propulsion vehicle and engine design. In *AIAA Propulsion and Energy 2019 Forum*, page 3943, 2019.

[49] Jack Mulqueen, Robert C Chiroux, Dan Thomas, and Tracie Crane. Nuclear thermal propulsion mars mission systems analysis and requirements definition. 2007.

[50] Kyle Shepard, Paul Sager, Sid Kusunoki, John Porter, Al Campion, Gunnar Mouritzan, George Glunt, George Vegter, and Rob Koontz. Clustered en-

gine study. In *NASA. Lewis Research Center, Nuclear Propulsion Technical Interchange Meeting, Volume 1*, 1993.

[51] Claude Joyner. Engine architecture recommendation and rationale. Technical report, Aerojet Rocketdyne, 2016.

[52] Yanping Guo and Robert W Farquhar. New horizons mission design. *Space science reviews*, 140:49–74, 2008.

[53] Mark D Hofstadter, Amy Simon, Kim Reh, and John Elliot. Ice giants pre-decadal study final report. *Report D-100520, NASA Jet Propulsion Laboratory, Pasadena, CA*, 2017.

[54] James Powell, George Maise, and John Paniagua. The compact mitee-b bomodal nuclear engine for unique new planetary science missions. In *38th AIAA/ASME/SAE/ASEE Joint Propulsion Conference & Exhibit*, page 3652, 2002.

[55] John C Paniagua, James R Powell, and George Maise. Design and development of the mitee-b bi-modal nuclear propulsion engine. In *AIP Conference Proceedings*, volume 654, pages 438–444. American Institute of Physics, 2003.

[56] Mike Houts, Larry Kos, David Poston, and Stephen L Rodgers. Potential operating orbits for the safe-400. In *2002 American Nuclear Society (ANS) Meeting-International Congress on Advanced Nuclear Power Plants (ICAPP)*, 2002.

[57] ROBERT FRISBEE, STEPHANIE LEIFER, and SHISHIR SHAH. Nuclear safe orbit basing considerations. In *Conference on Advanced SEI Technologies*, page 3411, 1991.

[58] Peter Venetoklis and John Metzger. A reduced-penalty nuclear-safe orbit strategy for nuclear thermal propulsion systems. In *30th Joint Propulsion Conference and Exhibit*, page 2760, 1994.

[59] Phillip Anz-Meador, John Opiela, and Jer-Chyi Liou. History of on-orbit satellite fragmentations. Technical report, NASA Lyndon B. Johnson Space Center, 2023.

[60] W Robbins. An historical perspective of the nerva nuclear rocket engine technology program. In *Conference on Advanced SEI Technologies*, page 3451, 1991.

[61] NASA/ESSCA NTP-RPT-0024. Historical Nuclear Thermal Propulsion Lessons Learned. Technical report, National Aeronautics and Space Administration, March 2020.

[62] John S Clark, Patrick Mcdaniel, Steven Howe, Ira Helms, and Marland Stanley. Nuclear thermal propulsion technology: Results of an interagency panel in fy 1991. Technical report, NASA, 1993.

[63] Robert R Corban. Ntp system definition and comparison process for sei. In *AIP Conference Proceedings*, volume 271, pages 1713–1722. American Institute of Physics, 1993.

[64] GARY BENNETT and THOMAS MILLER. Progress report on nuclear propulsion for space exploration and science. In *29th Joint Propulsion Conference and Exhibit*, page 2352, 1993.

[65] Christopher B Reynolds, Claude R Joyner, Timothy S Kokan, Daniel J Levack, and Brian J Muzek. Mars opposition missions using nuclear thermal propulsion. In *AIAA Propulsion and Energy 2020 Forum*, page 3850, 2020.

[66] ROBERT ZUBRIN and TAL SULMEISTERS. The application of nuclear power and propulsion for space exploration missions. In *28th Joint Propulsion Conference and Exhibit*, page 3778, 1992.

[67] C Russell Joyner, Michael Eades, James Horton, Tyler Jennings, Timothy Kokan, Daniel JH Levack, Brian J Muzek, and Christopher B Reynolds. LEU NTP engine system trades and missions. In *Nuclear and Emerging Technologies for Space*, 2019.

[68] Claude R Joyner, Tyler Jennings, Timothy S Kokan, and Daniel J Levack. NTP engine system–a robust evolutionary design. In *ASCEND 2021*, page 4109. AIAA, 2021.

[69] Saroj Kumar, L Dale Thomas, and Jason Cassibry. Development of integrated NTP mission model for planetary science missions. In *Proc. Conf. Nuclear and Emerging Technologies for Space*, 2022.

[70] Lawrence F Rowell, Robert D Braun, John R Olds, and Resit Unal. Multidisciplinary conceptual design optimization of space transportation systems. *Journal of Aircraft*, 36(1):218–226, 1999.

[71] BP Douglass. The harmony process. i-logix white paper, i-logix. *Inc.: Burlington, MA, USA*, 2005.

[72] Jeff A Estefan et al. Survey of model-based systems engineering (mbse) methodologies. *Incose MBSE Focus Group*, 25(8):1–12, 2007.

[73] Saroj Kumar, Lawrence Thomas, and Jason T Cassibry. Model-based approach for conceptual mission design for ntp enabled robotic missions. In *AIAA Propulsion and Energy 2021 Forum*, page 3598, 2021.

[74] Saroj Kumar, L Dale Thomas, and Jason T Cassibry. Decoding mission design problem for ntp systems for outer planet robotic missions. *Nuclear Technology*, 208(sup1):S67–S73, 2022.

[75] Dennis Nikitaev. *Implications of alternative in-situ propellants used in nuclear thermal propulsion engines*. The University of Alabama in Huntsville, 2021.

[76] Tyler Jennings. Cermet and cercer fuels in a block moderator configuration 15k leu ntp. *Virtual, Aug*, 20, 2020.

[77] Dennis Nikitaev and Dale L Thomas. Alternative propellant nuclear thermal propulsion engine architectures. *Journal of Spacecraft and Rockets*, 59(4):1149–1160, 2022.

[78] David L. Akin. Mass estimating relations - launch and entry vehicle design. In *ENAE791 University of Maryland*, 2016.

[79] Matthew M Berry and Liam M Healy. Implementation of gauss-jackson integration for orbit propagation. *The Journal of the Astronautical Sciences*, 52:331–357, 2004.

[80] Felix R Hoots and Richard G France. An analytic satellite theory using gravity and a dynamic atmosphere. *Celestial Mechanics*, 40(1):1–18, 1987.

[81] JJF Liu and RL Alford. Semianalytic theory for a close-earth artificial satellite. *Journal of Guidance and Control*, 3(4):304–311, 1980.

[82] JG Neeion, Paul J Cefola, and Ronald J Proulx. Current development of the draper semianalytical satellite theory standalone orbit propagator package. *Advances in the Astronautical Sciences*, 97:2037–2052, 1998.

[83] Daniel John Fonte, Beny Neta, Chris Sabol, Donald A Danielson, Walter R Dyar, and K Terry Alfriend. *Comparison of Orbit Propagators in the Research and Development Goddard Trajectory Determination System (R & D GTDS): Part I, Simulated Data*. American Astronautical Society, 1996.

[84] Carole Ann Jablonski. *Application of semianalytic satellite theory to maneuver planning*. PhD thesis, Massachusetts Institute of Technology, 1991.

[85] Srinivas J Setty, Paul J Cefola, Oliver Montenbruck, and Hauke Fiedler. Application of semi-analytical satellite theory orbit propagator to orbit determination for space object catalog maintenance. *Advances in Space Research*, 57(10):2218–2233, 2016.

[86] Paul A Lightsey and Erik Wilkinson. Importance of design reference missions for developing the next large missions concepts. Whitepaper, 2015.

[87] Saroj Kumar, L Dale Thomas, and Jason T Cassibry. Development of integrated NTP mission model for planetary science missions. In *Nuclear and Emerging Technologies for Space (NETS)*, pages 114–118, 2022.

[88] Saroj Kumar, L Dale Thomas, and Jason T Cassibry. Spacecraft integrated system model for NTP powered planetary science missions. In *73rd International Astronautical Congress, Paris, France*, 2022.

[89] Steven S Pietrobon. Analysis of propellant tank masses. *Submitted to Review of US Human Space Flight Plans Committee*, 6, 2009.

[90] Stanley K Borowski, David McCurdy, and Thomas Packard. Nuclear thermal propulsion (ntp): A proven, growth technology for'fast transit'human missions to mars. In *AIAA SPACE 2013 Conference and Exposition*, page 5354, 2013.

[91] Saroj Kumar, L Dale Thomas, and Jason T Cassibry. Nuclear thermal propulsion for jupiter and saturn rendezvous missions. *Journal of Spacecraft and Rockets*, 59(4):1171–1178, 2022.

[92] Bret G Drake, B Kent Josten, and Donald W Monell. Exploration requirements development utilizing the strategy-to-task-to-technology development approach. In *AIAA Space 2004 Conference*, number AIAA Paper 2004-5928, 2004.

[93] Vern Thorp, Will Crawford, and Bernard Kutter. Innovation in space access: History of unique capabilities begun with atlas, centaur and delta and the continuing innovation on vulcan centaur. In *70th International Astronautical Congress, Washington D.C, United States*, 2019.

[94] David Alan Smith. Space launch system (SLS) mission planner's guide. Technical report, NASA Exploration Systems Development (ESD) Division, NP-2018-09-089-MSFC, 2018.

[95] Claude R Joyner. Space technology mission directorate: Game changing development program: Nuclear thermal propulsion project - ntp mars opposition architecture analysis. 2020.

[96] Michael G Houts, Claude R Joyner, John Abrams, Jonathan Witter, and Paolo Venneri. Versatile nuclear thermal propulsion (ntp). In *70th International Astronautical Congress (IAC)*, 2019.

[97] Vulcan centaur, 2020.

[98] New glenn payload user's guide - revision c. Technical report, Blue Origin, LLC, 2018.

[99] L Naicker, R Wall, and D Perigo. An overview of development model testing for the leros 4 high thrust apogee engine. In *2014 Space Propulsion Conference*, volume 2969298, 2014.

[100] Todd Bayer, Brian Cooke, I Gontijo, and Karen Kirby. Europa clipper mission: the habitability of an icy moon. In *2015 IEEE Aerospace Conference*, pages 1–12. IEEE, 2015.

[101] M Marley, L Dudzinski, T Spilker, R Moeller, C Borden, W Smythe, et al. Planetary science decadal survey jpl rapid mission architecture neptune–triton kbo study final report. *NASA Mission Concept Study Report*, 2010.

[102] Scott J Bolton, J Lunine, D Stevenson, JEP Connerney, S Levin, TC Owen, F Bagenal, D Gautier, AP Ingersoll, GS Orton, et al. The juno mission. *Space Science Reviews*, 213:5–37, 2017.

[103] S Mitchell, R Ryan, and T Kokan. Engine Architecture Review and FY2016 Continuation Review for STMD Game Changing Development Program. *NASA NTP and AR Engine Analysis Study*, 2016.

[104] Carl Guernsey, Raymond Baker, David Plachta, and Peter Kittel. Cryogenic propulsion with zero boil-off storage applied to outer planetary exploration. In *41st AIAA/ASME/SAE/ASEE joint propulsion conference & exhibit*, page 3559, 2005.

[105] DW Plachta, RJ Christie, JM Jurns, and P Kittel. Passive zbo storage of liquid hydrogen and liquid oxygen applied to space science mission concepts. *Cryogenics*, 46(2-3):89–97, 2006.

[106] Mark S Haberbusch, Robert J Stochl, and Adam J Culler. Thermally optimized zero boil-off densified cryogen storage system for space. *Cryogenics*, 44(6-8):485–491, 2004.

[107] Richard L DeWitt and Robert J Boyle. *Thermal performance of an integrated thermal protection system for long-term storage of cryogenic propellants in space*, volume 8320. National Aeronautics and Space Administration, 1977.

[108] David Miao, James R Barber, and Richard L DeWitt. Design, fabrication, and structural testing of a lightweight shadow shield for deep-space application. Technical report, National Aeronautics and Space Administration, 1977.

[109] Elizabeth M Spiers, Jessica M Weber, Chandrakanth Venigalla, Andrew M Annex, Christine P Chen, Carina Lee, Patrick Clifton Gray, Kathleen J McIntyre, Jodi R Berdis, Shane R Carberry Mogan, et al. Tiger: Concept

study for a new frontiers enceladus habitability mission. *The Planetary Science Journal*, 2(5):195, 2021.

[110] Daria Nikitaeva and L Dale Thomas. Impacts of in situ alternative propellant on nuclear thermal propulsion mars vehicle architectures. *Journal of Spacecraft and Rockets*, 59(6):2038–2052, 2022.

[111] Georg Wilhelm Fredrich Hegel. *Hegel: Elements of the philosophy of right*. Cambridge University Press, 1991.

Appendix A. Publication History

A.1 Relevant Journal Publications

A.1.1 Published

1. Kumar, S., Thomas, D., and Cassibry, J, "Nuclear Thermal Propulsion for Jupiter and Saturn Rendezvous Missions." JSR, Vol. 59, No. 4 (2022), pp. 1171-1178 doi: doi/abs/10.2514/1.A35212.

2. Saroj Kumar, L. Dale Thomas and Jason T. Cassibry (2022): Decoding Mission Design Problem for NTP Systems for Outer Planet Robotic Missions, Nuclear Technology, 2022.

A.1.2 Submitted

1. Kumar, Saroj, L. Dale Thomas, and Jason T. Cassibry. "Application of Nuclear Thermal Propulsion for Sustainable Cislunar Exploration." Acta Astronautica *(submitted)*.

A.1.3 To be submitted

1. Kumar, S., Thomas, D., and Cassibry, J, "NTP Engine System Trades for Robotic Missions to the Outer Solar System.", will be submitted to the AIAA JSR.

2. Kumar, S., Thomas, D., and Cassibry, J, "Integrated System Model for Robotic Missions using NTP.", will be submitted to the Wiley Systems Engineering.

A.2 Relevant Conference Publications

1. Kumar, Saroj, L. Dale Thomas, and Jason T. Cassibry. "Nuclear Thermal Propulsion: Trades and Sensitivity Analysis for Robotic Missions." AIAA SCITECH 2024 Forum. 2024.

2. Kumar, Saroj, L. Dale Thomas, and Jason T. Cassibry. "Application of Nuclear Thermal Propulsion for Sustainable Cislunar Exploration." 74th International Astronautical Congress, Baku, Azerbaijan, October, 2023.

3. Kumar, Saroj, L. Dale Thomas, and Jason T. Cassibry. "Preliminary Nuclear Thermal Propulsion Engine System Trades for Robotic Missions to Jupiter." Nuclear and Emerging Technologies for Space (NETS), 41880, May, 2023.

4. Kumar, Saroj, L. Dale Thomas, and Jason T. Cassibry. "Spacecraft Integrated System Model for NTP Powered Planetary Science Missions." 73rd International Astronautical Congress, Paris, France, September, 2022.

5. Kumar, Saroj, L. Dale Thomas, and Jason T. Cassibry. "Development of Integrated NTP Mission Model for Planetary Science Missions." Nuclear and Emerging Technologies for Space (NETS), pp. 114-118, May, 2022.

6. Kumar, S., Thomas, D., and Cassibry, J. "Model-Based Approach for Conceptual Mission Design for NTP Enabled Robotic Missions." AIAA Propulsion and Energy Forum, AIAA-2021-3598, 2021.

7. Kumar, Saroj, Dale Thomas and Jason T. Cassibry. "Decoding Mission Design Problem for NTP Systems for Outer Planet Robotic Missions." Nuclear and Emerging Technologies for Space (NETS), 35952, April, 2021.

8. Kumar, S., Thomas, L., and Cassibry, J.T., "Nuclear Thermal Propulsion for Outer Planets Robotic Exploration," 52nd Lunar and Planetary Science Conference, 1613, March, 2021.

9. Kumar, Saroj, Lawrence Thomas, and Jason T. Cassibry. "Preliminary Trajectory Design for Jupiter Rendezvous Mission Using Nuclear Thermal Propulsion". AIAA Propulsion and Energy 2020 Forum. 2020.

10. Kumar, S., Thomas, L., Cassibry, J. T., and Frederick, R.A. (2020). "Review of Nuclear Propulsion Technology for Deep Space Missions". AIAA Propulsion and Energy 2020 Forum (p. 3815).

11. Kumar, Saroj, Dale Thomas and Jason T. Cassibry. "Nuclear Propulsion for Future Planetary Missions." Nuclear and Emerging Technologies for Space (NETS). 2020.

A.3 Other Publications

A.3.1 Journal

1. Spiers. M, Kumar, S., *et al.*, "TIGER: Concept Study for a New Frontiers Enceladus Habitability Mission", The Planetary Science Journal 2, no.5: 195 (2021).

A.3.2 Conference

1. Nikitaeva, D., Kumar, S., *et al.* "Details of the Spacecraft Integrated System Model for Nuclear Thermal Propulsion Applications." AIAA Propulsion and Energy Forum, AIAA-2021-3599, 2021.

2. Spiers. M, Kumar, S., *et al.*, "TIGER: JPL PSSS Architecture and Feasibility Study for a New Frontiers 5 Mission Concept to Enceladus", 52nd Lunar and Planetary Science Conference, March, 2021.

3. D. Nikitaeva, D. Thomas, A. Aueron, S. Kumar, and D. Nikitaev, "Nuclear Thermal Propulsion Spacecraft Integrated System Model," AIAA SciTech, January 11-15, 2021.

4. D. Nikitaev, S. Kumar, D. Thomas, and J. Cassibry, "Launch Vehicle Selection for Mars Transfer Vehicles Utilizing Seeded Hydrogen in a Nuclear Thermal Propulsion System," AIAA ASCEND, November 16-18, 2020.

Appendix B. 15 klbf NTP Engine Performance Profile

The following data is the performance of UAH NTP 330 MW engine model during the reactor startup and shutdown events using $LH2$ propellant.

Table B.1: UAH NTP 330 MW engine startup performance

Time (sec)	Thrust (lbf)	I_{sp} (sec)	$\dot{m}$ (kg/s)	Reactor Power (MW)
1	827.5904852	405.553688	0.196058482	1.936811474
2	6074.088142	451.391259	1.335732545	9.590685389
3	9171.981874	479.646672	1.896096798	16.39827755
4	11960.36342	503.94181	2.350640484	23.87649091
5	14599.54054	526.123288	2.745661288	31.92779896
6	17180.081	547.226578	3.104662387	40.56377228
7	19700.95418	567.506093	3.43403738	49.70715676
8	22184.28762	587.475954	3.7423915	59.38877858
9	24610.82647	607.420298	4.032958107	69.5696442
10	26954.38062	627.71289	4.309280073	80.26488181
11	29159.49089	648.180957	4.572656724	91.42716147
12	31188.80567	659.208484	4.82445215	103.0261393
13	33086.07691	665.780863	5.067409993	115.1209797
14	35002.30195	673.205747	5.301514745	127.6633616
15	37138.43396	685.288292	5.526080062	140.5758554
16	39580.06996	702.795198	5.74261588	153.9300748
17	42255.7766	723.832277	5.952661832	167.7858057
18	45028.03027	745.818119	6.156218117	182.1059048
19	47816.40102	767.44125	6.353246822	196.83205
20	50603.9163	788.40618	6.544818873	211.9876671

Table B.1 - continued

21	53392.66356	808.706673	6.732163207	227.6314424
22	56168.95497	828.243709	6.915156575	243.7169365
23	58931.07277	847.113494	7.093593941	260.1995154
24	61692.23788	865.422778	7.268857957	277.1717786
25	64427.74473	883.049881	7.439632901	294.4595549
26	65729.33747	891.262672	7.5199941	303.0456737
27	65750.53643	891.39564	7.521297761	303.5353411
28	65770.77711	891.522574	7.522542343	303.9972741
29	65790.13484	891.643949	7.523732496	304.4339696
30	65808.67667	891.760188	7.524872359	304.847623
31	65826.46253	891.871669	7.525965634	305.2401734
32	65843.5462	891.978732	7.527015638	305.6133404
33	65859.97611	892.081682	7.528025361	305.9686551
34	65875.79597	892.180794	7.5289975	306.3074858
35	65891.04544	892.276319	7.529934503	306.6310592
36	65905.76052	892.368483	7.530838589	306.9404788
37	65919.97404	892.457494	7.531711785	307.2367404
38	65933.71598	892.54354	7.532555939	307.520745
39	65947.0138	892.626795	7.533372746	307.7933102
40	65959.89271	892.707417	7.534163759	308.0551795
41	65972.3759	892.785552	7.53493041	308.3070311
42	65984.48476	892.861336	7.535674016	308.5494848
43	65996.23903	892.934892	7.536395795	308.7831084
44	66007.65701	893.006336	7.537096874	309.0084231

Table B.2: UAH NTP 330 MW engine shutdown performance

Time (sec)	Thrust (lbf)	I_{sp} (sec)	$\dot{m}$ (kg/s)	Reactor Power (MW)
1703	67199.7569	900.418937	7.610008889	325.4630205
1704	63720.77676	878.544639	7.395728112	308.5180475
1705	60574.23548	858.072907	7.198257457	286.29363
1706	57554.55944	837.7825	7.005064509	267.1720994
1707	54595.31434	817.240858	6.811915188	249.4867475
1708	51653.67019	796.127456	6.615804982	232.648755
1709	48743.39578	774.480415	6.417544227	216.6301526
1710	45849.7852	752.257782	6.214902711	201.2180435
1711	42982.55719	729.62058	6.007020515	186.3636797
1712	40196.2626	707.555157	5.792808557	172.0209361
1713	37631.4484	688.563036	5.57265517	158.2440985
1714	35392.9921	675.116047	5.345745335	144.9945301
1715	33424.83741	666.93055	5.110418305	132.1745315
1716	31517.6658	660.398217	4.866277992	119.782003
1717	29502.73054	650.928543	4.614409468	107.900282
1718	27326.1966	631.091723	4.353221507	96.49733664
1719	25015.72218	610.835007	4.080834919	85.54772835
1720	22635.33313	591.131301	3.797038232	75.10096484
1721	17924.08748	553.234704	3.203832396	56.18717217
1722	15521.9314	533.721841	2.876831073	47.24469106
1723	13155.24619	514.072073	2.533329456	38.86594856
1724	10828.37729	494.19607	2.171178393	31.06243065
1725	8535.930958	473.962939	1.786264634	23.78838813
1726	6378.249036	454.232054	1.393770822	17.33949102
1727	4004.928668	431.461591	0.922142704	10.69705428

Appendix C. STK Astrogator User Interface and Mission Control Sequence Segments

C.4 User Interface

Users can define the mission sequence using the graphical programming language or using the Astrogator connect commands. The command syntax is defined in three building blocks namely, the command block, the attribute path and the attribute block. The syntax for each command is as shown below:

$< Command >< AttributePath >< Attribute >$

The command block determines the location and the operation to be performed when it is executed by the user. There are three elements that define the command block.

$< Prefix > Objectorscenariopath < Operator >$

The attribute path defines the location of the attribute within the Astrogator module. The syntax of each attribute path depends on the attribute being executed. An example syntax of attribute path for mission control sequence is:

$Astrogator*/Spacecraft/Spacecraft1SetValuemainSequence.SegmentList.Propagate. < Attribute >< Value > [Unit]$

The final block, Attribute in the Astrogator connect command identifies the attribute that the command will interact with. The syntax for attribute block is:

$< Attribute >< Value > [Unit]$

With few exceptions, majority of the trajectory analysis performed is based on the GUI based graphical programming language.

C.5 Mission Control Sequence

Each operational requirement in the trajectory design acts as a 'segment'. The segment functions as the graphical programming language in Astrogator. The Mission Control Sequence (MCS) Toolbar in Astrogator consists the buttons which define the spacecraft operation.

C.6 Mission Control Sequence Segments

The MCS Segments are categorized into two types- the segments that generate ephemeris and the segments that affect the execution of MCS. The final ephemeris generated by each segment is used by the next segment to determine the trajectory accordingly. The segments that generate ephemeris are Initial State, Launch, Follow, Maneuver, Propagate, Hold and Update. The segments that affect the execution of the MCS are Sequence, Backward Sequence, Target Sequence, Return and Stop.

C.6.1 Initial State

The initial stage segment is used to define the initial conditions of the mission control sequence. In general, this segment specifies the spacecraft's initial condition by specifying its orbital elements, spacecraft parameters including propellant tanks.

C.6.2 Launch

The launch segment is the propagator for launch vehicle and can be used to model launch from any of the central bodies listed in STK. Launch segment can be used to determine the spacecraft injection and launch schedule based on the data provided by the launch vehicle manufacturer. The parameters required to define launch segment are Central body, step size, pre-launch time, ascent type, initial acceleration, launch coordinate type and epoch, location of burnout point and burnout velocity.

C.6.3 Follow

The follow segment is used to set the spacecraft to follow launch vehicle with an offset and separate once the required conditions are met. This segments requires the user to define epoch, separation conditions and spacecraft's physical values.

C.6.4 Maneuver

The maneuver segment is used to model the spacecraft's maneuver. There are two types of maneuver's available- impulsive and finite maneuver. The impulsive maneuver uses the spacecraft's velocity vector from the previous segment and adds the ΔV as specified by the user. The result is again sent as an output to the next MCS segment. The impulsive maneuver can be defined by the attitude, ΔV direction and engine specification. The finite maneuver uses the propagate seg-

ment along with the thrust due to longer burn times. Finite maneuvers are more complex as it requires the segment to propagate in the defined state and account for the acceleration from the thrust. The direction of the burn is defined from the maneuvers attitude control. The finite maneuver can be defined by attitude, thrust direction, engine specifications and propagator. The spacecraft engines can be modeled based on polynomial functions for thrust and I_{sp}, custom function to determine values for propagation start, update, eval and post function. Other simpler engine models include constant thrust and I_{sp}, constant acceleration and I_{sp} and Ion engine models.

C.6.5 Propagate

The propagator segment is used to model the spacecraft's trajectory until the stopping conditions within the specified tolerance defined by the user are met. The stopping conditions can be defined using the Astrogator components which consists many conditions such as a specified target orbital parameter, delta-V etc. The segment allows the use of many numerical integrators to integrate parameters such as velocity, acceleration and constants to control the step size and accuracy of the propagation. The 7th order Runge-Kutta-Fehlberg integrator with 8th order error control is used as the default integrator to solve ordinary differential equation. Other numerical integrators available are Bulirsch-Stoer integrator based on Richardson extrapolation, 12th Gauss-Jackson integrator for second order ODE's with fixed step size, and 4th order Runge-Kutta integrator with adapting step size.

C.6.6 Hold

The hold segments maintains the fixed attitude and position in a reference until the stopping conditions are met. The segments holds the attitude and position and updates the ephemeris based on the time specified in step size. This segment is usually helpful for rendezvous, entry decent and landing sequences where the spacecraft is required to maintain a specific attitude or position until the next sequence can begin.

C.6.7 Target Sequence

The MCS segments such as maneuvers and propagators are nested under target sequence to achieve the desired result. The target sequence is defined by the search and segment configuration. The search defines the desired results requirement by the user and the segment configuration changes the segments as per the target sequences. The search profiles consist of differential corrector, interior point optimizer and sparse nonlinear optimizer. The differential corrector is used to obtain the desired results by having control parameters within the specified correction limit, perturbation value and maximum step size. The equality constraints or results are defined based on the desired output within a specified tolerance range. The iterations can be restricted by defining the maximum tolerance and convergence criteria. Newton-Raphson method or Broyden's method with specified derivative calculation method are used for root-finding algorithm.

The segment configuration consist of change maneuver type, change propagator, change return segment, change stopping condition state and seed finite maneuver.

C.6.8 Stop

The stop segment is used to stop the MCS once the desired conditions are met or the required trajectory analysis is complete.

Appendix D. Approach for Establishing the Figures of Merit

The NTP's enhanced capability and limitations has often been projected by its higher specific impulse and poor thrust to weight parameters. However, it is important to analyze the propulsion systems performance from the mission context and eventually comparing the results from the traditionally available propulsion systems. This section discusses the performance factors that will be used to define the quantifiable figures of merit for Nuclear Thermal Propulsion powered robotic mission to the outer planets. The performance parameters are selected based on the system level which will have a weighty impact on the overall mission design. The approach for establishing the figures of merit was by constructing mission level and NTP system level criteria which will have a direct or indirect impact towards answering the overall research question.

NASA's strategy to task to technology development approach document which articulates the strategy towards developing technologies for future exploration of the solar system has been adapted towards establishing the performance parameters for this study [92]. The high level figures of merit from the referred study are effectiveness, extensibility and affordability. Using the top-down approach the technical figures of merit were established and divided into mission level and NTP system level parameters. The effectiveness is the measure of performance towards determining the mission needs for the given mission concept.

The parameters such as spacecraft class for the mission, mass and trip times can categorized as a measure of effectiveness. The extensibility is the measure of effectiveness associated with the extensibility focus on determining the technology for mission needs. The NTP system parameters are considered as a measure of extensibility for robotic mission using this advanced propulsion concept. Lastly, the affordability assessment is to make sure the robotic missions are within the budget constraints of the planetary science division, therefore the mission analysis using commercial launcher and spacecraft dry mass is within the cost margins of the flagship and new frontiers class missions.

A relationship between the mission level parameters and NTP system level parameters was then constructed to assess the impact on the overall engine and architecture performance. The mission level criteria identified are IMLEO, parking orbit, NTP system configuration, trajectory and NTP system level criteria being engine T/W, run time, propellant tank sizing, payload mass, and specific impulse sensitivity. The interdependence of mission and NTP system level criteria are presented in Table D.3. The criteria such as reliability, redundancy, operational flexibility, development cost are either non-quantifiable with the current development level of the NTP or are beyond the scope of this dissertation.

Table D.3: Mission and NTP system level relationship criteria

Relationship	IMLEO	Parking Orbit	Configuration	Trajectory
Engine T/W	direct	indirect	indirect	direct
Engine run time	indirect	indirect		direct
Tank sizing	direct		direct	
I_{sp} sensitivity	direct		indirect	indirect
Spacecraft class	direct	direct	indirect	indirect

Appendix E. Jupiter Rendezvous Mission Sequence Summary

Mission Control Sequence (MCS) Segment Type: InitialState

Name: Target Sequence.Initial State

User Comment: Initializes state data

Spacecraft State at End of Segment:

UTC Julian Date: 2460926.91666667

State Vector in Coordinate System: Earth Inertial

Parameter Set Type: Cartesian

X: 3118.1354338247369924 km, Vx: 5.8542295388555345 km/sec

Y: -6686.8630169232183107 km, Vy: 2.7298720665655440 km/sec

Z: 0.0000000000004564 km, Vz: 3.5071830349227398 km/sec

NTP Injection stage and Spacecraft Configuration:

Drag Area: 20 m^2, SRP Area: 20 m^2

Dry Mass: 9110 kg, Fuel Mass: 12650 kg

Total Mass: 21760 kg

Fuel Density: 71 kg/m^3

MCS Segment Type: Maneuver:Finite

Name: Target Sequence.TJI

User Comment: Maneuvers spacecraft with a finite burn

Propagator model used: Earth HPOP v10

Stopping Condition: Delta-V; Run Sequence STOP

Maneuver Summary:

Duration: 1574.61 sec

Fuel Used: 11903.86770087014 kg

DeltaV Magnitude: 6989.999999999779 m/sec

Maneuver Direction Specification: Along Velocity Vector

Maneuver direction is updated during maneuver.

Thrust vector at maneuver start with respect to VNC(Earth) axes:

X (Velocity): 1

Y (Normal): -2.220446049250313e-16

Z (Co-Normal): 3.202428264340972e-16

Azimuth: -1.272221872585407e-14 deg, Elevation:0 deg

Thrust vector at maneuver stop with respect to VNC(Earth) axes:

X (Velocity): 1

Y (Normal): 0

Z (Co-Normal): -4.163336342344337e-17

Azimuth: 0 deg, Elevation: 0 deg

NTP Engine values at beginning/end of segment:

Thrust: 66723.32000000001 N, Isp: 900 s

Mass Flow Rate: -7.559872354190498 kg/sec

Spacecraft State at Beginning of Segment:

UTC Julian Date: 2460926.91666667

State Vector in Coordinate System: Earth Inertial

Parameter Set Type: Cartesian

X: 3118.1354338247369924 km, Vx: 5.8542295388555345 km/sec

Y: -6686.8630169232183107 km, Vy: 2.7298720665655440 km/sec

Z: 0.0000000000004564 km, Vz: 3.5071830349227398 km/sec

Spacecraft State at End of Segment:

UTC Julian Date: 2460926.93489135

Vector in Coordinate System: Earth Inertial

Parameter Set Type: Cartesian

X: 8922.3523755249934766 km, Vx: 1.4751427544768838 km/sec

Y: 5649.9317788011394441 km, Vy: 11.7905906884448264 km/sec

Z: 5682.7211638041208062 km, Vz: 3.4253021376356183 km/sec

NTP Injection stage and Spacecraft Configuration:

Drag Area: 20 m^2, SRP Area: 20 m^2

Dry Mass: 9110 kg, Fuel Mass: 746.132 kg

Total Mass: 9856.13 kg

MCS Segment Type: Propagate

Name: Target Sequence.Propagate

User Comment: Propagates until stopping conditions are met

Propagator model used: Heliocentric

Stopping Condition: Duration; Run Sequence STOP

Spacecraft State at End of Segment:

UTC Julian Date: 2461026.93489135

State Vector in Coordinate System: Earth Inertial

Parameter Set Type: Cartesian

X: 3.1291296293095794e+07 km, Vx: 8.9644178273650219 km/sec

Y: 8.2677161025284380e+07 km, Vy: 16.3965074387668786 km/sec

Z: 2.4631986874884766e+07 km, Vz: 6.4404873874807027 km/sec

NTP Injection stage and Spacecraft Configuration:

Drag Area: 20 m^2, SRP Area: 20 m^2

Dry Mass: 9110 kg, Fuel Mass: 746.132 kg

Total Mass: 9856.13 kg

User-selected results:

Altitude Of Periapsis = 9.2611225819524080e+07 km

MCS Segment Type: Maneuver:Finite

Name: Target Sequence.DSM-1

User Comment: Maneuvers spacecraft with a finite burn

Propagator model used: Heliocentric

Stopping Condition:Duration; Run Sequence STOP

Maneuver Summary:

Duration: 98 sec

Fuel Used: 740.8674907106688 kg

DeltaV Magnitude: 689.6922137742814 m/sec

Maneuver Direction Specification: Thrust Vector

Maneuver direction is updated during maneuver.

Thrust vector at maneuver start with respect to VNC(Earth)

axes:

X (Velocity): -0.1729873939250899

Y (Normal): -0.9810602621904068

Z (Co-Normal): -0.08715574274765797

Azimuth: -100 deg, Elevation: -4.999999999999989 deg

Thrust vector at maneuver stop with respect to VNC(Earth) axes:

X (Velocity): -0.1729873939250898

Y (Normal): -0.981060262190407

Z (Co-Normal): -0.08715574274765825

Azimuth: -100 deg, Elevation: -5.000000000000004 deg

Spacecraft State at Beginning of Segment:

UTC Gregorian Date: UTC Julian Date: 2461026.93489135

State Vector in Coordinate System: Earth Inertial

Parameter Set Type: Cartesian

X: 3.1291296293095794e+07 km, Vx: 8.9644178273650219 km/sec

Y: 8.2677161025284380e+07 km, Vy: 16.3965074387668786 km/sec

Z: 2.4631986874884766e+07 km, Vz: 6.4404873874807027 km/sec

Spacecraft State at End of Segment:

UTC Gregorian Date: UTC Julian Date: 2461026.93602561

State Vector in Coordinate System: Earth Inertial

Parameter Set Type: Cartesian

X: 3.1292156264708709e+07 km, Vx: 8.5601960879357577 km/sec

Y: 8.2678760194197163e+07 km, Vy: 16.2490985851820575 km/sec

Z: 2.4632644622538801e+07 km, Vz: 6.9776056912275735 km/sec

NTP Injection stage and Spacecraft Configuration:

Dry Mass: 9110 kg, Fuel Mass: 5.26481 kg

Total Mass: 9115.26 kg

MCS Segment Type: Propagate

Name: Target Sequence.Propagate

User Comment: Propagates until stopping conditions are met

Propagator model used: Heliocentric

Stopping Condition:UserSelect; Run Sequence STOP

Spacecraft State at End of Segment:

UTC Gregorian Date: UTC Julian Date: 2461690.70833333

State Vector in Coordinate System: Earth Inertial

Parameter Set Type: Cartesian

X: -9.0452818827402484e+08 km, Vx: 15.1858212303064484 km/sec

Y: 1.9813996159930265e+08 km, Vy: -29.2303034602748788 km/sec

Z: 1.0320044040134162e+08 km, Vz: 23.1329470172551090 km/sec

Spacecraft State at End of Segment:

UTC Gregorian Date: UTC Julian Date: 2461690.70833333

State Vector in Coordinate System: Earth Inertial

Parameter Set Type: Cartesian

X: -9.0452818827402484e+08 km, Vx: 15.1858212303064484 km/sec

Y: 1.9813996159930265e+08 km, Vy: -29.2303034602748788 km/sec

Z: 1.0320044040134162e+08 km, Vz: 23.1329470172551090 km/sec

NTP Injection stage and Spacecraft Configuration:

Dry Mass: 9110 kg, Fuel Mass: 5.26481 kg

Total Mass: 9115.26 kg

NTP Injection stage and Spacecraft separation event

MCS Segment Type: Maneuver:Finite

Name: Jupiter Orbit Insertion

User Comment: Maneuvers spacecraft with a finite burn

Propagator model used: Jupiter HPOP (Jovian System)

Stopping Condition:Duration; Run Sequence STOP

Maneuver Summary:

Duration: 3400 sec

Fuel Used: 1180.724036079706 kg

DeltaV Magnitude: 1003.075916878957 m/sec

Maneuver Direction Specification: AntiVelocity Vector

Maneuver direction is updated during maneuver.

Thrust vector at maneuver start with respect to VNC(Earth) axes:

X (Velocity): -0.6935654222916597

Y (Normal):-0.6603048250352345

Z (Co-Normal):-0.2880356627860174

Azimuth:-136.4073051700 deg, Elevation: -16.74039050582 deg

Thrust vector at maneuver stop with respect to VNC(Earth) axes:

X (Velocity): -0.8356271763617373

Y (Normal): -0.5317849736603792

Z (Co-Normal):-0.1375934733726152

Azimuth: -147.5277230722 deg, Elevation:-7.908614755476 deg

Engine values at beginning/end of segment:

Thrust: 1100 N, Isp: 323 s

Mass Flow Rate:-0.3472717753175608 kg/sec

Spacecraft State at Beginning of Segment:

UTC Julian Date: 2461690.70833333

State Vector in Coordinate System: Earth Inertial

Parameter Set Type: Cartesian

X: -9.0452818834599197e+08 km, Vx: 15.1858211872965185 km/sec

Y: 1.9813996181221017e+08 km, Vy: -29.2303034680200291 km/sec

Z:1.0320044045272323e+08 km, Vz: 23.1329469984143046 km/sec

Spacecraft State at End of Segment:

UTC Julian Date: 2461690.74768519

State Vector in Coordinate System: Earth Inertial

Parameter Set Type: Cartesian

X: -9.0446242256870103e+08 km, Vx: 22.3888270319464766 km/sec

Y: 1.9801457200179037e+08 km, Vy: -44.0624648791080133 km/sec

Z: 1.0327494607528621e+08 km, Vz: 18.3940674842027718 km/sec

Spacecraft Configuration:

Dry Mass: 2300 kg, Fuel Mass: 869.276 kg

Total Mass: 3169.28 kg

MCS Segment Type: Propagate

Name: Target Sequence.Propagate

User Comment: Propagates until stopping conditions are met

Propagator model used: Jupiter HPOP (Jovian System)

Stopping Condition:Duration; Run Sequence STOP

Spacecraft State at End of Segment:

UTC Gregorian Date: UTC Julian Date: 2461791.74768519

State Vector in Coordinate System: Jupiter ICRF

Parameter Set Type: Cartesian

X: 2.0606572797138672e+06 km, Vx: 2.7334213760865427 km/sec

Y: -3.1502064776202394e+06 km, Vy: -5.0358718156885223 km/sec

Z: 625297.2378459015162662 km, Vz: -0.6042739136942937 km/sec

Spacecraft Configuration:

Dry Mass: 2300 kg, Fuel Mass: 869.276 kg

Total Mass: 3169.28 kg

_____